Transcriptional Regulation of Cystathionine---Y---lyase in Endothelial Cells by NADPH Oxidase 4---Dependent Signalling

Mistry, Rajesh Kumar

Awarding institution:
King's College London

Transcriptional Regulation of Cystathionine-ϒ-lyase in Endothelial Cells by NADPH Oxidase 4-Dependent Signalling

PhD Thesis

Rajesh Kumar Mistry

Cardiovascular Division

BHF Centre Of Research Excellence

King's College London

October 2015

Submitted for the Degree of Doctor of Philosophy from

King's College London

Supervisors: Dr. Alison C Brewer & Professor. Philip Eaton

'*At the final stage you teach me that this wondrous and multi-coloured universe can be reduced to the atom and that the atom itself can be reduced to the electron. All this is good and I wait for you to continue. But you tell me of an invisible planetary system in which electrons gravitate around a nucleus. You explain this world to me with an image. I realise then that you have been reduced to poetry*'

Albert Camus – The Myth of Sisyphus.

Abstract

Hypertension is a major risk factor implicated in the development of cardiovascular disease and is often associated with endothelial dysfunction. Studies have shown that hydrogen sulfide (H_2S) elicits beneficial actions in the regulation of vascular homeostasis where it modulates improved vascular tone. Evidence suggests that reactive oxygen species (ROS) may regulate the expression and activation of H_2S-generating enzymes within the vascular endothelium. Endothelial NADPH oxidase 4 (Nox4) is an enzyme that specifically generates the ROS, hydrogen peroxide (H_2O_2). It was therefore hypothesised that Nox4-derived ROS may be involved in the regulation of H_2S generation in the endothelium. Here it was shown, in human umbilical vein endothelial cells (HUVECs), that Nox4 regulates the expression of a major H_2S producing enzyme, Cystathionine γ-lyase (CSE) at the mRNA and protein level. Furthermore, this was shown to be dependent on the direct binding of the Activating Transcription Factor 4 (ATF4) to an intronic enhancer region of the CSE gene. Nox4 was also demonstrated to regulate CSE expression through the haem-regulated inhibitor kinase (HRI)/eukaryotic translation initiation factor 2α (eIF2α)/ATF4 signalling module. Finally, CSE mRNA and protein expression were increased in endothelial cells isolated from endothelial-specific Nox4 transgenic mice (eNox4 Tg) and using wire myography it was demonstrated that eNox4 Tg mouse aortae exhibit a hypo-contractile phenotype in response to phenylephrine, compared to Wild type (WT) littermates. This phenotype was ablated when vessels were incubated with the CSE inhibitor, Propargyl-glycine (PPG). To conclude, these data demonstrate a novel role for Nox4 in the regulation of CSE and hence vascular tone in endothelial cells.

Acknowledgements

I would like to extend a huge thank you to my primary supervisor Dr. Alison Brewer for providing me with complete and full support throughout my PhD project as well as allowing me the freedom to formulate, develop and test my own ideas as a junior scientist. This PhD would not have been possible without such an incredible mentor and I am exceptionally grateful to her for her unwavering commitment and belief in my abilities. I would also like to thank my second supervisor Prof. Philip Eaton for helping to clear up questions on complex chemistry and providing me with the equipment required for some of my experiments.

During my time in the lab I was encouraged and supported by a number of people, most notably Dr Thomas Murray, who patiently taught and guided me through a number of experimental procedures and has thus provided me with a wealthy skill set to which I can return in the future. I feel very privileged to have worked so closely with someone I regard as a rigorous, thorough, and accomplished scientist and most importantly, a close friend. Other heroes include, Matthew Hancock, Dan Martin, and Simon Burr.

Outside of the lab I would like to thank my parents for their continued support as well as my two brothers Jayran and Aneesh for their love, care and advice in all things far and wide, to which I consider myself extremely lucky. These thanks also extend to a mass of exceptional and truly incredible friends who have helped me party my way through the difficulties and successes of the past three years.

Declaration

I declare that I am the sole author of this thesis and that the work contained within it is my own unless otherwise stated.

Rajesh K Mistry

Table of Contents

Table of Figures

Table of Tables

Abbreviations

·OH: Hydroxyl Radicals

3-MST: 3-Mercaptopyruvate Sulfurtransferase

ACh: Acetylcholine

AdNox4: Adenoviral Nox4

AdBGal: Adenoviral beta-Galactosidase

AngII: Angiotensin II

ANS: Autonomic Nervous System

ATF4: Activating Transcription Factor 4

ATP: Adenosine Triphosphate

BH4: Tetrahydrobiopterin

Ca^{2+}: Calcium

CaM: Calmodulin

CAT: Cysteine Aminotransferase

CBS: Cystathionine β-Synthase

CD31: cluster of differentiation 31

cGMP: Cyclic Guanosine Monophosphate

ChIP-Seq: Chromatin Immunoprecipitation-Sequencing

ChIP: Chromatin Immunoprecipitation

CMEC: Cardiac Microvascular Endothelial Cells

CO: Carbon Monoxide

COX1/2: Cyclooxygenase 1/2

$CSE^{-/-}$: CSE Null Mouse

CSE: Cystathionine γ-Lyase

csNox4 Tg: Cardiac Specific Nox4 Overexpressing Mice

C_t: Cycle Threshold

CVD: Cardiovascular Disease

DPI: Diphenyleneiodonium chloride

EDHF: Endothelium Derived Hyperpolarising Factor

EDRF: Endothelium Derived Relaxing Factor

eIF2α: Eukaryotic Translation Initiation Factor 2α

eNOS: Endothelial Nitric Oxide Synthase

eNox4 Tg: Endothelial Specific Nox4 Overexpressing Mice

eNox4$^{-/-}$: Endothelial Specific Nox4 Null Mice

ER: Endoplasmic Reticulum

FAD: Flavin Adenine Dinucleotide

GCN2: General Control Non-derepressible-2 Kinase

GPx: Glutathione Peroxidase

GSH: Reduced Glutathione

GSSG: Oxidised Glutathione

GTP: Guanosine Triphosphate

GYY4137: Morpholin-4-ium 4-Methoxyphenyl(Morpholino) Phosphinodithioate

H_2O_2: Hydrogen Peroxide

H_2S: Hydrogen Sulphide

HBSS: Hanks Balanced Salts' Solution

Hcy: Homocysteine

HEK293: Human Embryonic Kidney Cells

HO: Haem Oxygenases

HRI: Haem-regulated inhibitor kinase

HUVEC: Human Umbilical Veins Endothelial Cells

IE: Intronic Enhancer

IK_{Ca}: Intermediate Calcium Gated K^+ Channels

iNOS: Inducible Nitric Oxide Synthase

IP: Prostaglandin I_2 Receptor

ISR: Integrated Stress Response

K^+: Potassium Ions

K_{ATP}: ATP-gated Potassium Channels

KCl: Potassium Chloride

KEAP1: Kelch-like ECH-associated Protein 1

K_{ir}: Inward Rectifying K^+ Channels

L-NAME: NG-Nitro-L-Arginine-Methyl Ester

L-NMMA: NG-Monomethyl-L-Arginine

L-NNA: L-Nitroarginine

MEFs: Mouse Embryonic Fibroblasts

mm Hg: Millimetres of Mercury

MOI: Multiplicity of Infection

mRNA: messenger RNA

MS: Methionine Synthase

N5-MTHF: N-5-Methyltetrahydrofolate

NAC: N-Acetyl Cysteine

NADPH: Nicotinamide Adenine Dinucleotide Phosphate

NaHS: Sodium Hydrosulphide

NaS: Sodium Sulphide

nNOS: Neuronal Nitric Oxide Synthase

NO: Nitric Oxide

NOS: Nitric Oxide Synthase

Nox: Nicotinamide Adenine Dinucleotide Phosphate Oxidase

Nrf2: Nuclear Factor Erythroid Derived

O.E: Overexpression

O_2^-: Superoxide

ORF: Open Reading Frame

PBS: Phosphate Buffered Saline

PCR: Polymerase Chain Reaction

PDE5A: Phosphodiesterase 5A

PDGF: Platelet-derived Growth Factor

PE: Phenylephrine

PEG-Cat: Catalase–Polyethylene Glycol

PERK: PKR-like ER Kinase

PGI_2: Prostacyclin

Phox: Phagocyte Oxidase

PI3K: Phosphatidylinositol-3-kinase

PIC: Pre-initiation complex

pKa: Acid Dissociation Constant

PKG: Protein Kinase G

PKR: Protein kinase double-stranded RNA-dependent kinase

PLP: Pyridoxal 5-Phosphate

Poldip2: δ–interacting protein 2

Pol II: RNA polymerase II

PPG: Propargylglycine

QPCR: Quantitative Reverse Transcription Polymerase Chain Reaction

ROS: Reactive Oxygen Species

S^-: Thiolate

SAH: S-adenosylhomocysteine

SAHH: S-adenosylhomocysteine hydrolase

SAM: S-Adenosylmethionine

SDS: Sodium Dodecyl Sulfate

Ser51: Serine 51

sGC: Soluble Guanylate Cyclase

SK_{Ca}: Small Calcium Gated K^+ Channels

SMC: Smooth Muscle Cell

SO_2H: Sulfinic Acid

SO_3H: Sulfonic Acid

SOD: Superoxide Dismutase

SOH: Sulfenic Acid

SP1: Specific Protein 1

SSH: Hydropersulphide Moiety

tBHP: Tert-Butylhydroperoxide

Tg: Transgenic

TxA_2: Thromboxane A2

uORF: Untranslated Open Reading Frame

UPR: Unfolded Protein Response

VEGF: Vascular Endothelial Growth Factor

Vmax: Maximal Velocity

VSMC: Vascular Smooth Muscle Cell

vWF: von Willebrand Factor

WT: Wild Type

Chapter 1: General Introduction

1.1 Cardiovascular Disease

Cardiovascular disease (CVD) remains a leading cause of morbidity and mortality in Western countries and generates a large economic burden[1]. A number of risk factors have been identified for CVD including hypertension, smoking and diabetes mellitus and of these, hypertension is the most prevalent risk factor worldwide[2]. Despite this, the aetiology of hypertension remains incompletely understood and thus an impetus toward further scientific exploration into the biochemical and physiological mechanisms of the disease has been established.

Perturbations in the normal homeostatic function of the endothelium, termed endothelial dysfunction, have been repeatedly recognised as a common participant in a number of CVD states including hypertension[3]. Indeed, traditional CVD risk factors are often associated with endothelial dysfunction and it seems that this may precede disease formation[4]. A detailed investigation of endothelial function in (patho)physiology may therefore provide the insights required for improved diagnostic and therapeutic interventions. An assessment of endothelial function may also present a useful prognostic marker for the identification of patients predisposed to long-term CVD events[5].

1.2 Blood Vessel Anatomy

Arteries and veins are structurally layered into three distinct regions identifiable as the tunica adventitia, media and intima (Figure 1.1). The tunica adventitia represents the outermost vessel layer and is composed of collagen, elastic fibres, nerves and fibroblasts. The middle layer, known as the tunica media, occupies the greatest area of the vessel wall and is composed of smooth muscle, collagen and elastic fibres. The tunica media is responsible for most of the mechanical properties of the vessel, where smooth muscle controls constriction and dilation, elastic fibres help to maintain blood flow by expanding the vessel wall (as blood pressure increases) and collagen ensures that excessive expansion and dilation of vessels is prevented. The tunica intima lines the luminal surface of the vessel and is composed of a monolayer of cells known as the vascular endothelium. In healthy vessels the endothelial cells of the intima are flat, elongated and aligned in the direction of flow[6]. The endothelium has a number of physiological functions that will now be discussed.

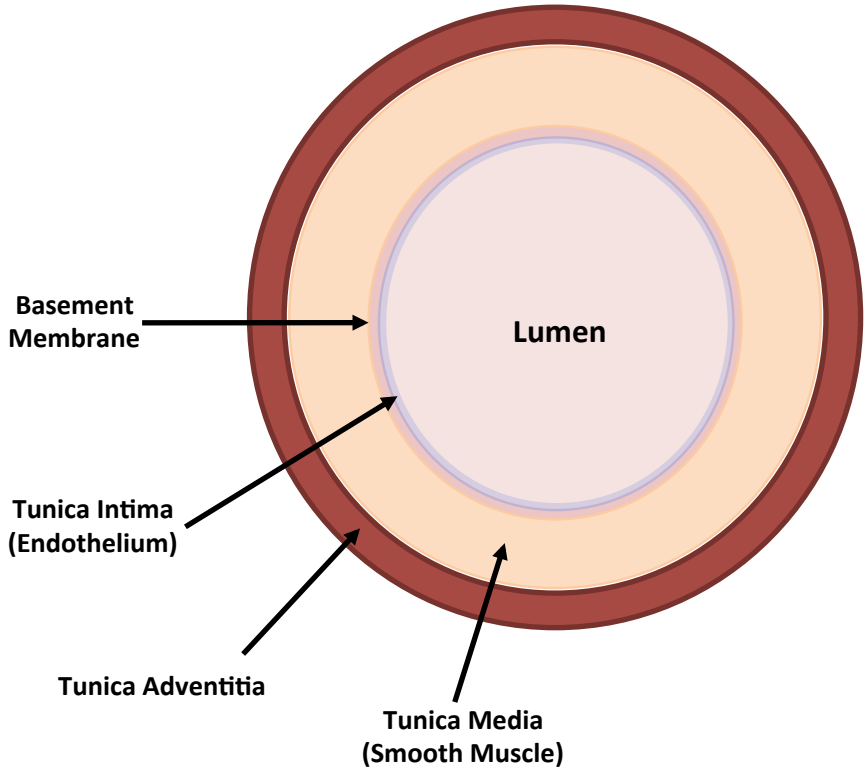

Figure 1.1: Artery Anatomy. A schematic diagram displaying the structure of an artery composed of the Tunica Intima, Media and Adventitia. The endothelium lines the luminal surface of the vessel and comprises the Intimal layer.

1.2.1 The Endothelium

The endothelium comprises a monolayer of individual endothelial cells that collectively line the interior surface of the entire vascular system. Initially, it was considered to function solely as a mechanical barrier that also facilitated the diffusion and transport of biomolecules across itself. In recent decades however, it has become apparent that the endothelium possesses fundamental basal and inducible synthetic and metabolic functions that are elicited through its ability to secrete and respond to, a number of autocrine, paracrine and endocrine molecules[7]. Indeed, its unique position at the interface between blood and surrounding tissue make it ideally placed to modulate vascular function and

homeostasis. As such, the endothelium represents a highly versatile and multifunctional 'organ' system. Like other organs the endothelium varies in its morphological and functional activity depending on the vascular bed in which it is situated. Thus structural and molecular endothelial heterogeneity exists on an organ-to-organ basis and even within different regions of the same tissue[8, 9]. The importance of the endothelium within the cardiovascular system is highlighted by the many diseases that arise from its dysfunction such as atherosclerosis, hypertension and metastatic disease[4, 10].

The endothelium in its quiescent state plays a fundamental role in regulating a number of homeostatic vascular processes[7]. Of these, the most widely studied and well-established function is in its control of blood flow and tissue perfusion through the modulation of vascular tone. The endothelium controls vascular tone by releasing, and reacting to, a number of vasoactive mediators that balance vasodilation and vasoconstriction. Alterations in this balance lead to pronunciations in the phenotype to which the vasoactive substance favours. For example Nitric Oxide (NO) release favours a vasodilatory phenotype, whereas angiotensin II (AngII) promotes vasoconstriction[11]. In addition to the regulation of blood-pressure, the endothelium is intimately involved in coordinating blood haemostasis and coagulation. Here, the basal-state endothelium acts to preserve a non-thrombogenic blood-tissue interface by preventing thrombosis, thrombolysis, platelet adherence and immune cell recruitment. By contrast, in its activated state, the endothelium causes a dynamic shift in phenotype, moving away from the maintenance of blood fluidity toward a pro-coagulant and pro-thrombotic milieu[12]. The activated endothelium achieves this through the release of von Willebrand

factor (vWF), platelet activating factor and thromboplastin[10]. In a similar process, the endothelium controls vascular inflammation and host defence by permitting the release of various cytokines and promoting cell adhesive and permeability properties upon its activation[13]. Finally, the endothelium has further roles in regulating neovascularisation through its engagement in angiogenesis *via* a proliferative response to vascular endothelial growth factor (VEGF)[14].

1.3 The Endothelium and Vascular Tone

As mentioned above, the endothelium can direct changes in vascular tone and therefore blood flow through its release and response to a number of vasoactive agents[11]. This process of modulating blood flow is fundamental in permitting individual tissues and organs to meet their changing metabolic demands both at rest and under stress conditions. To achieve this a number of biosystems and molecules that comprise metabolic, humoral and neuro-adrenergic components have evolved. Indeed, the control of vascular tone can be envisaged as an intimate interplay between autonomic nervous output and local endothelium-directed vasomotor actions. The autonomic nervous system (ANS) acts to innervate and modulate the vessel dynamics of small arteries and arterioles and therefore contributes to maintaining physiological vascular tone and blood pressure. This is achieved by a smooth muscle response to various neuro-adrenergic mediators that permit vasorelaxation through the activation of β-adrenergic receptors or vasoconstriction through binding α1 adrenergic receptors[15].

To complement the ANS-induced regulation of blood pressure the endothelium exerts local homeostatic control of vessel dynamics through its sensing of haemodynamic forces and in its response to various humoral agents. In its resting state, the endothelium maintains a balance between vasodilator molecules, that elicit their actions through smooth muscle cell relaxation, with vasoconstrictor agents that oppose this dilation by causing smooth muscle contraction. Vasodilatory molecules include endothelium-derived relaxing factors (EDRF) such as NO[16] and prostacyclin[17] as well as endothelium derived hyperpolarising factors (EDHF)[18] that include hydrogen peroxide (H_2O_2)[19] and hydrogen sulphide (H_2S)[20]. By contrast constrictor agents include catecholamines[21], angiotensin II[22], thromboxanes[23] and endothelin 1[24]. The balance of vasodilators and constrictors achieved by a normal functioning endothelium ultimately leads to precise tissue perfusion under physiological conditions. If perturbations in the levels or activities of these mediators occur, such as in states of endothelial dysfunction, it can result in a number of vascular diseases such as atherosclerosis and hypertension[4].

1.4 Endothelium-derived Vasodilators

As mentioned above a number of vasodilatory mediators exist, some of which are produced by the endothelium[25]. These endothelium-derived factors can broadly be defined as endothelium-derived relaxing factors (EDRF), of which NO is the prototypical example[16]. Other endothelium-derived substances that can be distinguished from EDRF by the ability to cause vascular smooth muscle cell hyperpolarisation are termed endothelium-derived hyperpolarising factors

(EDHF)[26]. In the following sections a detailed account of both EDRFs and EDHFs will be given as well as a discussion of gasotransmitter molecules and their potential contribution to these categories.

1.4.1 Nitric Oxide (NO)

In 1980, Furchgott and Zawadzki published their seminal research into the function of the endothelium in vasomotion. Here it was demonstrated that an intact endothelium is absolutely required for the mediation of acetylcholine (ACh)-induced vasorelaxation in rabbit aortic rings, since vessels denuded of their endothelium failed to relax to ACh and in fact became more contractile. These observations defined a role for the endothelium in the production of a vasoactive substance termed EDRF[27]. Subsequent research efforts culminated in Furchgott, Ignarro and Murad being awarded a Nobel prize in 1988 for the discovery and characterisation of NO as the elusive EDRF[16]. Since then the NO field has expanded exponentially and many important physiological roles have been ascribed to this gaseous mediator[28].

NO is synthesized enzymatically by a family of enzymes collectively termed Nitric Oxide Synthases (NOS). The NOS family encompasses three distinct isoenzymes encoded by separate genes that include neuronal NOS (nNOS, NOS-I), inducible NOS (iNOS, NOS-II) and endothelial NOS (eNOS, NOS-III). Within the vasculature, multiple NOS isoforms, in particular nNOS and eNOS are expressed[29]. In the

endothelium eNOS is the predominant isoform and will therefore form the focus of this discussion.

Endothelial NOS is a constitutively-expressed enzyme that utilises the amino acid L-arginine as a substrate for the production of NO and L-citrulline under physiological conditions[30, 31]. A number of agonists have been shown to induce endothelium–dependent relaxations through eNOS activation such as ACh, serotonin and VEGF[32]. These stimuli induce eNOS activity by enhancing intracellular calcium concentrations. Here, calcium (Ca^{2+})-bound calmodulin (CaM) binds to and displaces eNOS from caveolin, a protein that sequesters eNOS within membrane invaginations known as caveolae. The binding of Ca^{2+}/calmodulin is generally considered to promote the movement of electrons from nicotinamide adenine dinucleotide phosphate (NADPH) to flavin molecules in the NOS reductase domain. These electrons then pass into the oxygenase domain, where they reduce haem iron, permitting NO synthesis from L-arginine (Figure 1.2). In order for this series of reactions to occur correctly, eNOS needs to form a homodimer. Dimer formation is promoted by the binding of tetrahydrobiopterin (BH4), an eNOS cofactor. Indeed, loss of BH4 results in eNOS uncoupling and subsequent generation of the reactive oxygen species (ROS), superoxide (O_2^-). Therefore, effective eNOS activation requires, NADPH, oxygen, BH4 and the substrate L-arginine[33].

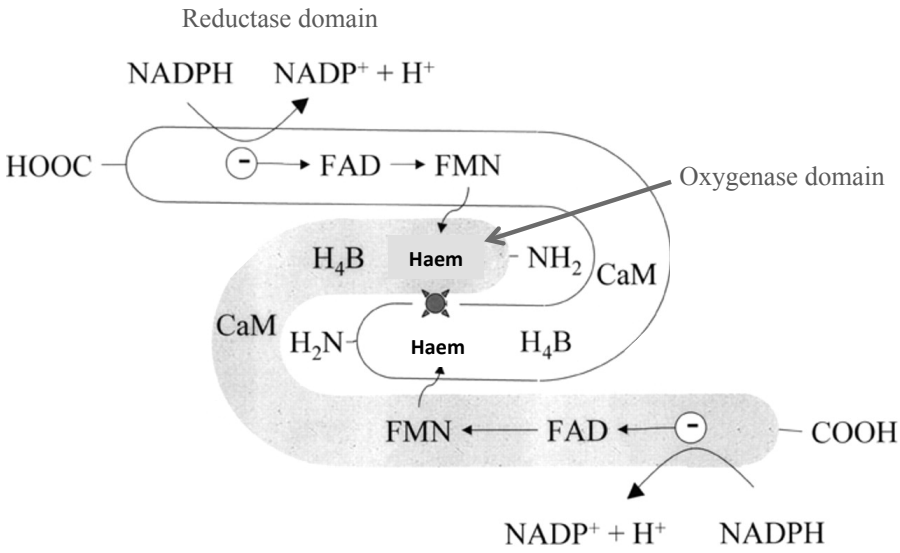

Figure 1.2: eNOS Structure and Mechanism of NO Generation. Electrons move from NADPH to flavin groups (FAD, FMN) in the reductase domain, these then reduce haem in the oxygenase domain permitting NO formation. Binding of Ca^{2+}/CaM is thought to activate electron transfer. Figure adapted from[33].

Once NO is formed in the endothelium, it diffuses across to neighbouring smooth muscle cells (SMC) where it activates soluble guanylate cyclase (sGC) by binding to its haem group. sGC converts guanosine triphosphate (GTP) into cyclic guanosine monophosphate (cGMP) which then goes on to activate Protein Kinase G (PKG). PKG has a number of downstream targets that act to cause vascular smooth muscle cell (VSMC) relaxation (Figure 1.6)[34]. The importance of eNOS in controlling vasodilation and blood pressure is highlighted by the effects of eNOS inhibitors such as NG-monomethyl-L-arginine (L-NMMA) and NG-nitro-L-arginine-methyl ester (L-NAME) on endothelium-induced vasodilation in *ex vivo* experiments. Treatment with these inhibitors causes vessel constriction, an effect that is reversed by L-arginine treatment[35]. Furthermore, direct genetic evidence for eNOS-induced control of blood pressure was confirmed in mice by disruption of

the eNOS gene, as these mice displayed enhanced systemic blood pressure compared to WT controls[36].

1.4.2 Prostanoids

The Prostaglandins represent a family of oxygenated 20-carbon fatty acid metabolites of arachidonic acid that play a role in a number of vascular processes including vasodilation, vasoconstriction and platelet aggregation. They are formed by the action of cyclooxygenase enzymes (COX-1 and COX-2) on arachidonic acid derived from membrane lipids such as phosphatidylcholine. Prostaglandin H2 is a common precursor for five major signalling fatty acids, which include the vasoconstrictor molecule, thromboxane A2 (TxA_2), and, of pertinence to this section, the vasodilator Prostacyclin (PGI_2)[17]. PGI_2 is produced in endothelial cells by the action of prostacyclin synthase in response to a variety of stimuli including bradykinin, adenine nucleotides and ACh[37]. In cultured endothelial cells PGI_2 is generated along with TxA_2 at a proposed ratio of 5:1 highlighting the importance of this prostanoid in endothelial cells[38]. Once formed, PGI_2 can mediate its vasodilatory actions by increasing cyclic adenosine monophosphate (cAMP) signalling in VSMCs through binding to the prostaglandin I_2 receptor (IP) (Figure 1.6)[39].

1.4.3 Endothelium-derived Hyperpolarising Factor

Nitric oxide and PGI_2 are well-established EDRFs that play a central role in vasodilation. In 1988 however, Chen and Weston described the existence of another endothelium-derived species that elicited vasodilation by hyperpolarising VSMCs in rat blood vessels[40]. The functional effects of this substance subsequently lead to its appellation; Endothelial Derived Hyperpolarising Factor (EDHF)[41]. The characterisation of EDHF came from studies in which the combined administration of NOS and COX inhibitors did not fully ablate vascular relaxation responses to endothelial agonist such as bradykinin and ACh *ex vivo* and *in vivo*[42]. These observations were further investigated in mice deficient in both eNOS and COX-1 where it was shown that ACh-induced vasodilation was preserved in eNOS/COX-1 null mice[43]. The hyperpolarisation activity of EDHF has been emphasised by the observation that the calcium-activated potassium channel blockers, Apamin and Charybdotoxin (as well as membrane depolarisation induced by high extracellular potassium) ablate the residual EDHF responses when NO and PGI_2 are perturbed[41-43].

The precise nature of EDHF remains contentious, indeed a number of different molecules and mechanisms have been proposed and it is likely that EDHF represents a combination of these. Edwards *et al* proposed that potassium ions (K^+) might function as an EDHF. They showed that endothelium-derived K^+ ions increased in the myoendothelial space following endothelial stimulation with ACh, an effect that was blunted by Apamin and Charybdotoxin, inhibitors of endothelial small (SK_{Ca}) and intermediate (IK_{Ca}) calcium-gated K^+ channels respectively. The

extracellular accumulation of K^+ was associated with VSMC hyperpolarisation elicited through the opening of inward rectifying K^+ channels (K_{ir}) and the activation of the sodium/potassium ATPase pump present on VSMC membranes. Inhibitors of these channels and pumps such as ouabain and barium abolished the hyperpolarisation of VSMCs (Figure 1.6)[44].

Another candidate for EDHF is H_2O_2 (Figure 1.6). Matoba *et al* demonstrated that human mesenteric arteries denuded of their endothelium hyperpolarised in response to exogenous H_2O_2 in a dose-dependent manner. Indeed, vascular relaxation in response to the endothelial agonist bradykinin was significantly blunted by treatment with the peroxidase enzyme, catalase, which also reduced membrane hyperpolarisation. In order to rule out any effect of NO and PGI_2, all of these studies were performed under the blockade of COX and NOS with indomethacin and L-nitroarginine (L-NNA) respectively[19]. To further verify a role for H_2O_2 as an EDHF, these findings were recapitulated in mice[45]. Moreover, studies conducted in mice deficient in BH4 revealed that endothelium-dependent relaxation to ACh occurred in both WT- and BH4-deficient phenotypes. Interestingly, this relaxation could be inhibited by catalase and enhanced by superoxide dismutase (SOD) only in the BH4-deficient mice. The authors concluded that during situations where eNOS becomes uncoupled, it generates ROS that can mediate vasorelaxation to compensate for the loss of NO[46]. Despite these observations, the source of H_2O_2 has yet to be identified. However studies performed by Ray *et al* using an endothelial specific NADPH Oxidase 4 (Nox4) overexpressing mouse (eNox4 Tg) suggest that H_2O_2 derived from Nox4 may be involved. Here, eNox4 Tg mice were shown to display a low blood pressure

phenotype that was accompanied by an enhanced aortic relaxation profile to a number of endothelial agonists, an effect that was reversed by catalase treatment. Although a mechanism was not identified it would appear that Nox4-derived ROS were potentially acting as an EDHF since K^+ channel blockade also ablated the enhanced endothelial-dependent relaxatory phenotype[47]. These data thus support previous findings by Matoba *et al*[45].

1.5 Gasotransmitters

A gasotransmitter is a gaseous messenger molecule that participates in cell signalling. Three major gasotransmitters are known to exist: NO, CO and H_2S[48] (Figure 1.3). The discovery and characterisation of these three family members has altered the conventional paradigm of intercellular signalling. Unlike peptide signalling molecules that are often stored in vesicles, gasotransmitters are synthesised enzymatically on demand. Furthermore, peptide signals tend to mediate their function by binding to plasma membrane receptors such as receptor tyrosine kinases. By contrast, gasotransmitters diffuse across membranes within and between cells and then interact with their target directly *via* post-translational modifications. These novel mechanisms of intercellular signalling have been the subject of much research, most notably in the NO field, but also more recently in H_2S biology[49]. Gaseous signalling molecules exert a wide range of effects within a variety of cell types that can then lead to a plethora of phenotypic consequences such as angiogenesis, cell survival and the regulation of vascular tone[49-51]. As NO

has previously been discussed, this section will focus on CO and H_2S in the control of vasomotion.

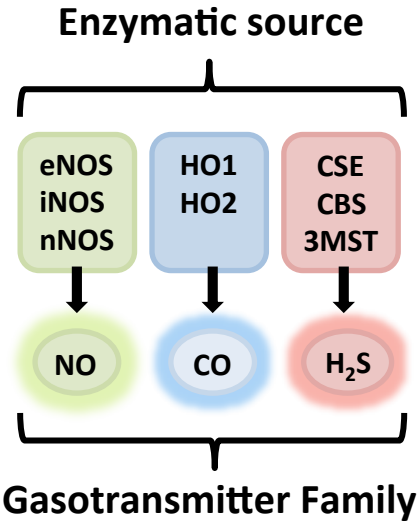

Figure 1.3: Gasotransmitters. A schematic diagram depicting major gasotransmitter and their respective enzymatic source. NO: Nitric Oxide, CO: Carbon Monoxide, H_2S: Hydrogen Sulphide. NOS: Nitric Oxide Synthase, HO: Haem-oxygenase, CSE: Cystathionine-γ-lyase, CBS: Cytathionine-β-synthase, 3MST: 3 mercaptopyruvate sulphur transferase.

1.5.1 Carbon Monoxide (CO)

Carbon monoxide (CO) is physiologically generated *via* haem catalysis by a family of enzymes known as haem-oxygenases (HO). This family comprises 3 isoenzymes; HO-1, HO-2 and HO-3, of which only HO-1 and 2 are catalytically active proteins. HO-1 is an inducible isoform that becomes active in response to inflammation and oxidative stress. HO-2 on the other hand is constitutively expressed and is responsible for basal CO production primarily in the brain and cardiovascular system[52]. CO has been shown to induce vasorelaxation in a number of vessels[53] including rat aorta and tail as well as mesenteric, renal and pulmonary arteries[54].

Some groups suggest that this occurs in an endothelium-dependent manner[55]. Despite these observations, the precise biochemical mechanisms through which CO induces vasodilation are not currently understood.

1.5.2 Hydrogen Sulphide (H_2S)

H_2S was first thought of as a toxic environmental pollutant until relatively recently when Abe and Kimura proposed it to be an endogenous signalling mediator in mammals[56]. Subsequent research efforts have established H_2S as the third member of the gasotransmitter family of signalling molecules and have ascribed a number of physiological functions to it in systems as diverse as the cardiovascular, immunological and nervous system [57].

The chemical properties of H_2S under physiological conditions have been studied; in aqueous solutions at pH 7.4, H_2S exists in a dissociated state with approximately two thirds of total H_2S existing as hydrosulphide anions (HS^-) and protons (H^+) and the remaining third as H_2S undissociated gas. HS^- can subsequently form sulphide ions (S_2^-) through further dissociation but only at high, non-physiological pHs. S_2^- are therefore considered negligible in physiological systems[58]. The term H_2S will be used to collectively denote both H_2S and HS^- anions in this thesis as it is unknown which of these is the most physiologically relevant species. H_2S is lipophilic and can diffuse through membranes in a similar manner to NO and CO, although due to its dissociation at physiological pH, it is considered to be less lipid-permeable than its other family members[59].

H_2S is synthesised endogenously through the action of 3 enzymes: cystathionine β-synthase (CBS), cystathionine γ-lyase (CSE) and the combined action of 3-mercaptopyruvate sulfurtransferase (3MST) and cysteine aminotransferase (CAT)[60]. These enzymes have been shown to have tissue-specific patterns of expression, with CBS playing a major role in H_2S generation in the brain and nervous system[61]. By contrast, 3MST is widely distributed in multiple cell types including neurons, hepatocytes, cardiac cells and endothelial cells[62, 63]. Within the vascular system however, the major enzymatic source of H_2S is CSE, which has been shown to be expressed and active in a number of vascular cell types including VSMCs[64], perivascular adipose cells[65] and importantly, endothelial cells[20, 66, 67]. Initially however, CSE expression was thought not to occur in the endothelium but it is now clear that CSE is both expressed and active in this cell type[63, 64].

CSE is a tetrameric protein that requires the binding of pyridoxal 5-phosphate (PLP or vitamin B6) in order to function[68]. It generates H_2S from a number of substrates including cysteine, cystine and homocysteine[69 70]. Figure 1.4 shows the substrates and products made by each of the H_2S-generating enzymes.

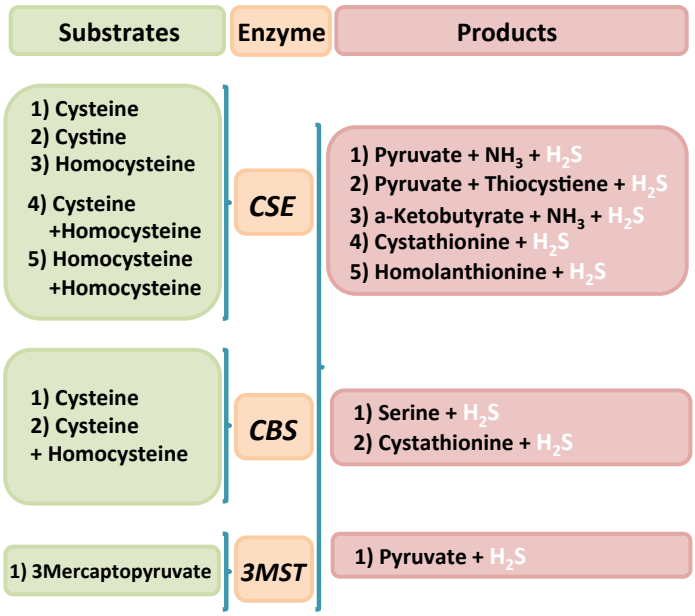

Figure 1.4: H_2S Biosynthesis. The enzymatic substrates and products generated by CSE, CBS and 3MST during H_2S biosynthesis (adapted from[69, 70]).

Once generated, H_2S is believed to function as a secondary messenger by post-translationally modifying cysteine residues on target proteins in a process known as S-sulfhydration[71]. Here, sulphur derived from H_2S becomes added to the thiol group of a target cysteine residue to render the formation of a hydropersulphide moiety (-SSH) (Figure 1.5 shows how H_2S can attack thiol groups to from -SSH). Indeed, 10-25% of the proteins in mouse liver were shown to exist in the S-sulfhydration state and a number of key proteins of diverse function are beginning to emerge as potential targets of H_2S[71].

Recently however, the precise mechanism through which H_2S induces its modifications has been questioned. Initially it was thought that H_2S attacks previously oxidised cysteine residues such as those in the sulfenic acid (SOH) or disulphide bonded (S-S) state in a reduction reaction[71] (Figure 1.5). However, recent studies have begun to show that in order to mediate its function, H_2S acts as

an oxidant molecule through its initial reaction with ROS to form polysulphides (H_2S_n). These polysulphides then oxidise cysteine residues on target proteins yielding the aforementioned persulphide moiety[72, 73].

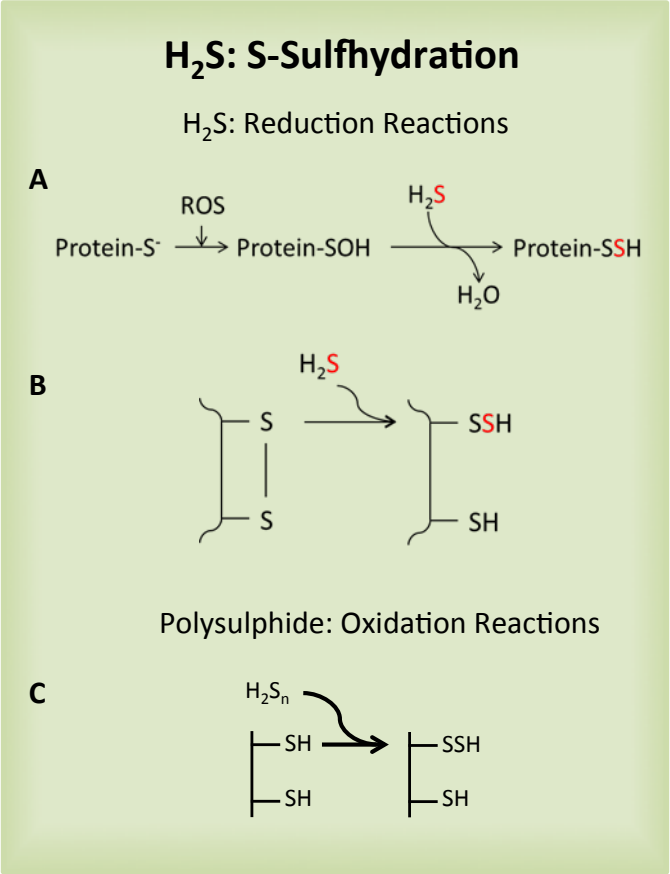

Figure 1.5: **Sulfhydration by H_2S and Polysulphide**. A schematic diagram depicting the proposed reaction mechanisms involved in hydropersulphide (-SSH) formation. **A)** reduction of sulfenic acids. **B)** reduction of disulphide bonds. **C)** Polysulphide (H_2S_n) induced thiol oxidation to –SSH.

1.5.3 Hydrogen Sulphide and Vascular Tone

One of the first biological activities attributed to H_2S was in the regulation of vascular tone[74]. A number of subsequent studies have helped define a clear role for

the CSE/H_2S signalling system in the modulation of this process, specifically with respect to vasodilation. Exogenous application of H_2S or polysulphides to vessels using donor compounds such as sodium sulphide (NaS), sodium hydrosulphide (NaHS) and the slow-releasing H_2S donor drug, GYY4137 (morpholin-4-ium 4-methoxyphenyl(morpholino) phosphinodithioate) have been shown to induce vasorelaxation in a plethora of *ex vivo* models[65 73, 75-77]. Furthermore, the CSE substrate, cysteine, can induce vasorelaxation in rat aortae, an effect that can be blocked by the CSE inhibitor propargylglycine (PPG)[78]. The direct physiological relevance of the CSE/H_2S pathway in vasorelaxation was subsequently confirmed in CSE-null mice ($CSE^{-/-}$) *in vivo.* Here, both homozygous and heterozygous deficiencies in CSE resulted in perturbed H_2S profiles[79]. Indeed, endogenous H_2S levels in the aorta and heart of homozygous CSE-null mice were reduced by around 80% and serum levels reduced by 50% compared to WT littermate controls. Consistent with the involvement of the CSE/H_2S pathway in vasomotion, $CSE^{-/-}$ mutants developed age-dependent hypertension that began at 7 weeks of age and peaked at over 135mm Hg at 12 weeks; this was approximately 18mm Hg higher than the blood pressure of control mice. It was also shown that eNOS protein levels were not augmented in these mice, suggesting that the hypertensive phenotype was not due to a loss in eNOS-mediated vasorelaxation but rather an effect of CSE ablation[79]. To further demonstrate that the H_2S reduction (itself due to a loss in CSE expression) was responsible for the hypertensive phenotype, $CSE^{-/-}$ mice were intravenously injected with the H_2S donor, NaHS. Following injection, mice demonstrated a dose-dependent and transient reduction in systolic blood pressure confirming a role for H_2S in blood pressure regulation. It was also shown that

$CSE^{-/-}$ mice display blunted endothelium-dependent vasorelaxation compared to WT littermates further confirming a role for endothelial CSE in vascular tone[79].

At the cellular and molecular level, studies have revealed that H_2S may exert its vasodilatory actions in VSMCs where it has been shown to cause the opening of ATP-gated K^+ channels (K_{ATP}) through S-Sulfhydration leading to SMC hyperpolarisation and subsequent vasodilation[71] [20]. To add to these findings, studies using patch clamp techniques demonstrated that H_2S could directly hyperpolarize VSMCs[80].

In addition to H_2S-induced hyperpolarisation of smooth muscle, H_2S signalling is thought to be important in the endothelium, where it can induce EDHF-type actions. *In vitro* experiments have shown that endothelial CSE can be activated by Ca^{2+}/calmodulin in response to cholinergic stimulation or by the calcium ionophore, A23187 leading to enhanced H_2S production[79]. Moreover, stimulation of endothelial cells with ACh resulted in hyperpolarisation in WT but not $CSE^{-/-}$ endothelial cells. It was further demonstrated that inhibition of small and intermediate calcium gated K^+ channels present on the endothelium using apamin and charybdotoxin blocked ACh-induced hyperpolarisation. By contrast, both WT and $CSE^{-/-}$ endothelial cells hyperpolarised in response to NaHS in an apamin- and charybdotoxin-sensitive manner[20]. These findings were further confirmed using patch clamp techniques[81]. At the whole vessel level, cholinergic stimulation of mesenteric arteries caused vasorelaxation, an effect that was blunted in $CSE^{-/-}$ mice. In vascular rings with an intact endothelium, NaHS-induced dilatation was partially inhibited by the separate addition of apamin, charybdotoxin and the

VSMC K_{ATP} channel blocker, glibenclamide. A combination of these inhibitors however completely ablated NaHS-induced relaxation. By contrast, in vessels denuded of the endothelium, apamin and charybdotoxin had no effect on NaHS-induced dilation but this was now completely blocked by glibenclamide alone[20]. Taken together, these data suggest that H_2S functions to hyperpolarise both VSMC and endothelial cells through the activation of various K^+ channels. The precise contribution of VSMC-expressed CSE and endothelial-expressed CSE to this process is yet to be determined but current data suggest that both are important contributors to H_2S-induced vasorelaxation.

In addition to eliciting endothelial and SMC hyperpolarisation, H_2S has been shown to induce vasorelaxation by other mechanisms. Firstly, Predmore *et al* showed that NaS induced the production of NO in bovine aortic endothelial cells, an effect reported to result from increased eNOS phosphorylation at serine 1177, a site consistent with its enhanced activation[82]. Interestingly, crosstalk between NO and H_2S has also been observed at the level of cGMP. Coletta *et al* demonstrated that NaHS significantly enhanced cGMP levels in an L-NAME dependent manner. Furthermore, NaHS inhibited phosphodiesterase 5A (PDE5A) to a similar extent as Sildenafil, a synthetic PDE5 inhibitor. It was concluded that NO acts in a classical manner to activate PKG through the sGC/cGMP pathway while H_2S potentiates this effect by inhibiting cGMP degradation by PDE5A (Figure 1.6)[83].

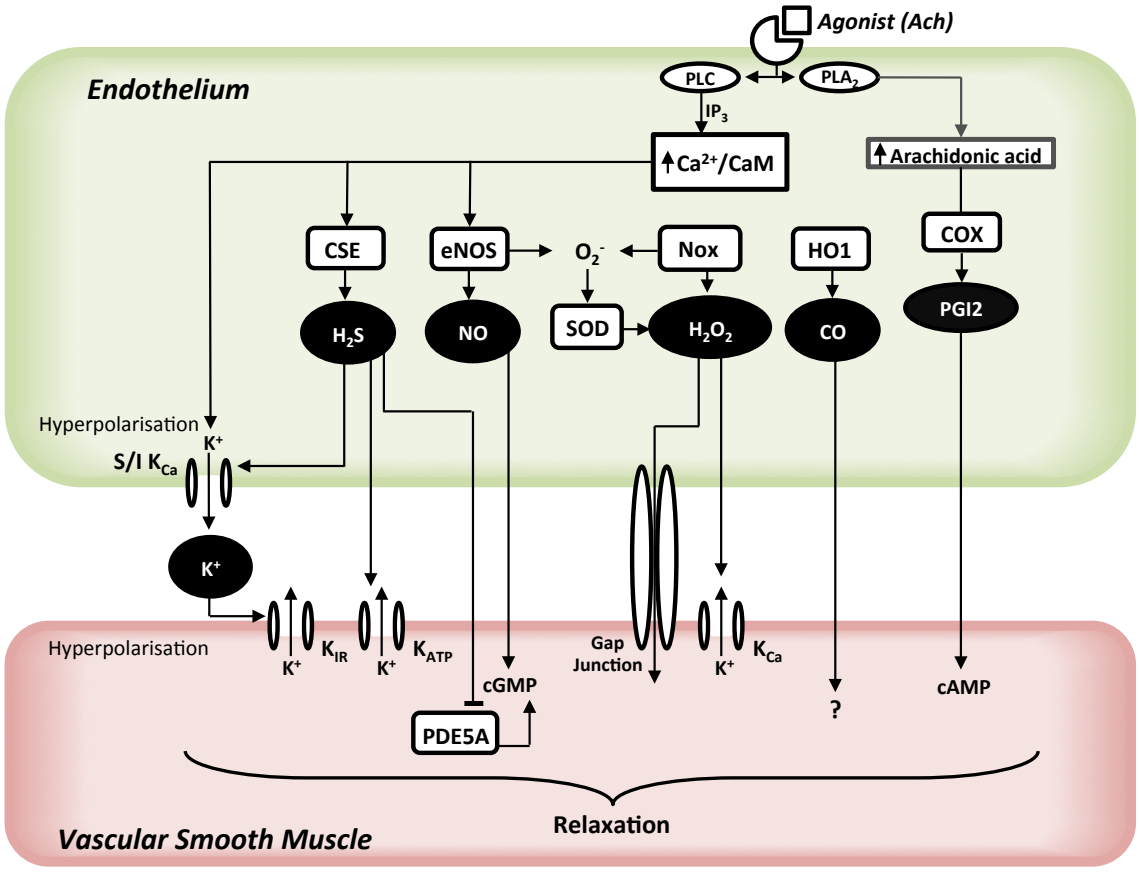

Figure 1.6: **Endothelial-derived Relaxation of Smooth Muscle.** A schematic diagram indicating the various mechanisms of endothelial cell-induced relaxation of VSMCs. The endothelium responds to various agonists by producing a number of signalling molecules (black ovals). These mediators can diffuse through the cell membrane or move through ion channels and gap junctions into adjacent VSMCs where they activate a variety of signalling pathways that culminate in vasodilation.

1.6 Homocysteine

Homocystiene (hcy) is a non-protein forming, sulphur-containing amino acid that has toxic, proinflammatory and prothrombotic effects[84, 85]. It has been positively associated with high blood pressure[86-89] as well as with impaired endothelium-dependent vasodilation and endothelial cell apoptosis[90, 91].

1.6.1 Homocysteine Metabolism

Intracellularly, hcy lies at the intersection between two metabolic pathways: remethylation and transsulfuration. These two pathways form part of a larger metabolic network, with the addition of the folate cycle[85]. Hcy is generated through the demethylation of the essential amino acid methionine. Here, methionine is converted to the universal methyl donor S-adenosylmethionine (SAM) by Methionine adenosyl transferases (MAT1A) and is utilised as a substrate by various methyl transferases and therefore contributes to a number of biologically important methylation reactions. The by-product of these reactions, S-adenosylhomocysteine (SAH) is then hydrolysed to hcy by the enzyme S-adenosylhomocysteine hydrolase (SAHH)[85] Hcy can then enter either the remethylation or transsulfuration pathway. During remethylation hcy acquires a methyl group from N-5-methyltetrahydrofolate (N5-MTHF) in a reaction catalysed by the vitamin B_{12} dependent enzyme, methionine synthase (MS) (Figure 1.7). Alternatively, hcy can enter the transsulfuration pathway, which involves the initial, irreversible conversion of hcy to cystathionine in a condensation reaction with serine catalysed by CBS[92]. Cystathionine is then hydrolysed to cysteine and α-ketobuterate by CSE. Subsequent to this, cysteine can then be anabolised to glutathionine (GSH) in a reaction involving the enzymes γ-glutamyl cysteine ligase and glutathione synthetase[84, 85, 92]. The transsulfuration pathway thus links hcy metabolism to the generation of a major redox buffer within the cell (Figure 1.7).

The dual-functionality of CBS and CSE in mediating both transsulfuration and H_2S biosynthesis is particularly intriguing. Indeed, perturbations in CBS and CSE

activity or expression are involved in hyperhomocysteinemia-induced vascular damage[93]. In recent years, the discovery that both enzymes can use hcy as a substrate to generate H_2S has further enhanced the complex aetiology of hcy related diseases and suggests that H_2S production may be intimately linked to hcy metabolism[94]. Interestingly, CSE is known to have 3 splice variants whose biological significance remains unknown. It is tempting to speculate that these variants may be involved in orchestrating the differential activities of CSE.

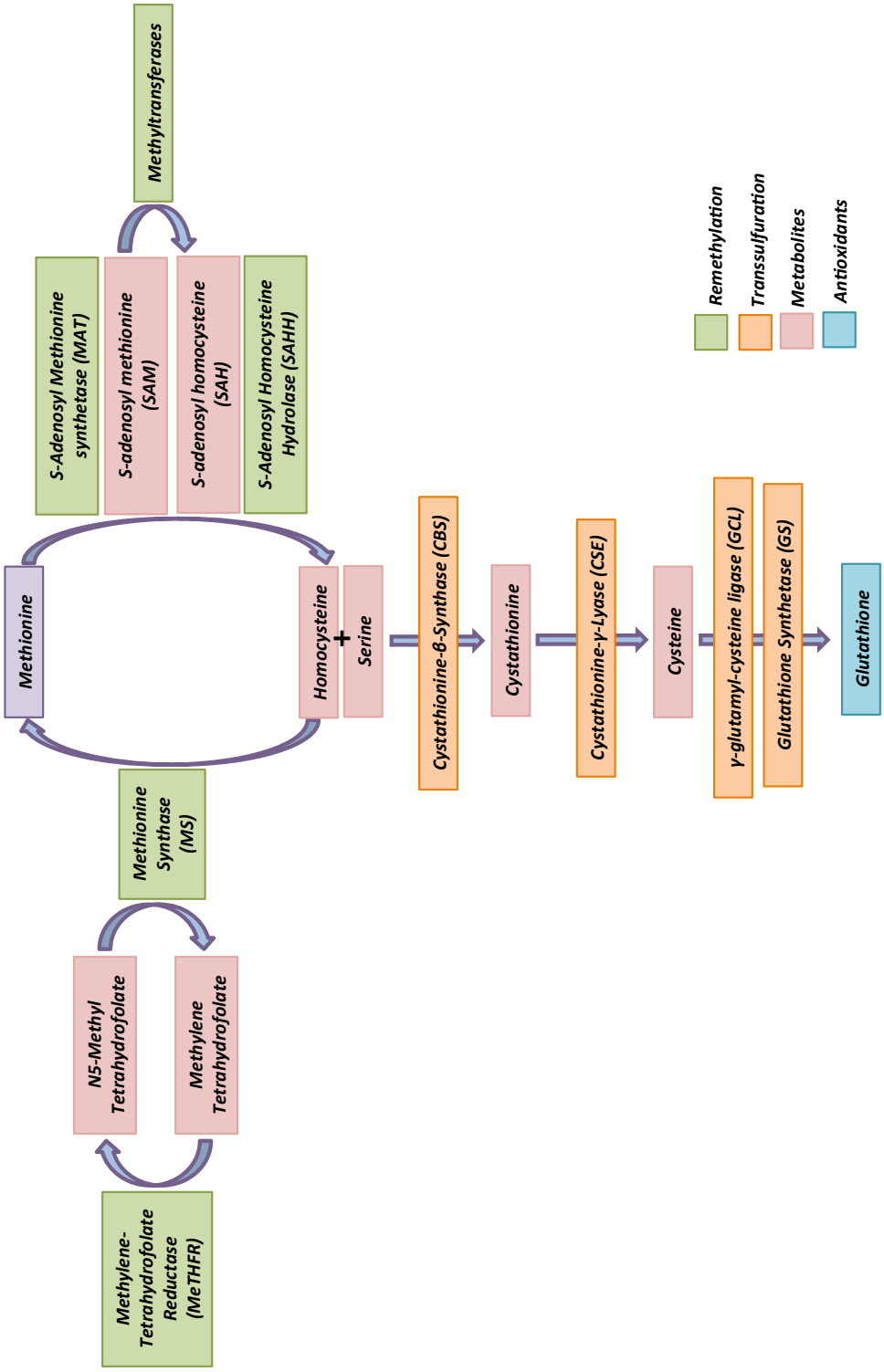

Figure 1.7: Homocysteine Metabolism. A schematic illustration of the metabolic networks involved in hcy metabolism. Hcy is generated from the demethylation of methionine. Once formed hcy can be converted to cysteine via the transsulfuration pathway or converted back to methionine by the remethylation pathway.

1.6.2 Redox Regulation of Transsulfuration and H_2S Production

Although the functions of CBS and CSE in transsulfuration and H_2S production have been characterised, little is known about the regulation of these enzymes at both the transcriptional and post-translational level. However, an emerging body of literature suggests that ROS may be involved in both the partitioning of hcy metabolism and in the regulation of H_2S production as discussed below.

Methionine synthase and CBS appear to be differentially regulated by H_2O_2. Mosharov *et al*[92] demonstrated that H_2O_2 was capable of increasing the flux of hcy through the transsulfuration pathway and suggest that this is because the activity of MS is reduced[95] and CBS is increased[96] in response to redox cues, thereby lowering hcy remethylation and promoting transsulfuration. These data are further supported in a study performed using neuronal cells. Here, the flux of radiolabeled [^{32}S]methionine through the transsulfuration pathway and subsequent incorporation into GSH was measured in the presence and absence of the oxidising agents tert-butylhydroperoxide (tBHP) and H_2O_2. Interestingly, it was shown that oxidants increased the incorporation of [^{32}S] into GSH[97], an effect that was recapitulated in T cells[98]. Collectively, these data suggest that ROS can increase GSH production by enhancing the activity of the transsulfuration pathway.

In addition to the redox regulation of CBS, ROS have also been shown to contribute to the regulation of CSE, primarily at the gene expression level. Studies performed by Wang *et al* show that exogenous H_2O_2 increased the luciferase activity of CSE promoter constructs in COS7 cells, an effect that was recapitulated at the mRNA

and protein level, although it was concluded that the ROS-induced regulation of CSE was complex and biphasic[99]. To further support a role for ROS in the regulation of CSE transcription, it has been suggested that CSE expression is under the control of the redox-driven transcription factor, Nrf2. Here, rat mesangial cells treated with platelet-derived growth factor BB (PDGF) increased Nrf2 activation and translocation to the nucleus, correlating with an up-regulation in CSE expression. This observed increase in CSE expression was abolished in response to the ROS scavenger, N-acetyl cysteine (NAC) and the broad-spectrum NADPH oxidase inhibitor, DPI[100].

In addition to ROS-induced transcriptional changes in CSE expression, ROS signalling can regulate CSE activity. A study published by Lin *et al*, who generated a cell-trappable fluorescent H_2S probe (SF7-AM), interrogated the involvement of CSE and endogenous H_2S production in VEGF-stimulated HUVECs. Here it was demonstrated that VEGF increased CSE-derived H_2S production in a H_2O_2-dependent manner. Moreover, Nox inhibition by DPI reduced H_2S production as measured by a reduction in SF7-AM activity upon VEGF stimulation. The authors concluded that crosstalk between H_2S and H_2O_2 may be an important, novel mechanism involved in angiogenesis[101]. Taken together these data highlight an emerging role for ROS in the modulation of metabolic flux through the transsulfuration pathway and in H_2S biosynthesis *via* both transcriptional and post-translational mechanisms.

1.7 Redox Biology

The evolution of aerobic organisms that utilise oxygen for their energetic needs has led to an extremely large diversification in the forms of life that have subsequently developed. This however, has not been without physiological consequence. An organism's reliance upon mitochondrial function, metabolic flux and turnover as well as protein catalysis results in its exposure to varying concentrations of chemically reactive, potentially deleterious, oxidant molecules broadly defined as ROS[102]. The study of these oxidants and their cellular effects constitutes the growing field of Redox Biology.

Historically, the redox biology field has focused heavily on mitochondrial functionality in adenosine triphosphate (ATP) production and the consequent generation of ROS as potentially detrimental by-products of this process. Indeed, the observation that ROS are generated as metabolic and enzymatic reaction by-products led, in part, to initial ideas surrounding their damaging effects[103]. Support for this comes from extensive evidence demonstrating that perturbations in cellular redox state can be a cause or consequence of various diseases such as cancer, neurodegenerative disorders and cardiovascular disease[104]. In the broad context of cellular biology however, growing evidence indicates that cellular redox status can also regulate various homeostatic aspects of intracellular and extracellular function. Indeed, the last two decades have seen a reversal in the view that ROS are necessarily detrimental to cellular heath and viability[105]. This turnaround perhaps coincided with the characterisation of the Nicotinamide Adenine Dinucleotide Phosphate Oxidase (NAPDH oxidase/Nox) family of proteins

that were found to function solely in the production of ROS[106, 107]. This discovery therefore lent credence to the notion that ROS may be important regulators of evolutionarily-conserved biological processes such as cell signalling and gene expression[108].

As a result of these studies our current understanding of redox biology is therefore complicated and at times contradictory. It is currently known that different ROS or sources of ROS play opposing roles in various settings; some promote deleterious phenotypes whilst others appear to elicit beneficial effects. Deciphering the functions of different ROS in various systems such as the cardiovascular system has therefore been challenging, but many advances have been made in understanding both their physiological roles and mechanistic actions[109].

1.7.1 Reactive Oxygen Species and Redox Signalling

Molecular oxygen is a biradical molecule that is able to accept electrons from multiple sources and ultimately become reduced to H_2O. Partially reduced oxygen species are however highly reactive and these are collectively termed ROS. The various types of ROS that can be formed include; superoxide (O_2^-), H_2O_2 and hydroxyl radicals (·OH) (Figure1.8). In addition, oxygen can react with nitrogen to form Reactive Nitrogen Species (RNS) such as NO.

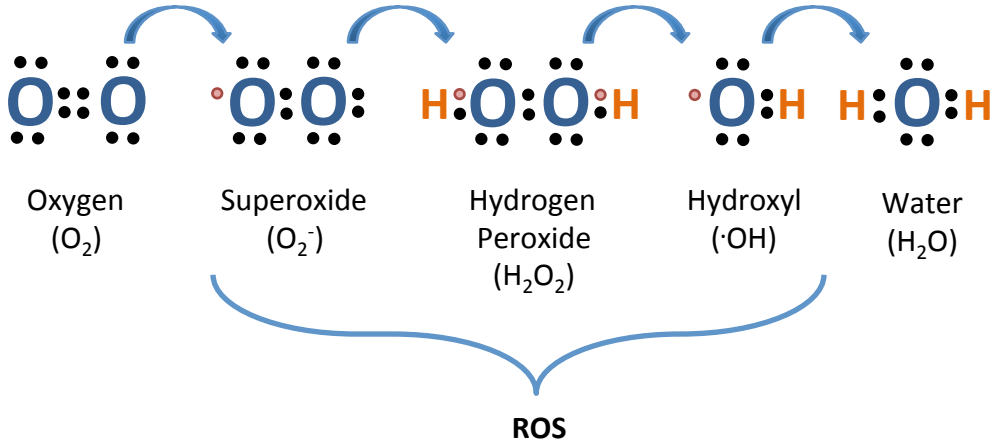

Figure 1.8: **Reactive Oxygen Species**. A diagrammatic illustration depicting the gradual reduction of oxygen, through its sequential gain of electrons, to form water. As oxygen is reduced various ROS are generated in the process including superoxide and hydrogen peroxide.

Early observations that cell signalling pathways could be regulated by ROS led to a multitude of studies aimed at identifying their biochemical and mechanistic roles[109, 110]. ROS are now known to act as secondary messengers in various cell signalling responses termed *redox signalling*. Due to inherent differences in the chemical properties of the differing types of oxidant species, not all ROS are able to function as efficient signalling mediators[111]. Indeed, the half-life and lipid solubility properties of a specific type of ROS are important factors in determining whether it will be an efficient signalling molecule. For example superoxide has a short half-life of 10^{-6} seconds and is membrane impermeable thus limiting its signalling capacity. By contrast, H_2O_2 is more stable and has a relatively long half-life of 10^{-5} seconds. In addition to this it can freely permeate biological membranes allowing relatively long range signalling[105, 111]. Moreover, of the many types of ROS, H_2O_2 has the greatest propensity to modify cysteine thiols on target proteins reversibly permitting signal transmission (as discussed below). Because of these properties,

H_2O_2 is thought to play a particularly important role in mediating redox signalling events[112].

In a similar manner to other cell signalling processes, physiological redox signals are transmitted through the reversible modification of target proteins. The presence of the sulphur-containing amino acids methionine and, especially, cysteine within a peptide sequence are believed to be primarily responsible for transmitting these redox cues[113]. The chemical properties that permit cysteine residues to function as redox sensors within proteins have been widely studied and well characterised. It is now known that ROS cannot mediate the oxidation of all cysteine residues, but specifically target cysteine thiol groups displaying low pKa thiolate anions (S^-). The pKa of a given cysteine thiol is thought to be determined by the microenvironment to which it is placed within a protein, with surrounding basic amino acids tending to deprotonate adjacent thiol groups better than acidic amino acids[105].

A number of different types of ROS-induced, post-translational modifications exist and the nature of these modifications is dependent on multiple factors such as amino acid localisation within a protein and the length of time to which a cysteine thiol is exposed to ROS. These time-dependent, ROS-induced modifications can be seen as a sequential oxidation reaction which proceeds through sulfenic acid (SOH), Sulfinic acid (SO_2H) and Sulfonic acid (SO_3H) states[114] (Figure 1.9). Of these oxidation states, sulfenic acid is the only reversible modification that can be reduced *via* the cell's intrinsic antioxidant systems and is therefore considered to have physiological effects. Sulfinic and sulfonic acid modifications, on the other

hand, occur under high levels of 'oxidative stress' and are irreversible oxidation states termed hyperoxidation[102]. However, in the specific case of sulfinic acid oxidation of peroxiredoxin, this modification can be reversed by the enzyme sulfiredoxin[115, 116]. In addition to these modifications, the localisation of cysteine residues within a proteins' tertiary or quaternary structure can result in ROS-induced covalent intra- and inter-disulphide bond formation that can subsequently elicit a functional change (Figure 1.9)[117, 118].

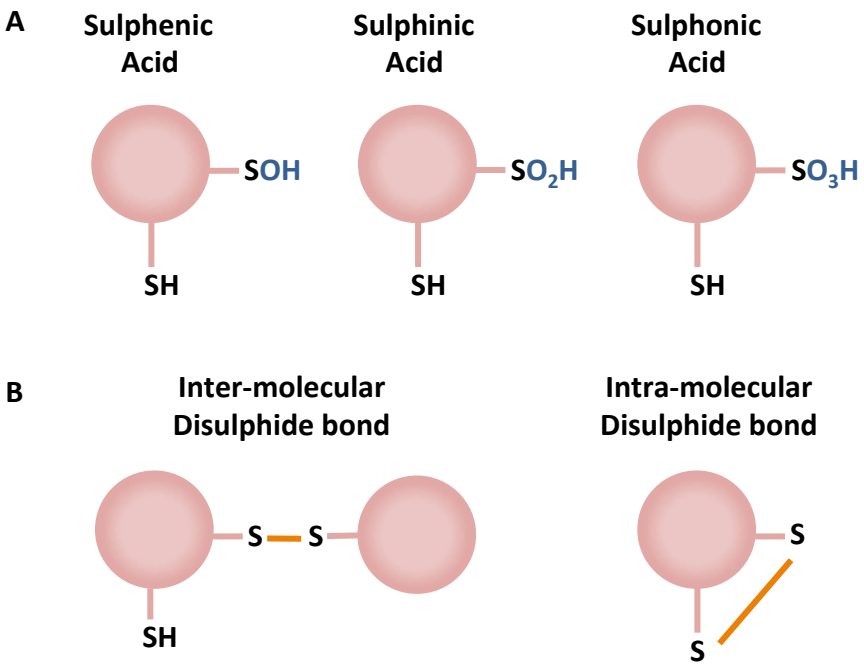

Figure 1.9: **ROS-induced Post-translational Modifications.** A schematic diagram indicating the various ROS induced post-translational modifications of cysteine residues on target proteins. **A)** Progressive oxidation of thiols through sulphenic, sulphinic and sulphonic acid states. **B)** Inter and Intra-disulphide bond formation. These modifications lead to functional changes within a protein.

1.7.2 Antioxidant Systems

The biological effects of ROS are countered by the actions of enzymatic and non-enzymatic antioxidants that collectively form the cellular antioxidant system. Enzymatic antioxidants include; superoxide dismutase (SOD) that converts O_2^- into H_2O_2, thereby removing the potentially damaging O_2^- and promoting the production of H_2O_2-mediated homeostatic signalling. Catalase and glutathione peroxidase (GPx) can subsequently scavenge H_2O_2 [119](Table 1.1).

Enzyme systems	*Reaction*
Superoxide dismutase	$O_2^{\cdot-} + O_2^{\cdot-} \longrightarrow H_2O_2 + O_2$
Catalase	$H_2O_2 + H_2O_2 \longrightarrow 2H_2O + O_2$
Peroxidase	$2GSH + H_2O_2 \longrightarrow GSSG + 2H_2O$

Table 1. 1: Enzymatic antioxidants and the reactions they catalyse.

Non-enzymatic antioxidants include vitamins C and E as well as the major redox buffer glutathione (GSH). GSH is present at millimolar concentrations in the cell and scavenges ROS through the formation of oxidised GSH (GSSG). The ratio of GSSG:GSH can be used as a readout of the intracellular redox state. Indeed, when the cells intrinsic antioxidant system is overwhelmed by excessive ROS production, 'oxidative stress' is induced which manifests in cellular damage and disease[103] [111](Figure 1.10).

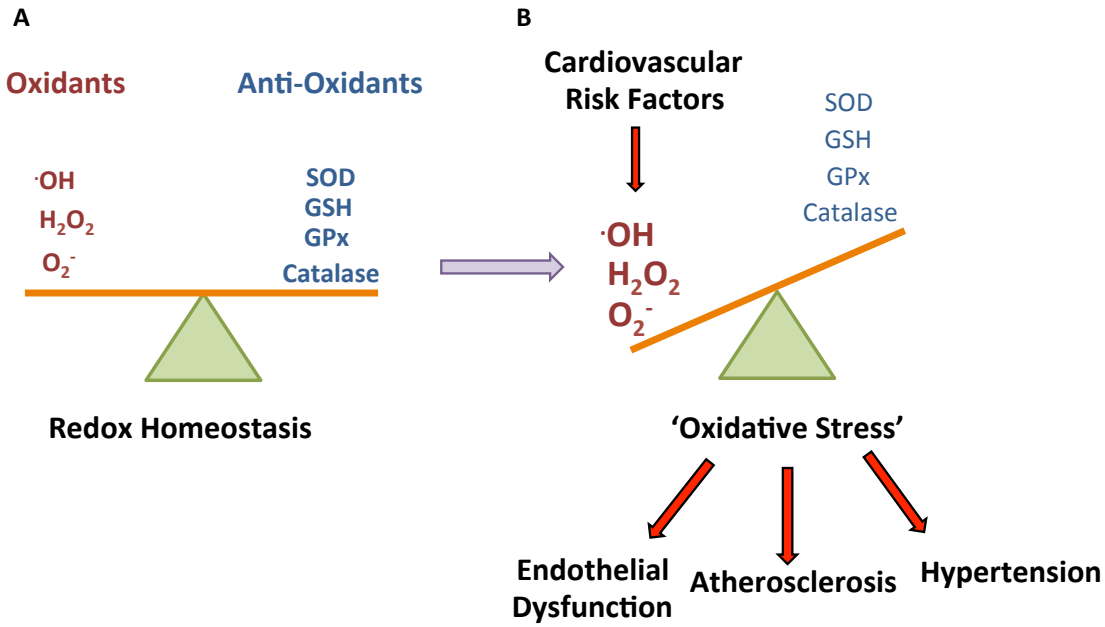

Figure 1.10: Vascular Oxidant and Antioxidant Production. A) normal physiological homeostasis maintains a balance between pro-oxidants and antioxidants. **B)** Cardiovascular risk factors such as smoking and elevated homocysteine increase ROS production and subsequently tip the balance between oxidants and antioxidants in favour of ROS. This results in 'oxidative stress' and vascular disease.

1.8 Endothelial Sources of ROS

ROS are derived from a number of sources within the endothelium. The mitochondria are organelles that generate energy in the form of ATP from aerobic metabolism by the electron transport chain. This process involves the shuttling of electrons through 4 protein complexes in order to generate a proton gradient across the mitochondrial inner membrane. Uncoupling of these complexes can lead to electron leakage and subsequent non-regulated O_2^- generation. Furthermore, mitochondrial SOD can convert O_2^- into H_2O_2 which can collectively contribute to oxidative stress and redox signalling[120]. Another source of vascular ROS comes

from endothelial Xanthine oxidases that convert hypoxanthine to xanthine and then to uric acid in a process that generates O_2^- and H_2O_2[121]. As mentioned previously eNOS is an enzyme that utilises L-arginine as a substrate for NO generation *via* electron transfer from NADPH. Uncoupling of eNOS due to low levels of L-arginine or reduced bioavailability of the eNOS co-factor BH4 results in electron transfer to O_2 instead of L-arginine and subsequent O_2^- formation[32]. In general, ROS derived from these processes are thought to be a result of mis-regulated metabolic functions. By contrast, Nox family enzymes generate ROS as their sole biological function, an observation that suggests that ROS may play a physiological role[122] (Figure 1.11).

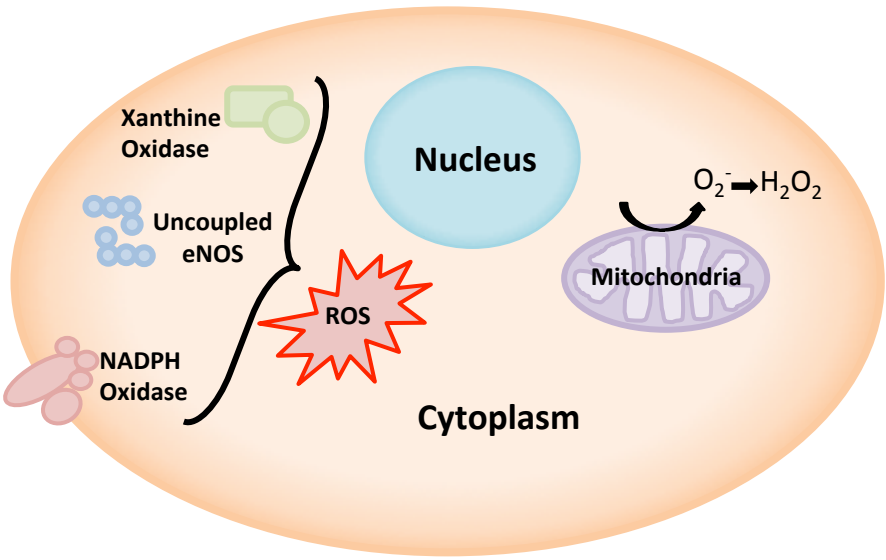

Figure 1.11: ROS Sources. A schematic diagram depicting the sources of ROS found in the endothelium. Uncoupled electron transport in the mitochondria as well as uncoupling of eNOS subunits and xanthine oxidase leads to non-specific ROS production. By contrast, Nox derived ROS is thought to be generated physiologically and contributes to cellular signalling responses.

1.9 NADPH Oxidases

In humans, NADPH oxidases comprise a family of 7 multi-subunit transmembrane proteins (Nox1-5 and duox 1 and 2) whose primary role is to synthesise ROS within the cell[107, 122]. Each family member is composed of a common catalytic Nox subunit that consists of at least 6 transmembrane alpha helicies and, with the exception of Nox5 and duox1/2, all isoforms associate with the transmembrane protein, $p22^{phox}$. Functionally, the Nox subunit shuttles electrons from NADPH down an electrochemical gradient across a membrane to molecular oxygen (O_2) in a process involving one C-terminal flavin adenine dinucleotide (FAD group) and two haem groups[106, 123]. Oxygen is subsequently reduced to O_2^- while NADPH is oxidised to $NADP^+$ and H^+. Newly-generated ROS can then be utilised by the cell in order to propagate a plethora of tightly-controlled, intracellular, homeostatic, redox signalling responses [107, 122, 124].

Although all Nox isoforms contain an integral Nox subunit, that functions similarly at the biochemical level, studies have demonstrated that each family member is associated with a number of different regulatory proteins that are required for the fine-tuning of ROS generation. For example, the prototypical Nox protein, Nox2 which was first discovered in phagocytic immune cells, associates with transmembrane $p22^{phox}$, cytosolic $p40^{phox}$, $p47^{phox}$, $p67^{phox}$ as well as the monomeric GTPase, Rac and the assembly of all these components is responsible for the Nox2 induced 'respiratory burst' seen in immune cells[107]. By contrast, Nox4 has been reported to associate only with transmembrane $p22^{phox}$, although more recently, a novel association between Nox4 and polymerase δ–interacting protein

2 (Poldip2) has been described in VSMCs where it is thought to increase Nox4 activity (Figure 1.12)[125, 126].

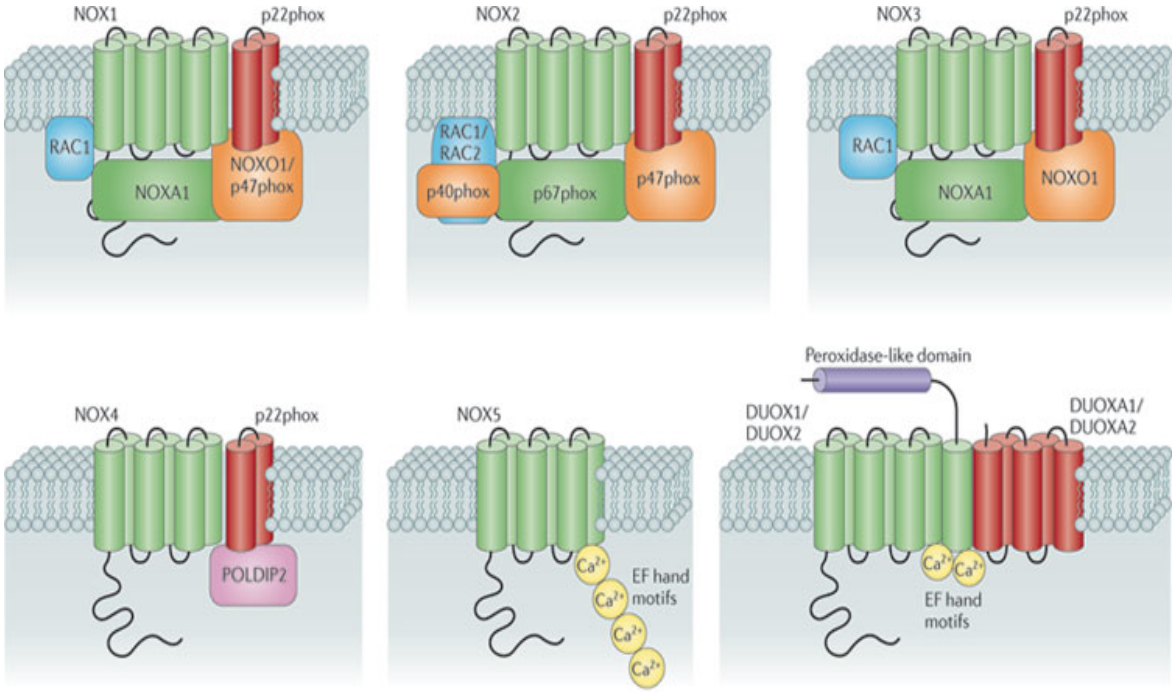

Figure 1.12: **NADPH Oxidase Family.** A schematic representation of each Nox isoform and their associated subunits. Nox2 associates with a number of cytosolic regulatory subunits including $p40^{phox}$, $p47^{phox}$, $p67^{phox}$, whereas Nox4 primarily only associates with the membrane protein $p22^{phox}$. From: Nature reviews Drug Discovery[127].

In addition to these differences in molecular structure, each Nox isoform displays distinct tissue- and developmental-stage specific patterns of expression, different subcellular locations and markedly different mechanisms of activation. Nox2 protein is found in a number of cell types including phagocytic immune cells[128] to cardiomyocytes, SMCs and endothelial cells[122, 129]. It is expressed primarily at the plasma membrane and has been shown to be regulated by agonist-induced post-translational modifications such as phosphorylation[130]. By contrast, Nox4 is

located in VSMC as well as in the endothelium. Subcellularly, Nox4 has been shown to occupy the endoplasmic reticulum (ER) of VSMCs[130, 131], as well as the nucleus and ER of HUVECs[129 132]. It is currently believed that Nox4 is a stress-inducible protein whose activity is regulated at least in part at the gene expression level[133]. Its transcriptional regulation is thus considered to be the primary determinant of its ROS-generating capacity[107, 133] and as a consequence its expression and activity are under highly-regulated and cell-type specific control[107]. More recently, it has been demonstrated that the activity of Nox4 may also be regulated post-translationally by phosphorylation[134], suggesting that the regulation of Nox4 occurs at multiple levels and *via* various mechanisms.

Finally, the type of ROS associated with each Nox isoform is also thought to differ. Whilst all Nox proteins make O_2^-, some Noxs (such as Nox4 and duox1/2) produce O_2^- that is very rapidly converted to H_2O_2. The exact mechanism through which Nox4 achieves this is still unclear although some studies suggest that the E loop of Nox4 may be involved in mediating an intrinsic superoxide dismutase activity[107, 122, 135]. Taken together, these differences in structure, activity, expression, regulation and the type of ROS produced may indicate that each Nox protein possesses its own distinct and defined functions [129, 130, 136].

1.9.1 Endothelial NADPH Oxidases

Nox proteins are expressed in a cell type-specific manner and in the endothelium, 4 Nox isoforms have been shown to be present; Nox1, Nox2, Nox4 and Nox5[137].

The importance of these enzymes in vascular patho(physiology) is potentially indicated by the changes in their gene expression patterns that occur during disease. Thus, in general, Nox1 and Nox2 expression levels increase during disease, and loss-of-function studies have shown that removal of these Noxs tends to elicit beneficial effects in certain pathophysiological settings[127]. Apolipoprotein–E-deficient mice ($ApoE^{-/-}$) are often used as a model of atherosclerosis and these mice display endothelial dysfunction with associated reductions in NO bioavailability. Interestingly, ablation of ApoE in a $P47^{Phox}$ null background resulted in protection from lesion development. This suggests that the presence of Nox isoforms that associate with $P47^{Phox}$ in order to function, such as Nox2, may exacerbate the development of atherosclerosis[138, 139]. Another model of vascular disease with a strong endothelial component is hypertension. Ang II is a major inducer of hypertension and as such is used routinely to model this disease. Indeed Nox1- and Nox2-derived O_2^- is thought to inactivate NO and enhance hypertension[140-143] and vascular dysfunction in angiotensin II-induced stress[144]. Interestingly, AngII treatment up-regulates Nox2 expression and activity in the endothelium[145] and the targeted overexpression of Nox2 increases blood pressure[146]. Furthermore Nox1 null mice display a reduced blood pressure phenotype compared to WT littermates[147]. Taken together these data suggest that, while Nox1 and Nox2 have important physiological functions, their mis-expression may promote perturbations in vascular function during disease.

1.9.2 Endothelial Nox4 and Vaso-protection

Nox4 is expressed in a number of vascular cell types and a diverse range of molecular and physiological effects have been attributed to its vascular expression[148, 149]. Interestingly, unlike Nox1 and Nox2, Nox4 expression is considered to positively regulate vascular homeostasis[47 150, 151]. Indeed, Nox4 is abundantly expressed in the endothelium and it is thought that this may underscore an important functional role for it in the vasculature[129, 149 152]. Thus, endothelial Nox4 has been shown to participate in the regulation of vascular tone in multiple models and, as stated previously, endothelial-specific Nox4-overexpressing transgenic mice show improved endothelial function, vasodilation and lower blood pressure when compared to WT controls[47]. Furthermore, a recent study using Nox4-null mice demonstrated that the ablation of Nox4 expression reduced the activity of eNOS and perturbed NO formation[151]. These data may be consistent with the observation that H_2O_2 can regulate aortic relaxation in an eNOS-dependent manner[153].

In addition to regulating vascular tone, the endothelium also orchestrates key aspects of angiogenesis. Here, endothelial-specific Nox4-overexpression has been shown to increase angiogenesis in the ischemic hind limb of mice[150], while conversely, studies in Nox4-null mice revealed that Nox4 expression is required to support exercise-induced angiogenesis[154]. Moreover, blood flow recovery after femoral artery ligation was significantly blunted in Nox4-null animals, an effect that was attributed to worsened endothelial cell-mediated angiogenesis in

matrigel plug assays[151]. Collectively these data suggest that endothelial Nox4 is a constitutive generator of H_2O_2 that positively affects vascular function.

1.10 Summary

To summarise, the endothelium can be considered as a multifaceted 'organ system' that orchestrates a number of physiological vascular processes. In order to achieve this, it has evolved to produce (and respond to) a range of signalling mediators. Of these, NO elicits vascular protection on a number of levels including the modulation of vascular tone, inflammation and thrombosis. In recent years it has become apparent that other gasotransmitter family members such as CO and most notably H_2S, also regulate similar processes and therefore represent novel potential therapeutic targets. Endothelial Nox4 has also been implicated in the modulation of vasodilation and it is becoming apparent that ROS may be important physiological regulators of gasotransmitter signalling. Indeed the regulation of H_2S generation by ROS is emerging as a novel research area that may yield important new insights into the (patho)physiological actions of gasotransmitters.

1.11 Hypothesis

I hypothesise that Nox4 may act as a physiological source of ROS that functions in the regulation of H_2S production and/or hcy metabolism by enhancing CSE activity and/or expression in the endothelium.

Chapter 2: Materials and Methods

2.1 Introduction

This chapter details the general methods that were employed in this thesis.

2.2 Reagents

All the reagents used in this thesis were ordered from Sigma Aldrich unless otherwise stated in the relevant section.

2.3 Cell Culture

Standard tissue culture techniques were implemented for culturing, expanding and freezing down cells. Pooled Human Umbilical Veins Endothelial Cells (HUVECs) (Lonza) were seeded and cultured in pre-coated (0.4% gelatin in PBS for 1 hour at 37°C) T75 tissue culture flasks, 6-cm dishes (seeding density $1x10^6$ cells/well), 24-well (seeding density $1x10^5$ cells/well) or 96-well (seeding density $1x10^4$ cells/well) plates and grown in EBM-2 HUVECs media (Lonza). Human Embryonic Kidney cells (HEK293) were grown in T175 flasks or 24-well plates in DMEM D6546 media supplemented with 10% Foetal Bovine Serum and 1% Penstrep/Glutamine. Both cell lines were grown in a humidified 37°C incubator in 5% CO_2. HUVECs were always used at passage 8.

2.4 Quantification of gene expression

2.4.1 RNA isolation.

RNA was extracted from HUVECs using the SV total RNA isolation kit (Promega). In brief, HUVECs were scraped into 200 µl of SV RNA lysis buffer before being spun through Qiashredder columns (Qiagen) at 13,000 rpm for one minute. RNA was isolated according to the manufacturer's specifications (Promega) with the addition of 1 µl of RNase-free DNase (Promega) at the DNase incubation step. The resultant RNA was eluted into 100µl nuclease-free water and placed in a lyophiliser for 40minutes to concentrate the RNA. RNA was re-suspended in 20 µl nuclease-free water before being quantified using a NanoDrop spectrophotometer (ND-1000, Labtech International).

2.4.2 Reverse Transcription – QPCR

Reverse transcription polymerase chain reaction (RT-PCR) is a process used in order to amplify single-stranded cDNA copies of an RNA template. Here, RNA isolates are converted enzymatically to single-stranded cDNA molecules by hybridising oligodeoxythymine primers (Oligo(dT)) to the polyadenine (Poly(A)) tail of mRNA templates before extending the cDNA using the RNA-dependent DNA polymerase, Reverse Transcriptase.

2.4.3 cDNA Synthesis

To prepare cDNA, 13 µl of isolated RNA (500 ng - 1 µg) was incubated with 1 µl of Oligo(dT)$_{18}$ primers (1 µg final) and 1 µl dNTPs (5 mM final concentration) at 70°C for 3 minutes in order to disrupt any secondary structure present within the RNA. The RNA was then incubated briefly on ice before the addition of 4 µl of 5X Murine Leukaemia virus (MLV) RT buffer (Promega), 0.5 µl of the RNase inhibitor, RNasin (Promega) and 0.5 µl Reverse Transcriptase RT- MLV enzyme (Promega) to give a final volume of 20 µl. Samples were incubated at 42°C for 90 minutes and then heated to 70°C for 10 minutes before the addition of 80 µl nuclease-free water. Negative controls comprising equivalent amounts of RNA were also prepared in the absence of reverse transcriptase (-RT). Both the cDNA and –RT reaction products were stored at -20 °C.

2.4.4 Quantitative Real-time (QPCR)

Quantitative real-time PCR (QPCR) was implemented in order to quantify relative levels of mRNA expression. The process relies on the detection of fluorescence emitted by a fluorescent probe that increases proportionally to the amount of cDNA amplicons present at any one time. The cDNA generated by reverse transcription was amplified using fluorescent SYBR Green PCR technology (Applied Biosystems) with gene-specific primers (detailed in Table 2.1 and 2.3) on the Applied Biosystems StepOnePlus™ Real Time PCR detection system. Each reaction was made up as follows; 12.5 µl Power SYBR® Green PCR master mix

(2X) (Applied Biosystems), 2.5 µl of 9 µM gene-specific forward primer, 2.5 µl of 9 µM gene-specific reverse primer, 5.5 µl of water and 2 µl of cDNA or –RT control.

Quantification of mRNA expression levels was determined using a plot of log fluorescence against cycle number. Here, a fixed fluorescence threshold or cycle threshold (C_t) was set in the linear phase of the observed exponential increase in the target PCR product. The C_t was thus determined as the cycle number at which fluorescence crosses the threshold. Relative mRNA expression was then quantified using the comparative Ct ($\Delta\Delta C_t$) method (equation shown below). Here, the target gene or gene of interest was normalised to a standard housekeeping gene (cytoskeletal β Actin unless otherwise stated) and this change was subsequently normalised to the C_t level of a calibrator or control sample. The specificity of each PCR product was determined by analysing the melt curve produced at the end of each QPCR reaction where a single melt curve indicated a single product, therefore validating the analysis.

$$(\Delta\Delta C_t)=(Ct_{\text{target(unknown sample)}}-Ct_{\text{standard(unknown sample)}})-(Ct_{\text{target(calibrator sample)}}-Ct_{\text{standard(calibrator sample)}})$$

2.5 SDS PAGE (Immunoblotting)

Sodium dodecyl sulfate polyacrylamide gel electrophoresis (SDS PAGE)/immunoblotting is a technique used to analyse the expression of proteins on a polyacrylamide gel and relies on the separation of these proteins according to molecular weight.

2.5.1 Sample Preparation

Protein was extracted from HUVECs by scraping cells into 1.5 mls of ice cold phosphate buffered saline (PBS). Cell suspensions were centrifuged at 0.4 rcf for 5 minutes at 4°C and then spun at maximum speed for 10 seconds to obtain a cell pellet. PBS was removed and cell pellets were re-suspended in 60 µl of protein lysis buffer (2 mM EGTA, 5 mM EDTA, 30 mM sodium fluoride, 40 mM β-glycerophosphate, 20 mM sodium pyrophosphate, 1 mM sodium orthovanadate, 1 mM phyenylmethylsulfonyl – fluoride, 3 mM benzamidine, 5 µM pepstatin A and 10 µM leupeptin in 25 mM Tris-HCL buffer; pH 7.2) supplemented with protease inhibitor cocktail (5 µl/ml).

Protein concentration was determined using a Bradford assay (Bio-Rad). This assay involves a change in absorbance of a Coomassie dye (Coomassie Brilliant Blue G-250) upon protein binding. The absorbance increases proportionally to the amount of protein bound to the dye. To perform the assay, a standard curve was made using increasing concentrations of bovine serum albumen (BSA) (0-50 µg/ml) supplemented with 2 µl of lysis buffer/well (since the Bradford reagent is sensitive to detergents in the lysis buffer) in a total of 200 µl/well of Bradford reagent. 2 µl of protein sample of unknown concentration was then added to 198 µl Brandford reagent in triplicate wells. The plate was incubated in the dark for 5 minutes to allow the reaction to proceed and then read on a microplate reader (GENios pro; Tecan) at a wavelength of 595 nm. The protein content of the samples was deduced from the BSA standard curve. 50 µl of HUVEC lysates were then added to 12.5 µl 5X Laemmli buffer (20% glycerol, 4% SDS in 250 mM Tris-HCL

with 10% β-mercaptoethanol) and boiled for 5 minutes to denature the proteins. Where possible, samples to be blotted for Nox4 alone were not boiled but rather added to 12.5 µl 5X Laemmli buffer containing 1 mM Tris(2-carboxyethyl)phosphine hydrochloride (TCEP) and left for 15 minutes at room temperature. Samples were then made up to a concentration of 15-25 µg/30 µl by dilution in 1X Lemelli buffer and stored at -80°C.

2.5.2 Blotting

10% resolving gels were cast and then topped with a stacking gel (See Table 2.7 for volumes and reagents used for gel casting). 15-25 µg of protein was loaded into each well alongside 6 µl of molecular weight marker (PageRuler™) and electrophoresed in running buffer (25 mM Tris-base, 192 mM glycine, 0.1% SDS) at 120V for 10 minutes to ensure proteins migrate evenly through the stacking gel before the voltage was increased to 200V until the dye front reached the bottom of the resolving gel. Wet transfer onto nitrocellulose membranes was performed at 100V for 70 minutes in transfer buffer (25 mM Tris-base, 192 mM glycine, 10% methanol). Membranes were subsequently stained with Ponceau S red to check for efficient transfer and loading before being washed in 0.1% PBS-Tween-20 (PBST) or Tris-buffered salt solution containing 0.1% Tween-20 for phosphoblots (TBST) and blocked for 3 hours with 10% milk powder (Marvel Original) in 0.1% PBST or TBST. Membranes were then probed using primary antibodies diluted in 10% milk powder overnight at 4°C. Membranes were then washed 3 times for 20 minutes in PBST/TBST and incubated at room temperature with a secondary horseradish

peroxidase-HRP conjugated antibody diluted in 10% milk powder for 2 hours (primary and secondary antibody information is indicated in Tables 2.8 and 2.9 respectively). This was followed by enhanced chemiluminescence (ECL) detection and development of blots onto autoradiographic film (GE healthcare). Membranes were reused to re-probe for other protein targets by washing for 5 minutes in PBST/TBST before the application of 6 ml Stripping buffer (Thermoscientific) for 15 minutes. Membranes were blocked in 10% milk for 30 minutes before incubation with the next primary antibody. Densitometry was performed on each sample band using the ImageJ image analysis program.

2.6 PCR

PCR reactions were set up as follows; 2 µl cDNA, 1 µl (9 µM) forward primer, 1 µl (9µM) reverse primer (primer details in Table 2.5), 12.5 µl REDTaq® ReadyMix™, 33.5 µl H_2O. PCR reactions were run as follows; 35 cycles of denaturation (30 seconds at 94 °C), annealing (30 seconds at 56 °C) and extension (30 seconds at 72 °C). Resultant PCR products were separated at a constant voltage by electrophoresis on a 1% agarose gel containing ethidium bromide (400 ng/ml) in 1xTAE buffer (40 mM Tris-acetate and 1 mM EDTA) and then visualized under ultraviolet light. A 100bp ladder (Hpa II digest of pBluescript II SK+) was also run in order to identify DNA bands according to size. To distinguish between CSE variant 2 and 3, DNA bands were excised from the gel and purified using the Qiagen gel extraction kit and resultant DNA sent for sequencing by Source Biosciences.

2.7 Adenoviral-mediated Nox4 Overexpression

HUVECs were transduced with either an adenoviral β-Galactosidase overexpressing control viral vector (AdBGal) or an adenoviral mouse Nox4 overexpressing viral vector (AdNox4) (both generated in-house) using a multiplicity of infection (MOI) of 5, 10 or 20 for AdNox4 or 10 and 20 for AdBGal. Each virus was diluted to its respective MOI (20 for most experiments) in Optimem (Invitrogen) and 2 ml of this solution were applied to cells. Cells were placed in a 37°C incubator for 5 hours after which the virus and Optimem were removed and replaced with 4 ml of EBM-2 HUVEC media and incubated for a further 19 or 43 hours (as indicated) or for Nox4 time-course experiments, cells were incubated in media for a further 1, 7 or 19 hours after transduction and then harvested for RNA or protein.

2.8 PEG-Catalase with Nox4 Overexpression

HUVECs were treated for 24 hours with either 500 units/ml of Catalase–polyethylene glycol (PEG-catalase) or vehicle control (H_2O) diluted in EMB-2 HUVEC media. Following this, cells were transduced at an MOI of 20 with either AdBGal or AdNox4 as described in section 2.7. Optimem was supplemented with either 500 units/ml of PEG-catalase or vehicle control (H_2O). Cells were then placed in a 37°C incubator for 5 hours after which Optimem was removed and replaced with 4 ml of EBM-2 HUVEC media supplemented with a further 500

units/ml of PEG-catalase or vehicle control and incubated for 19 hours before harvesting for RNA.

2.9 DPI Treatment with Nox4 Overexpression

HUVECs were transduced at an MOI of 20 with either an AdBGal or AdNox4 as described in section 2.7. Cells were then placed in a 37°C incubator for 5 hours after which Optimem was removed and replaced with 4 ml of EBM-2 HUVEC media supplemented with 10 μM DPI or equal volumes of vehicle control (DMSO) and incubated at 37°C for 19 hours before harvesting for RNA.

2.10 ATF4 Overexpression

HUVECs were transiently transfected with PCDNA3.1 expression vectors containing no ectopic cDNA (PCDNA3.1) or ATF4 cDNA (pATF4) (Addgene). Transfections were carried out using the Turbofect transfection reagent kit following the manufacturer's-specifications (Thermoscientific). In brief, 4 μg/well of each plasmid construct (PCDNA3.1 control or pATF4) was added to EBM-2 HUVEC media containing 6 μl/well Turbofect reagent and incubated at room temperature (RT) for 20 minutes whilst complexes formed. After which 4 ml of the Turbofect/plasmid complexes were added to each well and incubated for 24 hours before being harvested for either RNA or protein.

2.11 siRNA Transfections

HUVECs were serum starved for 1 hour in 2 ml of Optimem before being transfected with targeted siRNA (Table 2.10) or an equivalent concentration of control scrambled siRNA (all siRNA from Ambion Silencer Selects). Transfections were performed using the Lipofectamine 2000® Transfection Reagent kit (Invitrogen) according to the manufacturer's-specifications. In brief, scrambled control or targeted siRNA were first diluted to the relevant concentration (as indicated in Table 2.10) in Optimem and incubated at RT for 5 minutes. In a separate tube, Lipofectamine 2000® reagent was mixed at a 1 in 100 dilution with Optimem and allowed to incubate at RT for 5 minutes. Following this, the Lipofectamine mix was added at a 1:1 ratio to the siRNA Optimem mixes and vortexed 3 times. Lipofectamine/siRNA mixtures were incubated at RT for 30 minutes whilst lipid/siRNA complexes formed. 2 ml of each lipid/siRNA mixture were applied to the designated wells of HUVECs and incubated for 5 hours. Optimem was then removed and replaced with 4 ml EGM-2 HUVEC culture medium and cells were placed back into the incubator for a further 19 or 43 hours (as indicated) before harvesting for RNA or protein.

2.12 Transcription Factor and eIF2α Kinase Silencing with Nox4 Overexpression

HUVECs were serum starved for 1 hour in 2mls of Optimem before being transfected with 20 nM targeted siRNA designed against the transcription factors,

SP1, NRF2 and ATF4, or the eIF2α kinases, PERK and HRI, (Table 2.10). Scrambled siRNA were used as controls. Transfections were performed using the Lipofectamine 2000® Transfection Reagent kit as detailed in section 2.11. Cells were then transduced at an MOI of 20 with either AdBGal or AdNox4 as detailed in section 2.7 before harvesting for RNA or protein.

2.13 Hydrogen Peroxide and Tert-butylhydroperoxide Treatment

HUVECs were treated with increasing concentrations of either H_2O_2 or tert-butylhydroperoxide (tBHP). H_2O_2/tBHP were diluted in EBM-2 HUVEC culture media to give final concentrations of 1 μM, 10 μM, and 100 μM. Control wells were treated with water (for H_2O_2) or decane (for tBHP). Cells were incubated for 24 hours and then harvested for RNA.

2.14 Methionine/Cysteine Limitation and Glutathione Assays

HUVECs were seeded into opaque-white 96-well plates and incubated with control medium containing cysteine and methionine (DMEM-11995) (Invitrogen), or medium depleted in cysteine and methionine (DMEM-21013-024) (Invitrogen). DMEM-21013-024 was supplemented with filter-sterilized 584 mg/ml Glutamine and 110 mg/ml Sodium Pyruvate (made up in sterile H_2O) to match the components of control DMEM-11995 media. For experiments involving methionine and N-acetyl cysteine (NAC) repletion, DMEM-21013-024 media was supplemented with increasing concentrations of methionine or 0.063 mg/ml NAC

before being filter-sterilized. Cells were incubated with their respective media for 24 hours or for 4 and 6 hours (for time-course experiments). Total glutathione levels were assayed using the Promega GSH/GSSG-Glo™ Assay kit following the manufacturer's guidelines. Total GSH was determined by adding the reducing agent TCEP (1 mM final concentration) to the reaction mix. Plates were read on a luminometer.

2.15 Methylene Blue Assay

HUVECs were transduced at an MOI of 20 with either AdBGal or AdNox4 (as described in section 2.7) and incubated for 48 hours before performing the methylene blue assay. The conventional methylene blue assay protocol is detailed by Zhu *et al*[155]. In brief, 75 µl of tissue culture media was added to 250 µl 1% (weight/volume stock) zinc acetate and 425 µl distilled H_2O. This was then combined with 133 µl of a 20 mM N, N-dimethyl-p-phenylenediamine stock (Stock made up in 7.2 M HCl) and 133 µl of a 30 mM Iron 3 Chloride (FeCl3) stock (stock made up in 1.2 mM HCl) in a glass vial. The reaction was incubated for 10 minutes at room temperature before the addition of 250 µl of a 10% stock of trichloracetic acid (TCA). 200 µl of the reaction was transferred to a clear-bottom 96-well plate and the absorbance was measured at 670 nm on a plate reader (TECAN).

2.16 Cloning CSE Promoter Constructs

A deletion series of luciferase reporter plasmid constructs containing different sized fragments of the human CSE promoter as well as a construct containing a CSE intronic enhancer (IE) element were generated as described below (IE construct (-*764bp-luc-IE)* was generated in house by Dr. Thomas Murray).

The Pac clone RP11-42O15, which comprises the human CSE locus, was obtained from the BACPAC Resources Center, CHORI. Using this as a template, genomic CSE promoter fragments were generated by PCR using Herculase II Fusion DNA Polymerase (Stratagene). The forward primers (6414F and 764F) incorporated a KpnI restriction site within their 5′ ends, while the common reverse primer (+191R) incorporated an XhoI restriction site. After restriction digestion with KpnI and XhoI, the fragments were subcloned into the KpnI-XhoI cloning sites of the promoterless luciferase reporter vector, pGL4.22 (Promega), to generate -*6414bp-luc* and -*764bp-luc*. To generate the 2.4kb intronic enhancer fragment, the same Pac clone was used as a template for PCR using the primers, CSE Int Enh F/R, which both had BamHI sites incorporated into their 5' ends. After digestion with BamHI, this fragment was inserted into the unique BamHI site, downstream of the SV40 late poly (A) signal in -*764bp-luc*, to generate -*764bp-luc-IE* (primer details are given in Table 2.4), all constructs were sequence-verified by Source Biosciences.

2.17 Reporter Assays

2.17.1 ATF4 Overexpression

HEK293 cells were seeded into 24-well plates at a density of $1x10^5$ cells/well and transfections performed as follows; 400 ng of firefly luciferase construct (*-764bp-luc, -6415-luc or -764bp-luc-IE*), 200 ng pRL-TK cotransfected reference plasmid and 400 ng of either ATF4 overexpression plasmid or PCDNA3.1 control plasmid were added to 100 µl of Optimem containing 2 µl Turbofect reagent. This was incubated for 20 minutes at room temperature to allow DNA/Turbofect complexes to form. 100 µl of each transfection mixture was added to each well and then topped up to 1 ml using DMEM D6546 media and incubated for 24 hours before reporter assays were performed.

2.17.2 Reporter Assay

Luciferase reporter assays were performed using the Dual-Glo® Luciferase Assay System (Promega) following the manufacturer's-specifications. In brief, cell culture media was removed from each well of a 24-well plate and 75 µl of PBS was subsequently added to the cells. 75 µl of Dual-Glo® Luciferase reagent was then added and the plate left to incubate at RT in the dark on a rocker for 15 minutes. 140 µl of the PBS/Dual-Glo mix was transferred to an opaque-white 96-well plate and then read in a luminometer for Firefly activity. 70 µl of Dual-Glo® Stop and Glo

reagent was added to each well and the plate placed back on a rocker at RT for 15 minutes. The plate was then read for Renilla expression on a luminometer.

2.18 Chromatin Immunoprecipitation

ChIP assays were performed by Dr. Alison Brewer using the SimpleChIP enzymatic Chromatin Immunoprecipitation kit (Magnetic beads: Cell signalling). In brief, T175 tissue culture flasks containing approximately $4x10^7$ HEK293 cells were transfected with 25 µg total DNA, with 50µl lipofectamine 2000 reagent. The DNA comprised 12.5 µg *-764bp-luc-IE* and either 12.5 µg PCDNA3.1 or pATF4 (Addgene). Cells were incubated overnight in DMEM D6546 media before crosslinking with 675 µl of 37% formaldehyde for 10minutes at room temperature. This reaction was stopped with the addition of 2.5 ml/flask of 10x glycine solution and incubated for a further 5 minutes at room temperature. Subsequent nuclear and chromatin extraction was performed exactly as per the manufacturer's instructions. 10 µg of the resultant chromatin was used for each immunoprecipitation. Each immunoprecipitation was performed using a positive control antibody to Histone H3 (10 µl), negative control rabbit normal IgG (1 µl ; both antibodies provided in the kit) or ATF4 (5 µl; D4B8, Cell Signalling).

PCR conditions used to amplify site A and site B were as follows; 95°C for 2 minutes, 23 cycles of 95°C for 15 seconds, 55°C for 15 seconds, 72°C for 30 seconds, followed by 72°C for 7 minutes. PCR conditions used for negative control RPL30 primers (provided in the kit) were 95°C for 2 minutes, 28 cycles of 95°C for

15 seconds, 62°C for 15 seconds, 72°C for 30 seconds, followed by 72°C for 7 minutes. All PCR reactions were performed in 20 µl reaction volumes using REDTaq® ReadyMix™ PCR Reaction Mix with final primer concentrations of 200 nM (See Table 2.6 for details of primers not included in the kit)

2.19 Gene-modified Mice

An endothelial-specific Nox4-overexpressing transgenic mouse line (eNox4 Tg) in which Nox4 expression is driven by a Tie-2 promoter construct, and an endothelial-specific Nox4 null mice line (eNox4$^{-/-}$), in which Cre-recombinase was driven by a Tie-2 promoter were generated in our laboratory by Dr Alison Brewer.

2.20 Animal Husbandry

Mice were housed in a standard temperature and humidity controlled animal facility (BSU) with a 12-hour light/dark cycle (daylight from 7am to 7pm) and allowed free access to water and standard laboratory chow in accordance with the Housing and Care of Animals Used in Scientific Procedures Code of Practice. Same sex mice were housed up to 5 per cage. All experimental animals were used at ages 8-10 weeks unless otherwise stated. Control 'wild type' (WT) mice for each experiment represent age- and sex-matched litter mates on a C57Bl/6J background unless stated otherwise.

2.21 Genotyping

Genotyping was used to determine the presence of the Nox4 transgene or absence of the endogenous Nox4 gene in isolated genomic DNA from individual mice. Ear punches were harvested under anesthesia (2.5% isoflurane/97.5% oxygen (2 L/min)) by BSU staff and stored at -20°C until use. Ear punches were digested in a solution of 10 mg/ml proteinase K (Roche, UK) in a buffer containing 0.1 M Tris EDTA, 0.1 M Na_2EDTA, 1% SDS and 0.15 M NaCl, pH 8.0 for 1 hour at 56°C. Resultant genomic DNA was precipitated in isopropanol, washed with 80% ethanol and re-suspended in 50 µl of nuclease-free water. Amplification of genomic DNA was conducted using PCR in a thermal cycler (AB Applied Biosystems, UK) as follows: 35 cycles of denaturation (30 seconds at 94 °C), annealing (30 seconds at 56 °C) and extension (30 seconds at 72 °C). Each reaction contained 12.5 µl REDTaq® ReadyMix™ (Sigma), 0.5 µl gene-specific forward primer (10 µM stock), 0.5 µl gene-specific reverse primer (10 µM stock), 0.5 µl GAPDH forward primer (10 µM stock), 0.5 µl GAPDH reverse primer (10 µM stock) (see Table 2.2 for primer details), 8.5 µl water and 2 µl of genomic DNA. Resultant PCR products were separated at a constant voltage by electrophoresis on a 1.5% agarose gel containing ethidium bromide (400 ng/ml) in 1xTAE buffer (40 mM Tris-acetate and 1 mM EDTA) and then visualized under ultraviolet light. A 100bp ladder (Hpa II digest of pBluescript II SK+) was loaded alongside the genotyping samples to permit the identification of DNA bands according to size.

2.22 Endothelial cell isolation

2.22.1 Antibody Preparation

50 µl of well vortexed streptavidin coated Dynabeads (Invitrogen) were washed 5 times in Hanks' Balanced Salt Solution (HBSS) and then incubated at RT with a biotinylated antiCD31 (cluster of differentiation 31) antibody (R&D Sytems BAF3628) (50 µg/ml) for 1 hour on a tube rotator to allow for biotin-streptavidin interaction and subsequent antibody conjugation to the beads. After this the beads were washed gently 3 times in HBSS to remove any unbound antibody.

2.22.2 Collagenase A Digestion and Endothelial Cell Affinity Isolation

8-10 week old male or female mice (WT, eNox4 Tg) were given an intra-peritoneal injection with 45 mg/kg pentobarbital to anaesthetise the animal terminally. Hearts were dissected out and 2-3 whole hearts from either male or female, age-matched WT and eNox4 Tg mice were pooled according to genotype. Hearts were finely chopped into 2mm^3 pieces in HBSS and allowed to collect at the bottom of a Sterilin tube on ice for two minutes. HBSS supernatant was carefully discarded and the remaining chunks of heart were washed twice in HBSS to remove any excess blood. Once washed, the heart pieces were added to 10 ml of HBSS containing 100 mg/ml collagenase A (Roche). This was then incubated at 37°C in a shaker for 20 minutes during which heart digests were mixed by pipetting half way through the incubation. Heart chunks were then allowed to settle at the bottom of the tube,

after which the collagenase A solution now containing any liberated cells was removed, added to a fresh tube and supplemented with 1 ml calf serum to stop the collagenase reaction. A fresh solution of HBSS containing collagenase A was then added to the heart chunks. This process was repeated twice more. This step was performed to allow extracellular matrix degradation and subsequent liberation of cardiac cell types without over-digesting the cells. After the final incubation, digests were pooled, passed through a 2 μm cell strainer and spun at 1200 rcf for 5 minutes. The supernatant was carefully removed, taking care not to disturb the cell pellet. Cells were re-suspended in 500 μl HBSS. For RNA isolations, 50 μl of this suspension was removed and added to 700 μl of Qiagen qiazol reagent (representing the input sample) and 450 μl added to the previously prepared antiCD31 conjugated Dynabeads. Mixtures were placed on a tube rotator for 3 hours at RT to allow endothelial cell binding. After this any unbound cells were removed by washing 3 times with HBSS. Cells bound to the beads (representing the output sample) were then lysed in 700 μl qiazol reagent. For protein isolations, the entire cell suspension (500 μl) was added to the previously prepared antiCD31 conjugated Dynabeads and placed on a tube rotator for 3 hours at RT. Any unbound cells were removed by washing 3 times with HBSS. Cells bound to the beads were then lysed directly into 60 μl of protein lysis buffer.

RNA was extracted from cardiac microvascular endothelial cells (CMEC) using the Qiagen RNeasy isolation kit. In brief, CMEC were incubated with 700 μl of Qiazol solution and vortexed vigorously for 10 seconds, beads were removed using a magnet and the remaining qiazol was spun through Qiashredder columns (Qiagen, UK) at 13,000 rpm for one minute. RNA was isolated according to the

manufacturer's specifications (Qiagen RNeasy). The resultant RNA was eluted into 30 µl of nuclease-free water respectively and quantified using a NanoDrop spectrophotometer (ND-1000, Labtech International, UK).

Protein was extracted from CMEC by the addition of 60 µl of lysis buffer (detailed in section 2.5.1) directly to the cells on the magnetic beads and incubated at room temperature for 5 minutes. Beads were subsequently removed using a magnet, protein concentration was determined using a Bradford assay before 50 µl of lysed CMEC sample were added to 12.5 µl 5X Laemmli buffer and boiled for 5 minutes to denature the proteins. Protein samples were diluted to 25 µg/30 µl in 1X laemmli buffer and stored at -80°C.

2.23 Measuring H_2S using the Unisense H_2S Microsensor

Hydrogen sulphide was measured using the Unisense H_2S Microsensor probe following the manufacturer's specifications. In brief, 150-200 mg organ slices were incubated at 37°C with a buffer containing 1 ml Hepes solution (pH 7.4), 60 µM pyridoxyl 5 phosphate (PLP) and 1 mM cysteine. The Microsensor probe was then placed through a rubber stopper into a glass vial containing the organ and buffer. The reactions were allowed to proceed for up to 1 hour after organ addition and H_2S standards were measured by incubating the probe with increasing concentrations (10 µM, 100 µM, 300 µM, 1 mM) of NaHS. Data were collected on the Unisense Sensor Trace suite software. Analysis was made by taking the

millivolt reading obtained 30 minutes after initial H_2S detection. A diagram of the experimental set up used is shown in figure 2.1.

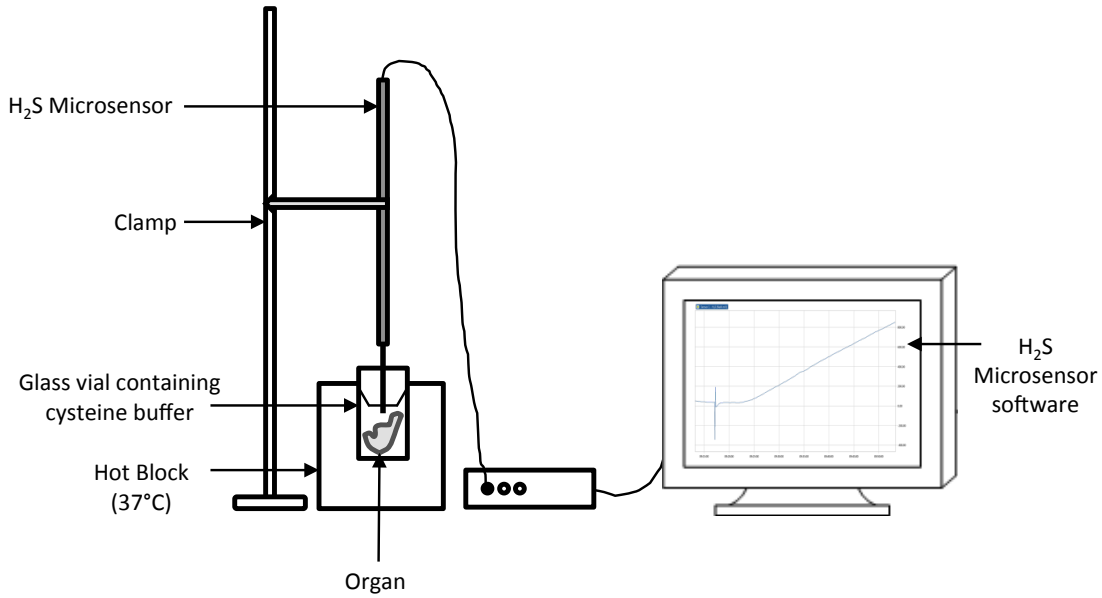

Figure 2.1: Polarographic Micro-sensor Setup. A schematic illustration of the experimental setup used for measuring H_2S *ex vivo*.

2.24 Wire Tension Myography

8-10 week old male mice (WT, eNox4 Tg or eNox4$^{-/-}$) were given an intra-peritoneal injection with 45 mg/kg pentobarbital mixed with heparin to anaesthetise the animal terminally whilst preventing coagulation of the blood. The thoracic aorta was removed by dissection along the spine and then immersed in cold (4°C) Krebs-Ringer solution (2.5 mM $CaCl_2x2H_20$, 118 mM NaCl, 11 mM Glucose D(+), 25 mM $NaHCO_3$, 4.7 mM KCl, 1.18 mM KH_2PO_4, 1.16 mM $MgSO_4$). The aortae were cut into 3mm long rings and mounted in a Danish Myo Technology (DMT) wire tension myograph. Rings were bathed in Krebs-Ringer solution at 37°C and supplied with a continuous gas mixture of 95% O_2/5% CO_2. Prior to treatment,

the vessels were stretched to the optimal pre-tension condition (~2 mN) using the DMT normalisation modules. Rings were then tested for contraction to 60 mM potassium chloride (KCl) before being washed 3 times and treated with 10 μM phenylephrine (PE) to induce contraction, this was maintained for 20 minutes before the addition of 10 μM acetylcholine to test the endothelium for its ability to relax the vessel. Aortic rings were then washed 3 times and incubated for 30 minutes in Krebs-Ringer before the addition of 20 mM PPG to inhibit CSE or 2000 Unit/5 ml of PEG-catalase to scavenge H_2O_2, all diluted in Krebs-Ringer. Vehicle controls composed of Krebs-Ringer were run alongside each inhibitor and inhibitors were incubated with vessels for 30 minutes and 20 minutes respectively. This was then followed by a cumulative dose-dependent contraction to PE (up to 30 μM). For eNox4$^{-/-}$ mice, no inhibitors were used and so after relaxation to ACh and subsequent wash steps, vessels were dose-dependently contracted with PE. Results were then analysed using LabChart software.

Strict exclusion criteria were implemented in the analysis of the results obtained whereby vessels that failed to contract above 1 mN to 10 μM PE and those that failed to relax to ACh more than 50% of the PE induced constriction were excluded from analysis. This was performed in order to rule out any vessels that may have been damaged during preparation.

2.25 Statistical Analysis

Data are expressed as mean ± standard error of the mean (SEM). Statistical calculations were performed using Graphpad Prism (version 6) and significance was considered acceptable when P≤0.05. The statistical tests implemented in this thesis are as follows; 1) One-way ANOVA followed by Tukey's post-hoc test, 2) Two-way ANOVA followed by Tukey's post-hoc test, 3) Unpaired Students *t*-Test.

2.26 Tables

Primer name (Human)	Forward (5'-3')	Reverse (5'-3')
CSE	ACACTTTTATGTCACCATATTTCCAG	TGTTGCAGAATACATAGAAATATCAGC
CSE (Full length Variant 1)	GAGGCAGCAATTACACCAGA	GTGCACAGCCTTCAATGTCA
CSE (Variant 2)	TTACACCAGAAACCAAGCGC	AGACACCAGGCCCATTACAA
CSE (Variants 1-3)	CCGTTCTGGAAATCCCACTA	GGAGATGGAACTGCTCCAAC
CBS	AAACAGATCCGCCTCACG	CTTCCCGGTGCTGTGGTA
ATF4	TCTCCAGCGACAAGGCTAA	CAATCTGTCCCGGAGAAGG
PERK	CCAGCCTTAGCAAACCAGAG	TCTTGGTCCCACTGGAAGAG
HRI	CCACTTCGTTCAAGACAGGTG	GCTAAACTCGTCACTACAAGTGAAA
Nox4 (Human/Mouse)	GCCAACGAAGGGGTTAAACA	TGGCCCTTGGTTATACAGCA
βActin	GCGAGAAGATGACCGAGATCA	TCACCGGAGTCCATCACGAT
3MST	ACATCAAGGAGAACCTGGAATC	GATGTGGCCAGGTTCAATG
Nrf2	GAGAGCCCAGTCTTCATTGC	TGCTCAATGTCCTGTTGCAT
SP1	CTATAGCAAATGCCCCAGGT	TCCACCTGCTGTGTCATCAT
MAT1A	AGGGCTCTGCCGGAGAGT	GCTCGGCCACACCAATG
SAHH	GGTTCATTTCCTGCCCAAG	TGGTCAATTCACATTCAGCTT
MeTHFR	GCCCGATTGTAGTTGTGCTT	TGGGAAATACGTGGTGGTG
MS	CAGAGTGCTTAACGGCACAG	TAACAGTGGCCAGCACGAT

Table 2.1: Primer sequences used for QPCR on HUVEC samples.

Primer name (Mouse)	Forward (5'-3')	Reverse (5'-3')
Nox4	AGCTTGATTCGACGGTATCGAT	CATATTACAGGATGAAAATCG
Cre	TGCCAGGATCAGGGTTAAAG	CCCGGCAAAACAGGTAGTTA
GAPDH	CCTAGACAAAATGGTGAAGG	GACTCCACGACATACTCAGC

Table 2.2: Genotyping primer sequences

Primer name (Mouse)	Forward (5'-3')	Reverse (5'-3')
CSE	GAGGATGAACAGGACCTTCTT	CAGCTTTGACTCGAACTTTTAAGG
CBS	GTCCACGAGCAGATCCAATAC	GGCAGTGACAACCCCAAA
NOX4	CCGGACACTCCTCGCTTATC	TGCTTTTATCCAACAATCTTCT
VWF	CCAAGGAGGGTCTGCAACT	AAAGGAAGACTCTGGCAAGCTA
βActin	CTGTCGAGTCGCGTCCACCC	ATGCCGGAGCCGTTGTCGAC

Table 2.3: QPCR primer sequences (mouse).

Primer name (Human)	Forward (5'-3')	Reverse (5'-3')
6414 F	AGAGAGGGTACCTGAAGTATGCTGCCCCTC	
764 F	AGAGAGGGTACCCTTTTAGGAAGCTGCCAG	
p 191 R		AGAGAGCTCGAGAGAAGAAGAGAGGAAAAGAACAC
Int Enh	TTAATGGATCCGTGAGCTGGGTCTGTCTG	TTAATGGATCCCAGAGGTGAATCACCTGAG

Table 2.4: Primer sequences used for cloning luciferase reporter constructs.

Primer name (Human)	Forward (5'-3')	Reverse (5'-3')
CSE splice variants	CCGTTCTGGAAATCCCACTA	GGAGATGGAACTGCTCCAA

Table 2.5: Primer sequences used for PCR.

Primer name (Mouse)	Forward (5'-3')	Reverse (5'-3')
Site A	ACCAACTCCTAGGCACTCAG	AGTAGCTGAGATTACCCGCC
Site B	TCTTGCTCTCTTGCCCAGG	CAGAGGTGAATCACCTGAG

Table 2.6: Primers used for ChIP assays.

Reagents	Resolving Gel	Stacking Gel
30% Acrylamide	3300µl	680µl
Water	4000µl	2720µl
1.5M Tris-HCL: pH 8.8	2500µl	X
1M Tris-HCL: pH 6.8	X	500µl
10% SDS	100µl	40µl
10% Ammonium persulfate (APS)	100µl	40µl
TEMED	10µl	4µl

Table 2.7: Reagents and dilutions used for casting and stacking gels

Primary Antibody	Dilution	Species	Company	Catalog Number
CSE	1 in 3000	Rabbit (Polyclonal)	Aviva	ARP46068_T100
CBS	1 in 3000	Rabbit (Polyclonal)	AbCam	Ab96252
Nox4	1 in 2000	Rabbit	In house	In house
ATF4 (CREB-2)	1 in 2000	Rabbit (Polyclonal)	Santa Cruz	SC-200
$p22^{Phox}$	1 in 2000	Rabbit (Polyclonal)	AbCam	ab75941
Total eIF2α	1 in 2000	Mouse (Monoclonal)	Santa Cruz	SC-133132
Pi-eIF2α (Ser51)	1 in 2000	Rabbit (Polyclonal)	Millipour	07-760
βGalactosidase	1 in 5000	Rabbit (Polyclonal)	AbCam	Ab616
βActin	1 in 5000	Rabbit	Sigma	

Table 2.8: Primary antibodies and dilutions.

Secondary Antibody	Dilution	Species	Company	Catalog Number
IgG-HRP linked	1 in 5000	Goat anti-Rabbit	Cell signalling technologies	7074S
IgG-HRP linked	1 in 5000	Horse anti-Mouse	Cell signalling technologies	7076S

Table 2.9: Secondary antibodies and dilutions.

Name	Concentration	Company
siNox4	5nM	Ambion (s27015)
siATF4	20nM	Ambion (s1702
sip22phox	20nM	Ambion (s194371)
siHRI	20nM	Ambion (s25823)
siPERK	20nM	Ambion (s18102)
siNRF2	20nM	Ambion (s9441)
siSP1	20nM	Ambion (s13320)

Table 2.10: siRNAs and final concentrations used.

Chapter 3: Results 1

3.1 Introduction

As discussed in chapter 1, studies have identified a role for ROS in the regulation of hcy metabolism[92, 96, 97, 156] and H_2S production[101] in various cell types. The endogenous source of ROS that regulates these processes however remains elusive.

3.1.2 NADPH Oxidase 4 as a Potential Source of ROS

Nox enzymes represent physiological enzymatic generators of ROS that are expressed and active in a diverse range of cell types and systems[122]. Indeed, some studies have indirectly implicated Nox as a potential ROS source in the regulation of hcy metabolism and H_2S biosynthesis, through the use of Nox inhibitors such as DPI[100 101, 157]. Of the 7 Nox family members, vascular Nox4 has been extensively characterised as an endogenous generator of H_2O_2 that participates in a diverse range of physiological intracellular signalling responses[149]. Interestingly, H_2O_2 has been shown to regulate the expression and activity of some of the enzymes involved in hcy/H_2S metabolism[92, 99]. Moreover, direct genetic evidence supporting a role for Nox4 in hcy metabolism comes from a large-scale, genome-wide screen which investigated the associations between high plasma hcy levels and over 300,000 single-nucleotide polymorphisms (SNPs) in 13,974 women. The results of this study reaffirmed the role of a number of enzymes integral to hcy metabolism and further demonstrated highly-significant associations between high hcy concentrations and polymorphisms in 4 novel genetic loci. One of these loci was that of Nox4[157]. Perhaps consistent with this, a striking observation was made

from a micro-array screen performed in our group[158] which compared the transcriptomes of hearts taken from cardiac-specific Nox4 transgenic mice and WT littermate controls. Significant changes in some of the enzymes known to be involved in hcy metabolism were identified. Of note, an expressed-sequence-tag (EST) corresponding to the CSE gene was very significantly elevated in Nox4 transgenic (Tg) hearts compared with WT littermates.

Finally, the gene expression of CSE has been shown to be ROS-inducible in some systems[99] [100]. Moreover, Nox-derived H_2O_2 has been shown to regulate CSE derived H_2S production in endothelial cells *in vitro*[101]. It is therefore tempting to speculate that Nox4, which specifically generates H_2O_2 and, accordingly has been shown previously to generate significantly increased amounts of H_2O_2 upon its overexpression in HUVECs[47], may function in the regulation of hcy metabolism and/or H_2S production in endothelial cells.

Aim

To characterise the effects of Nox4 mis-expression on the expression of enzymes involved in hcy metabolism in the endothelium.

3.2 Results

3.2.1 Characterising Adenoviral-mediated Nox4 Overexpression in HUVECs

To begin to investigate the potential role of Nox4 in the expression of hcy/H_2S metabolism-associated enzymes in HUVECs, experiments were performed to assess the efficiency of adenoviral-mediated ectopic overexpression of Nox4. Nox4 was transduced using three multiplicities of infection (MOI 5, 10 and 20) alongside a B Gal control overexpressing virus. Figure 3.1A and B show that Nox4 and B Gal can be overexpressed in a dose-dependent manner and that an MOI of 20 induces the highest level of overexpression of both proteins. An MOI of 20 was selected for future experiments. Figure 3.1A also shows that endogenous Nox4 protein expression can be detected in HUVECs.

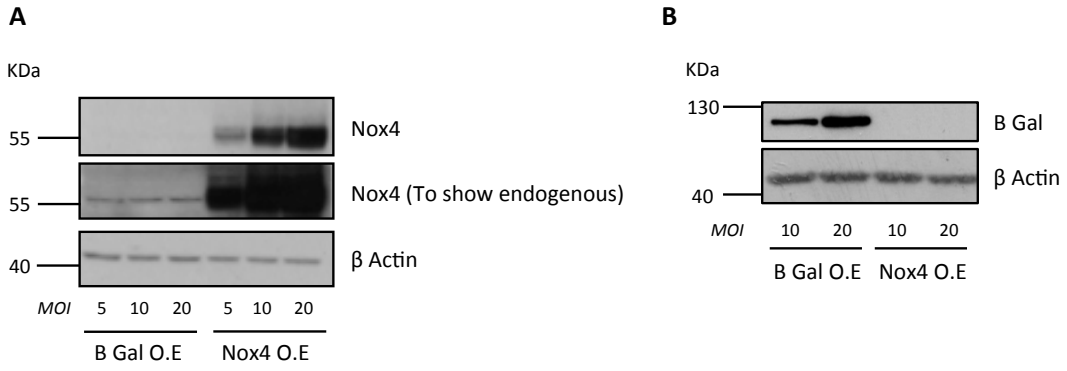

Figure 3.1: **Optimisation of Adenoviral-Mediated Nox4 Overexpression**. Immunoblots depicting an MOI-dependent increase in **A)** Nox4 and **B)** B Gal protein expression following a 24 hour overexpression in HUVECs. β Actin protein expression was used as a loading control for each experiment. **A** also shows an overexposed Nox4 blot depicting endogenous Nox4 protein. O.E = Overexpression. N=1.

3.2.2 Nox4 Overexpression Induces the Transcription of CBS and CSE

To determine whether a relationship exists between the expression of Nox4 and the transcription of enzymes involved in hcy metabolism and H_2S biosynthesis in the endothelium, Nox4 was overexpressed in HUVECs and the expression of hcy/H_2S metabolism-associated enzymes was quantified by QPCR. Figure 3.2 shows the results obtained from these experiments. Figure 3.2A indicates that Nox4 was highly overexpressed at the protein level and that this did not change the mRNA expression of methionine- and folate-cycle associated enzymes (Figure 3.2 B-E). By contrast, the transsulfuration-associated enzymes, CBS and CSE, are highly significantly and robustly up-regulated following 24 hours of Nox4 overexpression (Figure 3.2 F,G).

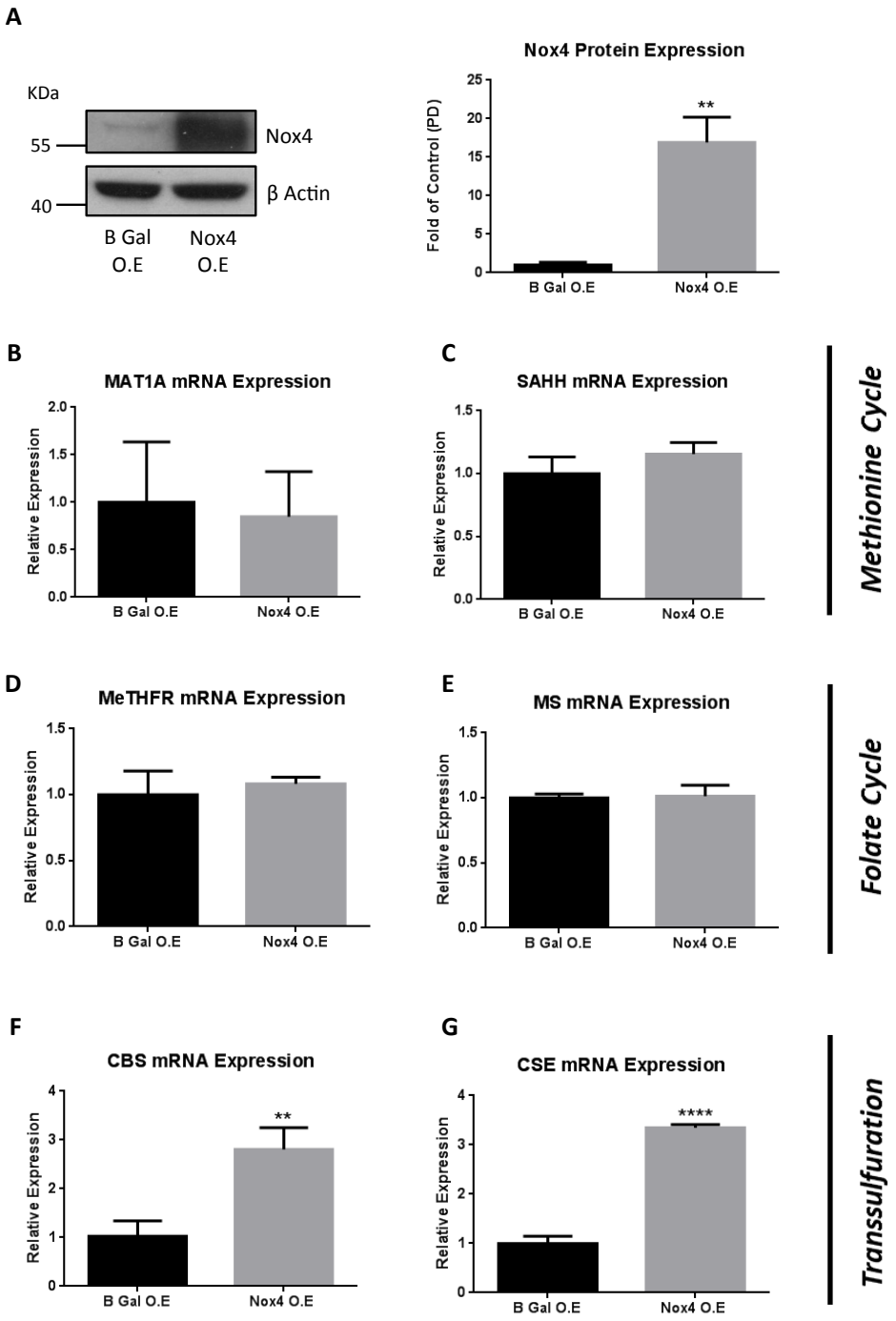

Figure 3.2: **Nox4 Overexpression Increases CBS and CSE mRNA Expression. A**) A representative immunoblot and densitometric analysis confirming Nox4 overexpression after 24 hours overexpression in HUVECs, normalised to β Actin protein expression. **B-G)** Corresponding QPCR data showing the mRNA expression of **B,C)** Methionine cycle, **D,E)** Folate cycle and **F,G)** Transsulfuration enzymes following B Gal (B Gal O.E) and Nox4 (Nox4 O.E) overexpression. Data normalised to β Actin mRNA expression. O.E = Overexpression. N=3, ** = P<0.01, **** = P<0.0001. Statistical analyses performed using an unpaired Students *t*-test.

3.2.3 Nox4 Silencing Reduces CSE mRNA Expression

To assess the physiological contribution of endogenous Nox4 on the expression of hcy/H_2S metabolism-associated enzymes in HUVECs, Nox4-silencing experiments were performed. Figure 3.3 indicates the results of these experiments. Figure 3.3A shows that Nox4 was significantly silenced at the mRNA level following targeted siRNA treatment. No significant changes in the expression of methionine and folate cycle enzymes were observed following Nox4 silencing (Figure 3.3 B-E). By contrast, there was a trend toward a reduction in the expression of CBS (Figure 3.3 F), and CSE expression was significantly reduced following Nox4 silencing, with respect to scrambled siRNA controls (Figure 3.3 G).

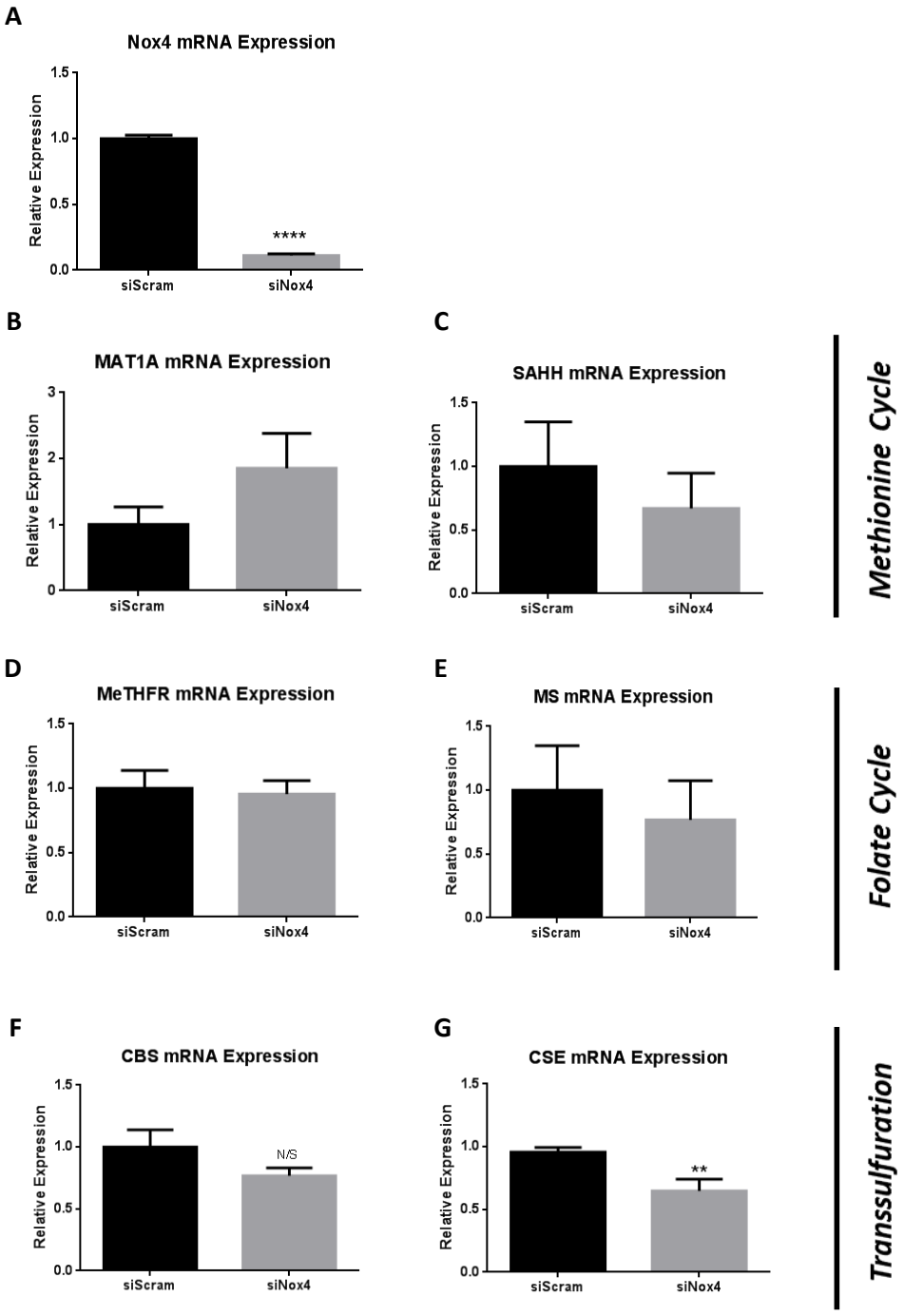

Figure 3.3: Nox4 Silencing Reduces CSE mRNA Expression. QPCR data showing the mRNA expression of **A)** Nox4, **B,C)** Methionine cycle, **D,E)** Folate cycle and **F,G)** Transsulfuration associated enzymes following 24 hours Nox4 silencing with Nox4 siRNA (siNox4) compared to scrambled siRNA controls (siScram) in HUVECs. All data normalised to β Actin mRNA expression. N=3, ** = P<0.01, **** = P<0.0001, N/S = Not significant. Statistical analyses performed using an unpaired Students *t*-test.

3.2.4 CSE Protein Expression can be Detected in HUVECs

There has been some debate as to whether significant CSE protein expression occurs in endothelial cells[63, 64]. To investigate whether endogenous CSE protein was expressed in HUVECs, immunoblotting to detect CSE protein levels was performed. Figure 3.4 indicates that a band at the anticipated molecular weight for CSE (44 KDa) is detected in HUVECs. To further confirm the identity of this band, siRNA-mediated silencing of CSE protein reveals a depletion in its intensity, consistent with the expression of CSE protein in HUVECs.

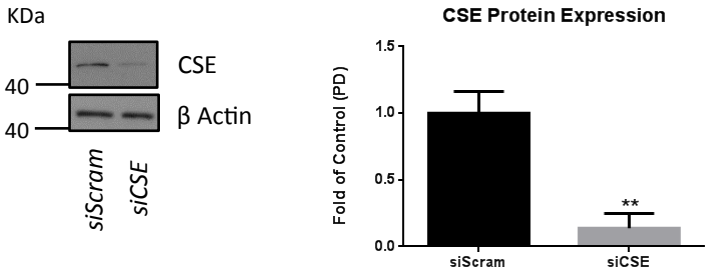

Figure 3.4: Endogenous CSE protein Expression is Detectable by Immunoblotting in HUVECs. A representative immunoblot and corresponding densitometric analysis of CSE expression in HUVECs following 48 hours of CSE silencing using CSE siRNA (siCSE) or scrambled siRNA controls (siScram). Data normalised to β Actin protein levels. N=3, ** = P<0.01. Statistical analyses performed using an unpaired Students *t*-test.

3.2.5 Nox4 Overexpression Increases CSE Protein Expression in HUVECs

Nox4 overexpression robustly up-regulated CSE mRNA expression (figure 3.2 G). To determine whether this resulted in a corresponding increase in CSE protein expression, Nox4 was overexpressed in HUVECs, and CSE protein expression was quantified. Figure 3.5A and B indicate that CSE protein levels are significantly increased upon Nox4 overexpression, compared to B Gal transduced control cells.

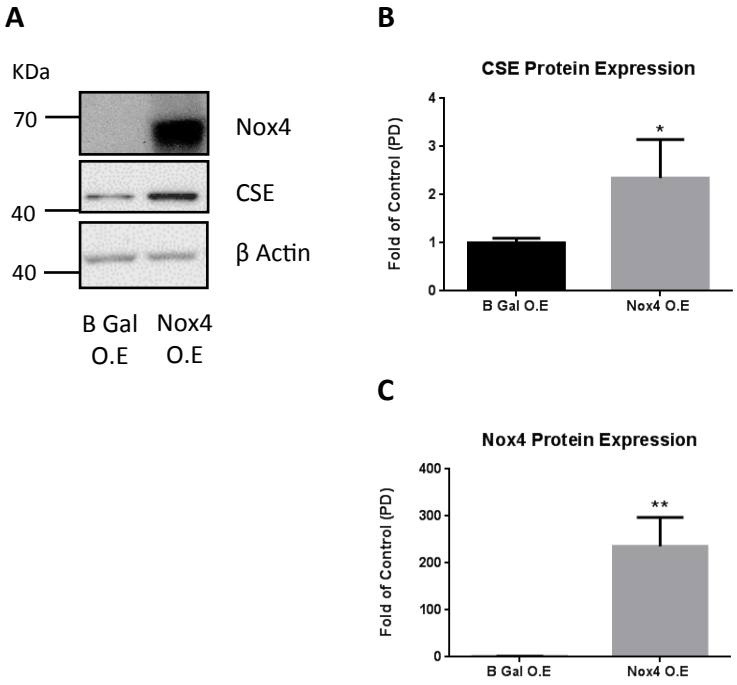

Figure 3.5: **CSE Protein Expression is Increased Upon Nox4 Overexpression. A)** A representative immunoblot showing CSE and Nox4 protein expression following 48 hours Nox4 overexpression (Nox4 O.E) or B Gal overexpression (B Gal O.E) in HUVECs. **B,C)** Corresponding densitometric analysis for CSE and Nox4 protein expression respectively. All data normalised to β Actin protein levels. N=3, * = P<0.05, ** = P<0.01. Statistical analyses performed using an unpaired Students *t*-test.

3.3.6 Nox4 Silencing Reduces CSE Protein Expression in HUVECs

The silencing of endogenous Nox4 significantly reduced CSE mRNA expression (figure 3.3 G). To determine whether this resulted in a concommitant reduction in CSE protein expression, Nox4 was silenced in HUVECs and CSE protein levels were analysed by immunoblotting. Figure 3.6 shows that the silencing of Nox4 for 48 hours significantly reduced CSE protein levels, consistent with the mRNA data obtained for the same experiment. This suggests that Nox4 is a physiological regulator of CSE expression in endothelial cells *in vitro*.

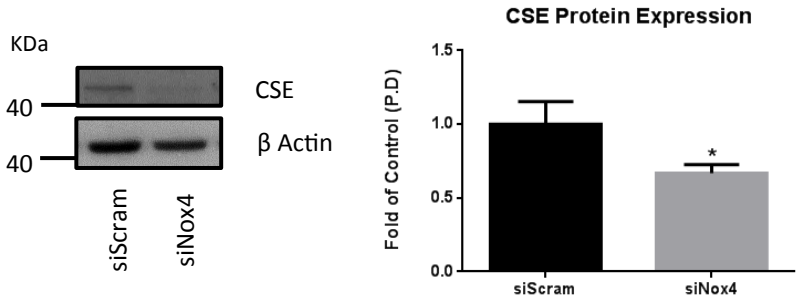

Figure 3.6: CSE Protein Expression is Reduced Following Nox4 Silencing. A representative immunoblot and corresponding densitometric analysis showing CSE protein expression following 48 hours Nox4 silencing using Nox4 siRNA (siNox4) or scrambled siRNA controls (siScram) in HUVECs. Data normalised to β Actin protein levels. N=3, * = P<0.05. Statistical analyses performed using an unpaired Students *t*-test.

3.2.7 CBS Protein Expression is Unaffected by Nox4 Overexpression and Silencing

Nox4 overexpression significantly increased CBS mRNA expression (figure 3.2 F) although, by contrast, Nox4 silencing did *not* significantly reduce CBS mRNA levels (a trend toward a reduction however was observed) (figure 3.3 F). To assess whether Nox4 affects CBS protein expression in HUVECs, Nox4 overexpression and silencing experiments were performed as described above. Figure 3.7A and D demonstrate that CBS protein expression remains unchanged following Nox4 overexpression and silencing respectively.

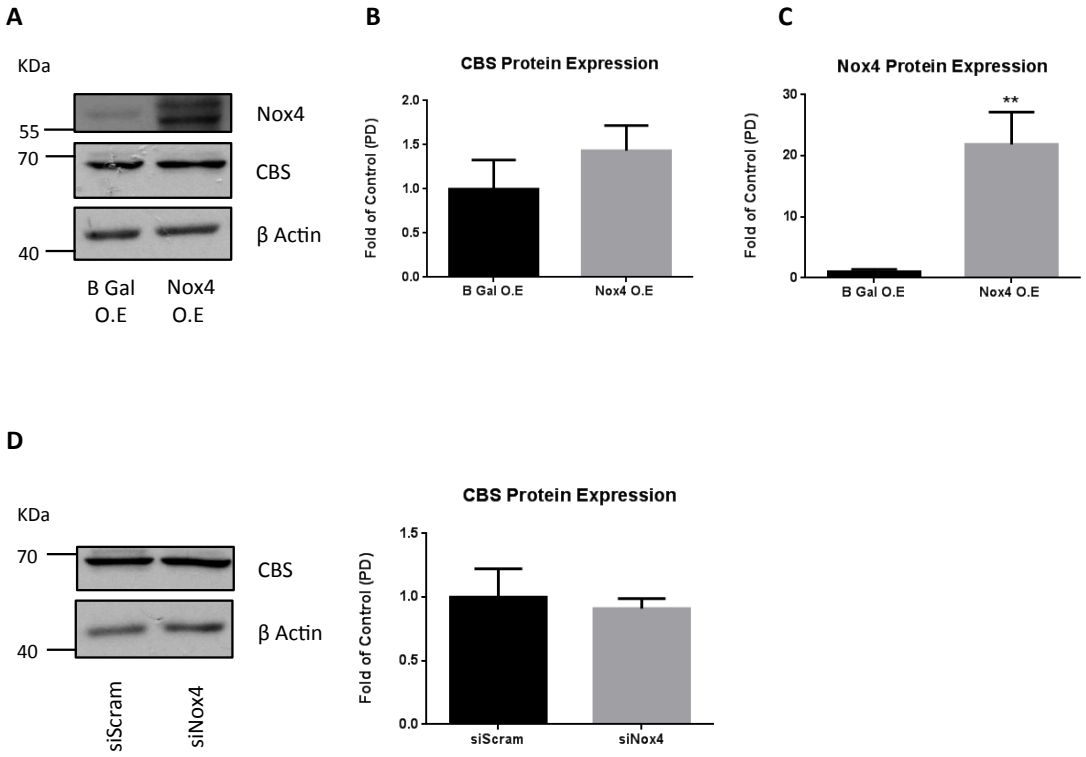

Figure 3.7: CBS Protein Expression Remains Unchanged Upon Nox4 Mis-expression. A) A representative immunoblot showing CBS and Nox4 protein expression following 48 hours Nox4 (Nox4 O.E) or B Gal (B Gal O.E) overexpression in HUVECs. **B,C)** Corresponding densitometric analysis for CBS and Nox4 protein expression respectively. **D)** A representative immunoblot and corresponding densitometric analysis showing CBS protein expression following 48 hours Nox4 silencing using Nox4 siRNA (siNox4) or scrambled siRNA controls (siScram) in HUVECs. All data normalised to β Actin protein levels. O.E = Overexpression. N=3, ** = P<0.01. Statistical analyses performed using an unpaired Students *t*-test.

Taken together, these data suggest that Nox4 is a physiological regulator of both the mRNA and protein expression of CSE. Nox4-induced changes in CSE expression will therefore form the focus of the following results.

3.2.8 Endothelial Nox4 is Highly Expressed Relative to Nox1 and Nox2.

It has previously been shown that Nox4 is highly expressed in endothelial cells[129]. To confirm these previous observations and to determine the relative expression of endothelial Nox1, Nox2 and Nox4, QPCR was used to measure the mRNA levels of these Nox isoforms. Figure 3.8 shows that Nox4 is highly expressed compared to Nox1 and Nox2, highlighting its potential functional importance in this cell type.

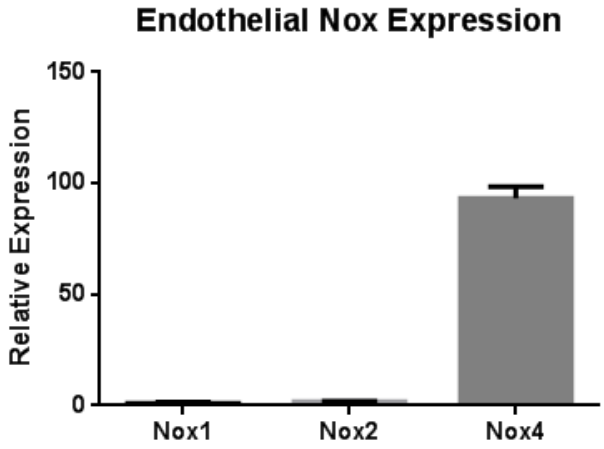

Figure 3.8: Endothelial Nox4 is Highly Expressed Relative to Nox1 and Nox2. QPCR data showing the relative mRNA expression of Nox1, Nox2 and Nox4 in HUVECs. All data normalised to β Actin mRNA expression. N=3.

3.2.9 Silencing of $p22^{phox}$ Significantly Reduces CSE mRNA Expression in HUVECs

Nox4 is the most abundantly expressed Nox isoform that associates with $p22^{phox}$ in the endothelium (Figure 3.8). The Nox subunit of Nox4 is stabilised by its association with the membrane protein $p22^{phox}$ [159]. To further investigate a role for Nox proteins in the transcriptional regulation of CSE, $p22^{phox}$ was silenced. Figure

3.9A shows that p22^{phox} was successfully silenced using siRNA and figure 3.9B demonstrates that this silencing of p22^{phox} significantly reduced CSE mRNA expression. These data further support a role for endogenous NADPH oxidase(s) in the physiological regulation of CSE expression and, consistent with the high level of expression of Nox4 in the endothelium compared to other Nox isoforms, further point to the involvement of Nox4 in this process.

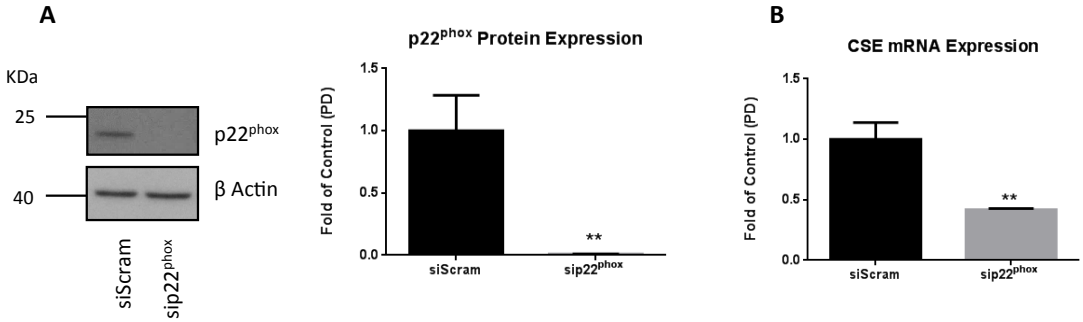

Figure 3.9: CSE mRNA Expression is Reduced Following p22^{phox} Silencing. A) A representative immunoblot and corresponding densitometric analysis showing p22^{phox} protein expression following 48 hours p22^{phox} silencing with siRNA (sip22^{phox}) or scrambled siRNA controls in HUVECs. Data are normalised to β Actin protein levels. **B)** Corresponding QPCR data showing CSE mRNA expression following 48 hours p22^{phox} silencing. Data normalised to β Actin mRNA expression. N=3, ** = P<0.01. Statistical analyses performed using an unpaired Students *t*-test.

3.2.10 24 Hours Exogenous H_20_2 Treatment Does Not Mimic the Effects of Nox4 on CSE Expression

Nox4 is unique among other Nox family members in that it generates H_2O_2 rather than O_2^-. Indeed, previous studies have shown that Nox4 overexpression using the same Nox4 adenovirus utilised here significantly increases extracellular ROS

production in HUVECs[47]. Furthermore, administration of H_2O_2 to COS7 cells was shown previously to increase CSE transcription[99]. Thus, in an attempt to confirm the involvement of H_2O_2 in the Nox4-induced up-regulation of CSE expression, HUVECs were treated with increasing concentrations of H_2O_2 for 24 hours. Figure 3.10 shows that CSE mRNA expression failed to increase significantly in response to all H_2O_2 concentrations used, although a slight trend toward an increase was observed in all cases.

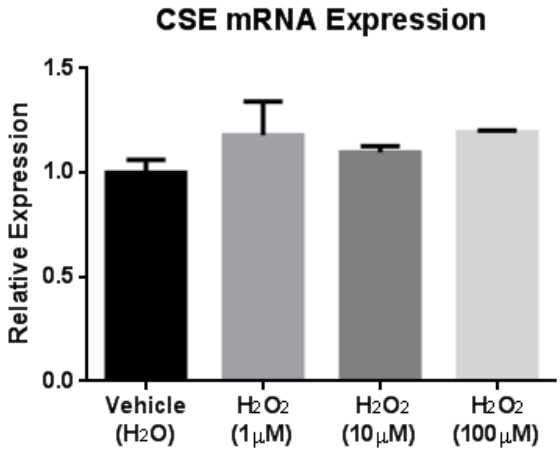

Figure 3.10: 24 Hour Treatment with Exogenous H_2O_2 Does Not Significantly Enhance CSE mRNA Expression in HUVECs. QPCR data showing the mRNA expression of CSE following 24 hours incubation of HUVECs with increasing concentrations of H_2O_2. All data normalised to β Actin mRNA expression. N=3, Statistical analysis performed using a one-way ANOVA and a Tukeys post-hoc test did not reveal any significant differences between groups.

3.2.11 Exogenous Tert-Butylhydroperoxide Fails to Increase CSE mRNA Expression

H_2O_2 is potentially labile and therefore to overcome the experimental caveats associated with H_2O_2 instability, Tert-butylhydroperoxide (tBHP), a peroxide donor, was utilised. Incubation of HUVECs with varying concentrations of tBHP did not however, increase CSE expression as shown in Figure 3.11.

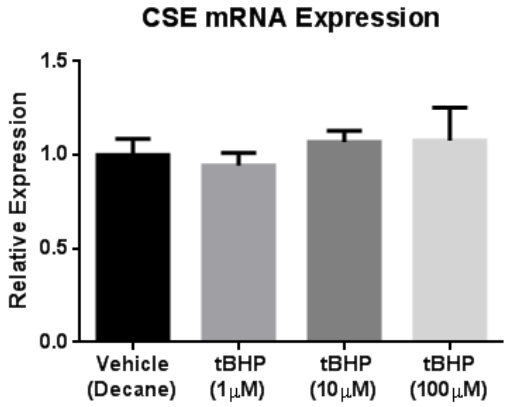

Figure 3.11: **Exogenous tBHP Does Not Enhance CSE mRNA Expression.** QPCR data showing the mRNA expression of CSE following 24 hours incubation of HUVECs with increasing concentrations of tBHP. All data normalised to β Actin mRNA expression. N=3, Statistical analysis performed using a one-way ANOVA and a Tukeys post-hoc test, did not reveal any significant differences between groups.

3.2.12 The Nox Inhibitor, DPI, Enhances the Nox4-induced Up-regulation of CSE

Previous reports have shown that CSE expression can be inhibited by the broad-spectrum Nox inhibitor, DPI in rat mesangial cells[100]. To further investigate whether the Nox4-induced increase in CSE mRNA expression was due to a

functional effect of Nox4, Nox4 was overexpressed in HUVECs followed by incubation with 10 μM DPI. Figure 3.12 shows that the combination of Nox4 overexpression with DPI treatment surprisingly resulted in a significant *enhancement* in the Nox4-induced up-regulation in CSE mRNA expression.

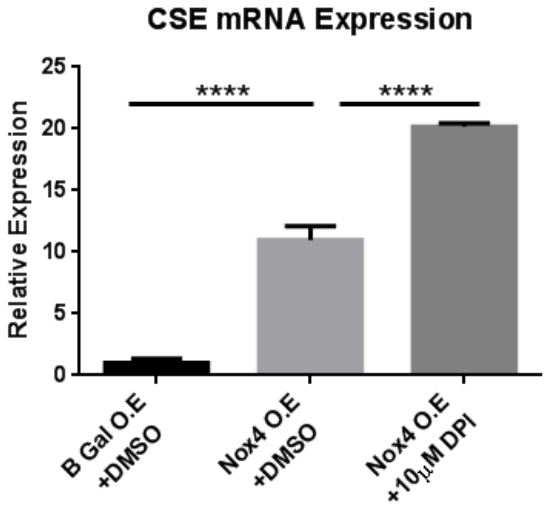

Figure 3.12: DPI Exacerbates Nox4-induced CSE Expression. QPCR data showing the mRNA expression of CSE following 24 hours Nox4 overexpression (Nox4 O.E) in the presence or absence of 19 hours DPI treatment compared to B Gal overexpression (B Gal O.E) in HUVECs. All data normalised to β Actin mRNA expression. O.E = Overexpression. N=3, **** = P<0.0001. Statistical analyses performed using one-way ANOVA and a Tukeys post-hoc test.

3.2.13 PEG-Catalase Reduces the Nox4-induced Increase in CSE mRNA Expression

To determine whether Nox4-derived H_2O_2 was involved in secondary messenger-signal mediated transcriptional activation of CSE, PEG-Cat was applied to HUVECs that were overexpressing Nox4. Figure 3.13 shows that incubation of HUVECs with

500units of PEG-Cat resulted in a small but significant blunting in the Nox4-induced transcriptional induction of CSE.

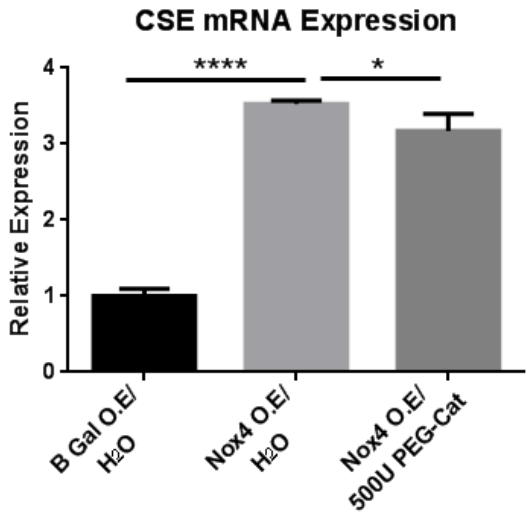

Figure 3.13: PEG-Catalase Blunts Nox4-induced CSE Expression. QPCR data showing the mRNA expression of CSE following treatment of HUVECs with 500units of PEG-Cat (500U PEG-Cat) for 48hours and Nox4 overexpression (Nox4 O.E) for 24 hours compared to a B Gal overexpression (B Gal O.E) control. All data normalised to β Actin mRNA expression. O.E = Overexpression. N=3, * = $P<0.05$, **** = $P<0.0001$. Statistical analyses performed using a one-way ANOVA and a Tukeys post-hoc test.

3.2.14 A Functioning Transsulfuration Pathway is not Present in HUVECs

CSE participates in both hcy metabolism and H_2S biosynthesis. During hcy metabolism, methionine is first utilised as a methyl donor where its demethylation results in the formation of hcy. When methionine levels are high, hcy enters into the transsulfuration pathway, an effect mediated by an S-adensylmethionine-induced up-regulation in CBS activity[160]. Hcy is subsequently converted into

cysteine by the sequential action of CBS and CSE. Once generated, cysteine can then, for instance be used as a substrate for GSH synthesis. To begin to determine whether endothelial CSE participates in canonical transsulfuration activity (the conversion of hcy to cysteine), an assessment of the transsulfuration capacity of HUVECs was made by assessing intracellular GSH level. Figure 3.14 B and C show that incubation of HUVECs with medium lacking cysteine and methionine results, as expected, in a significant reduction in glutathione levels. This effect is rapid and detectable just 4 hours after cysteine depletion (Figure 3.14 B). In an attempt to recover GSH levels through transsulfuration, HUVECs were subsequently incubated with medium lacking cysteine but containing high concentrations of methionine, which would be expected to result in an increase in transsulfuration activity *via* enhanced CBS activity. However, Figure 3.14 B and C show that both increasing the dose and time to which cells are incubated with methionine does *not* recover GSH levels, suggesting that the cysteine (and hence GSH) levels could not be replenished *via* the transsulfuration pathway in HUVECs.

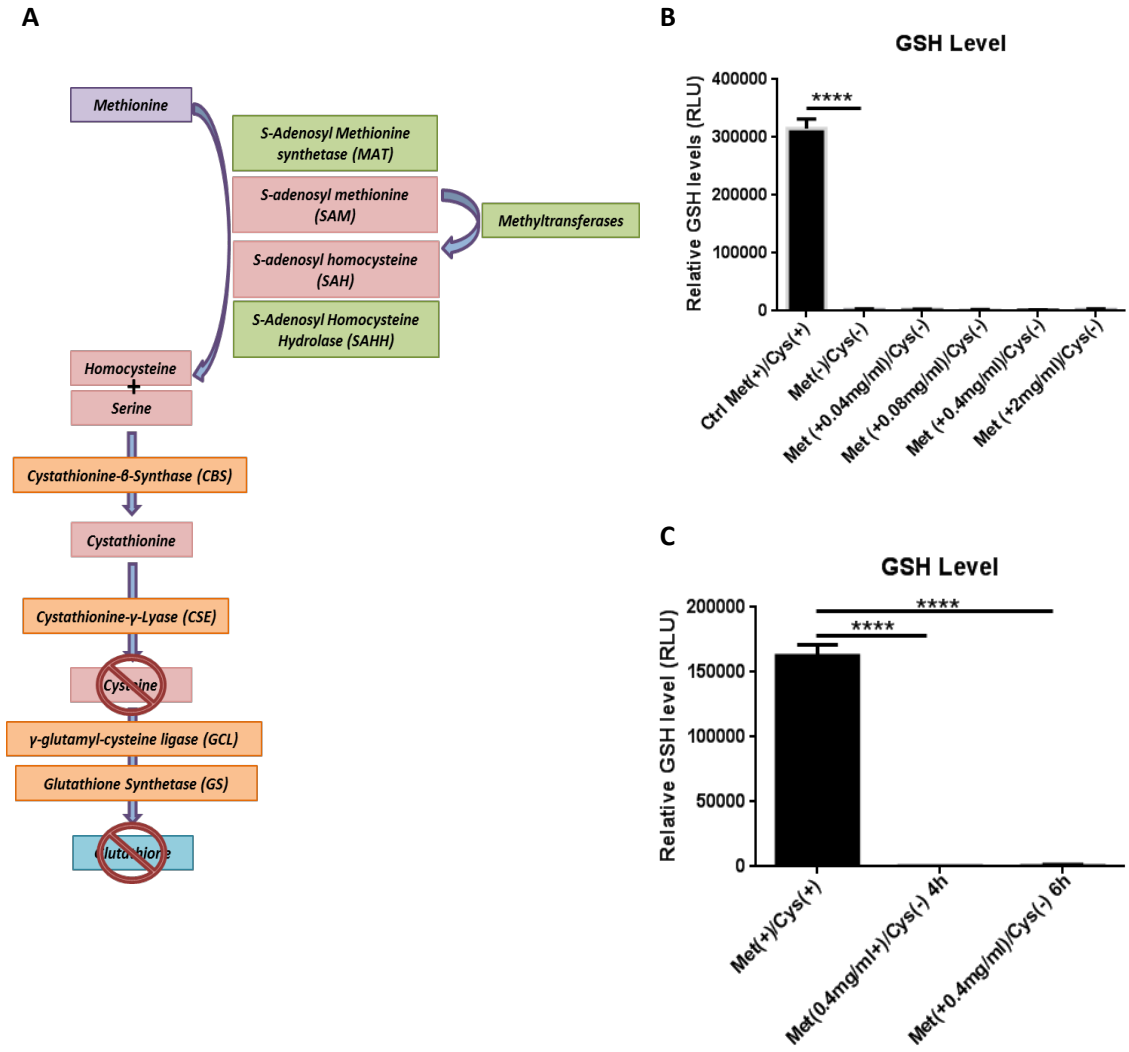

Figure 3.14: Methionine Repletion Does Not Recover GSH Levels In HUVECs. **A)** A schematic diagram depicting the demethylation and transsulfuration pathways indicating the presence of methionine and absence of cysteine as well as a loss in glutathione (GSH) arising from reduced cysteine bioavailability. **B)** Total GSH levels in HUVECs when cysteine and methionine are removed from tissue culture media (Met(-)/Cys(-)) and when methionine is supplemented at increasing concentrations (Met(+)/Cys(-)) for 24 hours. **C)** Total GSH levels in HUVECs when cysteine is removed from tissue culture media and methionine is supplemented at 0.4mg/ml (Met(0.4mg/ml+)/Cys(-)) for 4 and 6 hours. N=3, **** = P=<0.0001. Statistical analyses performed using one-way ANOVA and a Tukeys post-hoc test.

To further confirm that the loss of GSH in HUVECs treated with media lacking cysteine and methionine was due to an inability of cells to generate cysteine

through transsulfuration, HUVECs were incubated with media lacking both methionine and cysteine but containing 0.063mg/ml NAC, a cysteine donor. Figure 3.15B shows that the presence of NAC rescued GSH levels in HUVECs despite methionine being absent. Taken together these data suggest that an active transsulfuration pathway is not present in HUVECs.

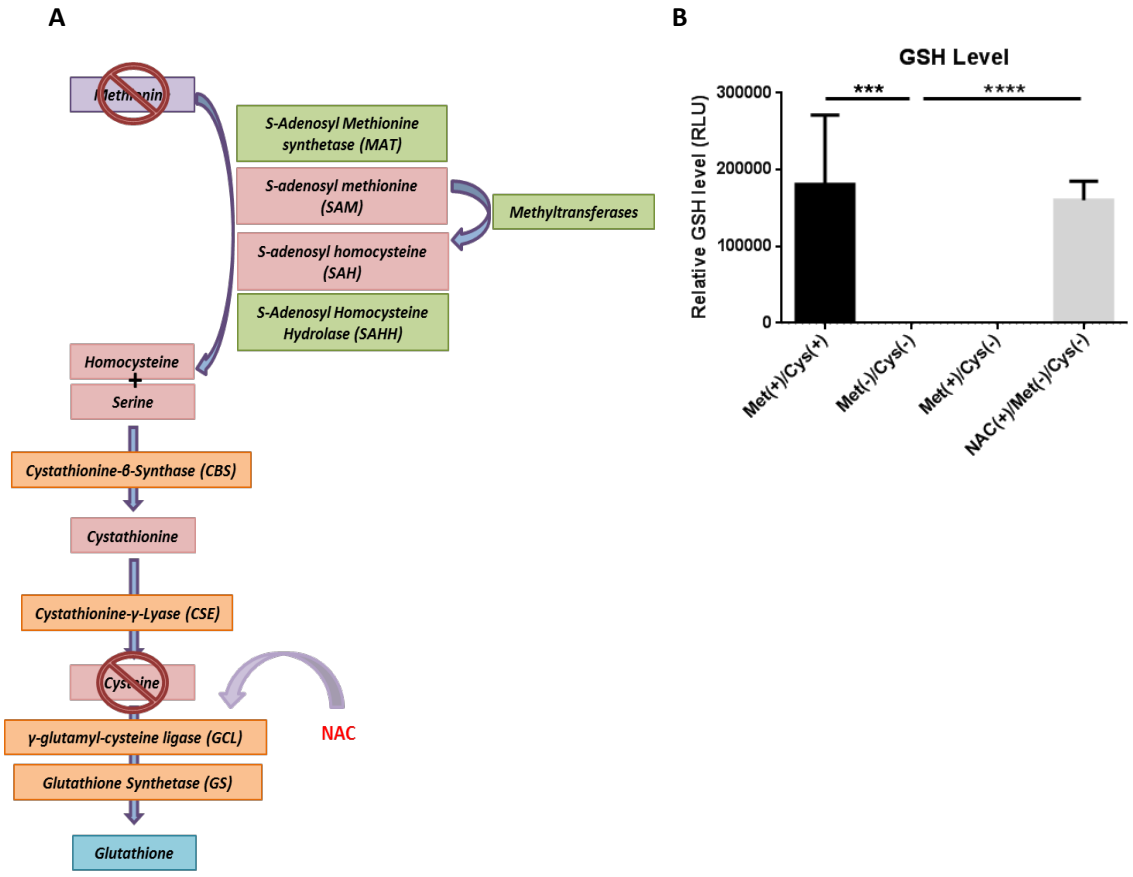

Figure 3.15: NAC Rescues GSH Levels in HUVECs. A) A schematic diagram depicting the demethylation and transsulfuration pathways indicating the absence of methionine and cysteine and the addition of NAC leading to GSH rescue. **B)** Total GSH levels in HUVECs when cysteine and methionine are removed from tissue culture media (Met(-)/Cys(-)), when methionine is supplemented at 0.4mg/ml (Met(+)/Cys(-)) and when 0.063mg/ml NAC is added (NAC(+)/Met(-)/Cys(-)) for 24 hours. N=3, *** = P<0.001, **** = P=<0.0001. Statistical analysis performed using a one-way ANOVA and a Tukeys post-hoc test.

3.2.15 Nox4 Overexpression Increases H_2S Levels in Tissue Culture Media

In addition to transsulfuration, CSE is also a primary mediator of H_2S production in the endothelium. To determine whether the Nox4-induced increase in CSE protein expression functioned to increase H_2S generation in HUVECs, H_2S levels were determined in the culture media of HUVECs overexpressing Nox4 or B Gal using the methylene blue assay. Figure 3.16 shows that H_2S levels are slightly, but significantly increased in the tissue culture media of cells overexpressing Nox4 compared to B Gal controls. Taken together with the transsulfuration data shown above, these data suggest that CSE is likely to be functioning in the production of H_2S and not in the *de novo* synthesis of cysteine in HUVECs.

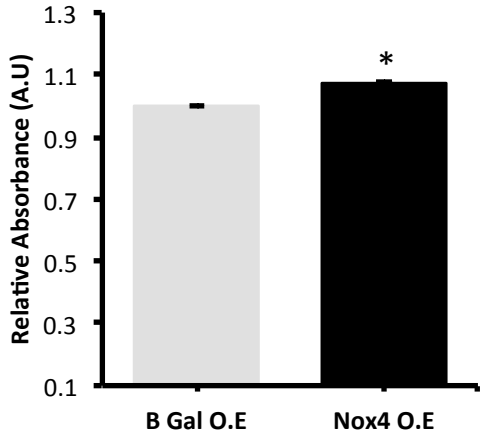

Figure 3.16: H_2S Levels are Increased Upon Nox4 Overexpression. Relative H_2S levels in tissue culture media following 48 hours Nox4 (Nox4 O.E) or B Gal (B Gal O.E) overexpression in HUVECs. N=8, * = P<0.05. Statistical analysis performed using an unpaired Students *t*-test.

3.2.16 CSE Splice Variants 1 and 2 are Up-regulated in Response to Nox4 Overexpression

The mechanism by which CSE switches between canonical transsulfuration and H_2S biosynthesis is unknown. However, the human CSE gene is known to give rise to at least 3 protein-coding splice variants (http://www.ensembl.org/Homo_sapiens/Gene/Summary?db=core;g=ENSG00000116761;r=1:70411218-70439851) whose expression may provide clues as to their functional significance.

To investigate which of these are expressed in HUVECs, primers were designed that could detect all 3 variants and the expression of these isoforms was determined by PCR and subsequently confirmed by DNA sequencing. Figure 3.17 indicates the presence of splice variants 1 and 2 in HUVECs, while splice variant 3 was not readily detectable. Of the 2 variants observed, variant 1 appears to be more abundantly expressed than variant 2.

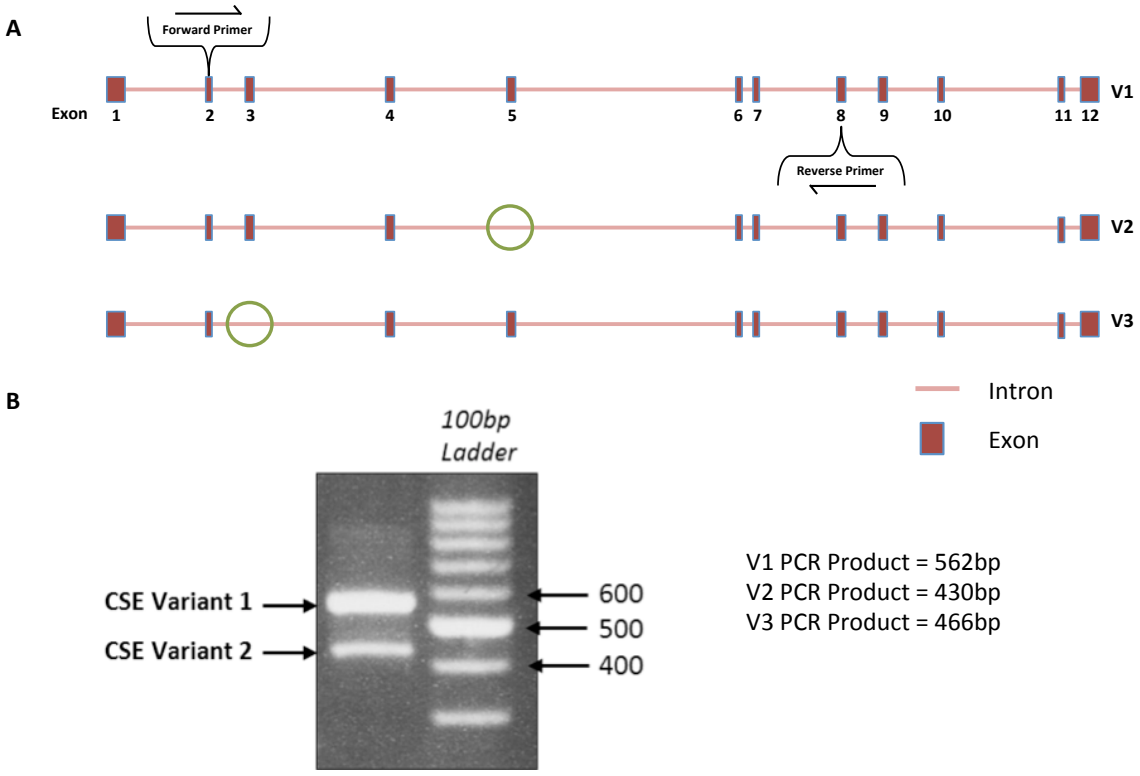

Figure 3.17: CSE Splice Variants 1 and 2 are Detectable in HUVECs. A) A schematic alignment of all 3 protein-coding CSE splice variants showing that the forward primer anneals to sequences in exon 2 and the reverse primer anneals to sequences in exon 8. The schematic also depicts the absence of exon 5 in variant 2, and exon 3 in variant 3 (green circles). **B)** Separation of PCR fragments generated from HUVEC cDNA, using the indicated primers, indicates the expression of CSE splice variants 1 and 2, by comparison to a 100bp ladder. The expected sizes of each PCR amplicon for each variant are indicated. V = variant. N=1.

To investigate which CSE splice variant(s) responded to Nox4 overexpression QPCR was used in combination with exon-specific primers to detect the relative levels of these two isoforms in HUVECs. Figure 3.18A confirms that CSE splice variant 1 is the most abundant form of CSE expressed in HUVECs at base line, and that both variant 1 and 2 are increased in response to Nox4 overexpression. Figure

3.18B shows that there is no difference in the relative Nox4-induced increase in both variant 1 and 2.

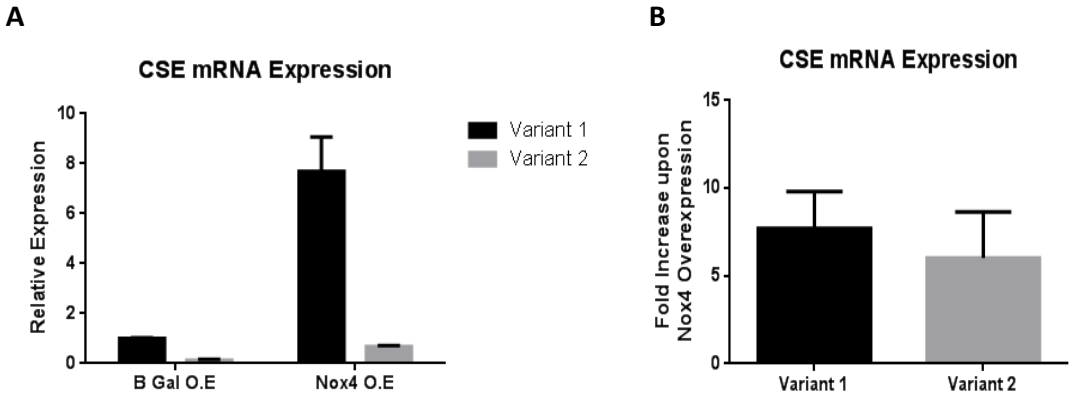

Figure 3.18: CSE Splice Variants 1 and 2 both Respond to Nox4 Overexpression. A) QPCR data depicting the relative expression of CSE splice variants 1 and 2 between B Gal (B Gal O.E) and Nox4-overexpressing (Nox4 O.E) HUVECs. **B)** a comparison of the relative Nox4-induced increase in CSE expression between variant 1 and 2. All data normalised to β Actin mRNA expression. O.E = Overexpression N=3.

3.2.17 Nox4 Does Not Affect the Expression of 3MST in HUVECs

A third H_2S-generating enzyme, known as 3MST, is also present in endothelial cells[63]. To investigate whether Nox4 was involved in regulating 3MST expression, Nox4 overexpression and silencing experiments were performed as above. Figure 3.19 A and B demonstrate that neither overexpression nor silencing of Nox4 have any significant effect on 3MST mRNA expression levels. Thus these data suggest that in HUVEC, Nox4 overexpression results in increased CSE transcription that subsequently increases the production of the gasotransmitter H_2S.

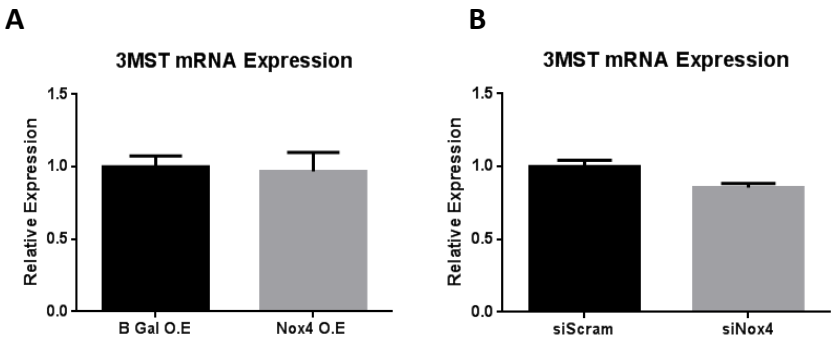

Figure 3.19: 3MST mRNA Expression Remains Unchanged In Response to Nox4 Overexpression. A) QPCR data depicting the relative mRNA expression of 3MST resulting from the overexpressing B Gal (B Gal O.E) and Nox4 (Nox4 O.E) in HUVECs and **B)** HUVEC in which Nox4 has been silenced (siNox4) compared to control cells (siScram). All data normalised to β Actin mRNA expression. N=3. Statistical analysis performed using an unpaired Students *t*-test.

3.3 Discussion

3.3.1 Endothelial Nox4 Regulates CSE Expression

Various aspects of hcy metabolism and H_2S biosynthesis have previously been shown to be redox regulated, particularly with regard to the post-translational activation of CBS[92, 156] and the transcriptional regulation of CSE[99, 100]. Interestingly, indirect evidence derived from the use of broad-spectrum Nox and ROS inhibitors suggest that these redox mechanisms may be Nox dependent[100]. Moreover, direct genetic evidence derived from a genome-wide association study point to the involvement of Nox4 in regulating hcy levels[157]. Bioinformatic analysis revealed that the SNP in Nox4 identified by this study is located in an intron, suggesting that it may be potentially involved in either the positive or negative regulation of Nox4 expression. Indeed, this may hold functional significance since Nox4 activity is thought to be regulated at the gene expression level[133]. Collectively these data allude to Nox4 as a potential source of ROS involved in the regulation of hcy/H_2S metabolism.

To investigate whether endothelial Nox4 is involved in regulating hcy/H_2S metabolism *in vitro*, Nox4 was misexpressed in HUVECs and the gene expression levels of core enzymes involved in hcy metabolism were analysed. Nox4 misexpression was shown to have little effect on the mRNA expression of methionine- and folate-cycle associated enzymes. By contrast, Nox4 overexpression promoted a highly significant and robust up-regulation in the mRNA expression of both the transsulfuration-associated enzymes, CBS and CSE.

Moreover, Nox4 was shown to be the most abundantly expressed $p22^{phox}$-associating Nox isoform in HUVECs and the silencing of both endogenous Nox4 and $p22^{phox}$ significantly reduced CSE expression. Collectively these data suggest that Nox4 is a physiological regulator of endothelial CSE expression.

The endothelial protein expression of CSE is debated by some research groups[63, 64]. However, CSE silencing experiments performed here demonstrate that CSE protein is indeed detectable at baseline in HUVECs, a finding consistent with some other studies[67]. Nox4 overexpression was shown to significantly enhance CSE protein expression, an effect that was reversed by Nox4 silencing. Interestingly, CBS protein expression was unchanged in response to Nox4 misexpression, despite a robust increase in its mRNA expression upon Nox4 overexpression. This suggests that post-transcriptional mechanisms may be in place to regulate CBS translation in the endothelium. Furthermore, it appears that the redox-driven post-translational regulation of CBS is an important factor in regulating its function[92, 156]. These data shed light on a role for endothelial Nox4 as a potential source of ROS involved the regulation of CSE gene expression and further contribute to the growing body of evidence that suggests that CSE transcription is redox regulated[99, 100].

3.3.2 Exogenous Oxidants and Antioxidants on CSE Expression

As mentioned above, previous studies have shown that CSE transcriptional expression is regulated by H_2O_2[99] and have suggested that Nox-derived H_2O_2 can

also regulate CSE activity[101]. Nox4 is considered to mediate its cellular functions through its regulation of redox-dependent signalling pathways by producing H_2O_2. Previous studies using the same Nox4 adenovirus utilised in the experiments conducted here, have shown that it produces significant levles of H_2O_2 in HUVECs[47]. Investigations were therefore performed to interrogate the involvement of Nox4-derived ROS in the transcriptional regulation of CSE. Perhaps surprisingly, exogenous application of peroxide, to mimic the effects of Nox4 overexpression, failed to increase CSE expression significantly at the mRNA level, although a slight trend toward an increase was observed. These data are somewhat inconsistent with previous findings showing that CSE expression can be regulated by H_2O_2 in COS7 cells, although that study concluded that the H_2O_2-induced regulation of CSE expression was complex and biphasic[99]. Furthermore, studies performed here assessed CSE expression after a 24 hour H_2O_2 incubation period, whereas these previous reports assessed the H_2O_2-induced induction of CSE expression after a maximum of 1.5 hours. These differences in time-points may suggest the existence of a temporal window in which H_2O_2 can induce CSE expression. Alternatively, H_20_2 may be unstable and therefore lose its signalling efficiency at longer time points. It should also be noted that the use of exogenous ROS to recapitulate the effects of endogenously-generated ROS are not always consistent[161, 162]. A potential explanation for this lies in the fact that exogenous ROS are not compartmentalised in the same way that endogenously-produced ROS are expected to be. Indeed, in the case of Nox4, its signalling capacity is thought to be discrete and environment- specific, owing to its occupation of specific subcellular locations[129]. Taken together, it seems that although treating cells with exogenous ROS can prove useful in helping to decipher the redox regulation of a signalling

pathway[161] it does not directly mimic the effect of endogenously-generated ROS such as that produced by Nox4. This may therefore explain why exogenous ROS does not increase CSE expression in the same way that Nox4 does, at least at the time-points assessed here.

Antioxidants and Nox inhibitors have been frequently used to study the effects of Nox functionality in various systems[163]. DPI is a broad-spectrum Nox inhibitor that functions by inhibiting flavoproteins. Surprisingly, DPI promoted the effect of Nox4 overexpression in the endothelium, an effect that contrasts to the blunting of CSE expression observed in DPI-treated mesangial cells[100]. This suggests that in endothelial cells Nox4 overexpression in the presence of DPI, further activates CSE expression. A potential explanation for this lies in the fact that DPI is non-specific and inhibits all flavoproteins including other Nox isoforms as well as the gasotransmitter producing enzyme, eNOS. Furthermore, DPI has been shown to induce GSH efflux from some cell types leading to apoptosis[164] suggesting that in addition to oxidant inhibition, cellular antioxidant defence is also perturbed. Indeed, the complex cross talk and homeostatic balance integral to redox systems as well as between gasotransmitter signalling may mean that interventions such as DPI administration further displace the Nox4-induced imbalance in redox homeostasis that leads to CSE transcription, resulting in increased CSE expression.

PEG-Cat is an antioxidant involved in converting H_2O_2 into water. Treatment with PEG-catalase resulted in a small but significant blunting in Nox4-induced CSE expression. These data support a role for Nox4-derived H_2O_2 in the regulation of CSE expression but the effect is perhaps surprisingly small. Nox4 was expressed at

a high MOI of 20, which would result in dramatically-enhanced ROS production. PEG-cat was used at 500U/ml and, being an enzyme, it may have rapidly reached its maximal velocity (Vmax) in the presence of high amounts of Nox4-derived H_2O_2. The small blunting effect observed could therefore be a result of Nox4 continuing to signal when catalase activity is saturated. This discrepancy could possibly be resolved by further increasing the amount of catalase used or reducing the MOI of the Nox4 adenovirus, thereby changing the stoichiometry of the reaction. In addition, studies in bacteria have shown that sulphide can inhibit catalase[165], suggesting that H_2S produced by CSE could potentially inactivate PEG-cat and thus prevent a more robust blunting in the Nox4-induced increase in CSE expression. Finally, with regard to all antioxidants and exogenous ROS used in these assays, an important factor that has not been investigated is the temporal relationship between the ROS-induced CSE expression and antioxidant treatment. It may be that antioxidants can blunt CSE expression in response to Nox4 overexpression, but only when applied at a specific time-point or for a longer duration. This is something that merits further work.

3.4.3 HUVECs Do Not have a Functional Transsulfuration Pathway but can Generate Increased H_2S levels in Response to Nox4

CBS and CSE have been shown to be bi-functional enzymes, in that they can perform canonical transsulfuration which involves the conversion of hcy into cysteine, as well as generating H_2S from cysteine, homocyteine and cystine[166]. Most of the literature surrounding the role of endothelial CSE focuses on its H_2S-generating capacity as opposed to its role in transsulfuration[20, 67, 79, 83, 101]. To

determine whether HUVECs were able to mediate transsulfuration and therefore provide clues as to the endogenous function of CSE in endothelial cells, HUVECs were grown in media lacking in cysteine but containing increasing concentrations of the indirect substrate for transsulfuration, methionine. To assess cysteine bioavailability arising from transsulfuration activity, GSH levels were used as a measure as reported previously[97, 98]. Methionine failed to increase GSH levels in a time- and dose-dependent manner in HUVECs, and only the repletion of cysteine by the addition of NAC could recue GSH levels. These data demonstrate that HUVECs are unable to generate cysteine *via* the transsulfuration pathway and therefore suggest that endothelial CSE likely functions in the generation of H_2S. Indeed, the assessment of H_2S production in HUVECs showed a small but significant elevation in the levels of H_2S detected in tissue culture media upon Nox4 overexpression. It would also appear from these data that the Nox4-induced increase in H_2S levels is a result of increased CSE expression and not due to an effect of other H_2S-generating enzymes. Thus CBS protein expression failed to change in response to Nox4 overexpression, and 3MST mRNA expression was not augmented upon Nox4 misexpression.

3.4.4 Experimental Caveats in H_2S measurements using Methylene Blue

The methylene blue assay is the most commonly used analytical procedure for measuring sulphide as it has a low detection limit (micromolar), is cheap and is simple to perform. Despite this, there are a number of caveats associated with it. Firstly, the assay relies on the use of strong acid to liberate H_2S from a zinc trap,

and this acid can mobilise H_2S from cellular acid labile stores, leading to errors in endogenous enzymatically- produced H_2S measurements. However, this is unlikely to affect the experimental protocol used in this investigation, since extracellular H_2S was being measured and acid labile stores are found in primarily in the mitochondria[167, 168]. Furthermore, methylene blue has been shown to produce monomers, dimers and trimers when reacted with H_2S and therefore measuring absorbance at 670nm (corresponding to the dimeric product) may lead to erroneous read-outs, since trimeric products are not considered[168-170]. The experimental protocol used here involved the removal of media from incubated cells to take a "snapshot" of H_2S levels. This is difficult to achieve since H_2S is readily oxidised and dissipates quickly in air preventing accurate quantification of its cellular levels. Overexpression of Nox4, and its subsequent enhancement in ROS production, may therefore deplete H_2S through oxidation and further complicate its accurate quantification[171]. In spite of this, the assay continues to be used extensively in measuring H_2S levels in tissue as well as cells, and can be used relatively reliably to compare levels of H_2S. Despite these caveats, the data presented here suggest that the Nox4-induced increase in CSE expression results in a concomitant increase in H_2S levels in HUVECs.

3.4.5 CSE Splice Products

Alternative splicing is reported to occur in around 40-60% of genes and this form of regulation is important in controlling the differential activities of specific genes[172]. Human CSE is known to have at least 3 protein-coding splice variants that

differ from each other by the absence of either exon 5 (splice variant 2) or exon 3 (splice variant 3). It is currently unknown what the functional significance of each splice variant is. It was shown here that variants 1 and 2 are present in HUVECs with variant 1 being the most abundantly expressed. Interestingly, Nox4 up-regulates the expression of both variant 1 and variant 2, and a comparison between the relative Nox4-induced increase between variants reveals that both transcripts are up-regulated to a similar extent. These data suggest that CSE splice variants 1 and 2 are both responsive to Nox4 overexpression and may therefore play a role in H_2S production.

To summarise, the data collected in this chapter demonstrate that endothelial Nox4 is a physiological regulator of CSE expression, an effect that appears to be important for H_2S generation. These data contribute to the growing body of evidence that suggest that ROS can regulate CSE expression and further implicates endothelial Nox4 as a potential source of ROS in this process.

Chapter 4: Results 2

4.1 Introduction

In the previous chapter data are presented which describe a physiological role for Nox4 in the regulation of CSE mRNA and protein expression, which appears to be important in the generation of the gasotransmitter, H_2S. CSE and H_2S are known to be mediators of blood pressure regulation[79] and vascular tone[20, 81], in that they have been shown to induce vasorelaxation, potentially in an endothelium-dependent manner[20]. With this in mind, eNox4 Tg mice were used to investigate the effect of Nox4 overexpression on CSE expression and activity *ex vivo.*

Aim

To determine whether endothelial-specific overexpression of Nox4 in the mouse also functions to regulate CSE expression and to determine the functional significance of this.

4.2 Results

4.2.1 Genotyping eNox4 Transgenic Mice

The following studies involve the use of eNox4 Tg mice which were generated in our laboratory. The transgene comprises the previously-described endothelial-specific Tie2 promoter/enhancer construct[173] driving the expression of the entire mouse Nox4 cDNA coding region. Heterozygous Tg/WT crosses were set up in order to generate equal numbers of WT and eNox4 Tg mice, and the presence or absence of the Nox4 transgene was determined by genotyping. Figure 4.1 depicts a representative genotyping result for the eNox4 Tg mouse line. Here, two WT and one eNox4 Tg mouse are present among the litter. The Nox4 transgene is identified as a band at ~120bp which is apparent in the positive control DNA isolated from a previously characterised eNox4 Tg mouse. Primers which detect a genomic region corresponding to a GAPDH pseudogene were used as a positive control to confirm that the PCR reactions were successful.

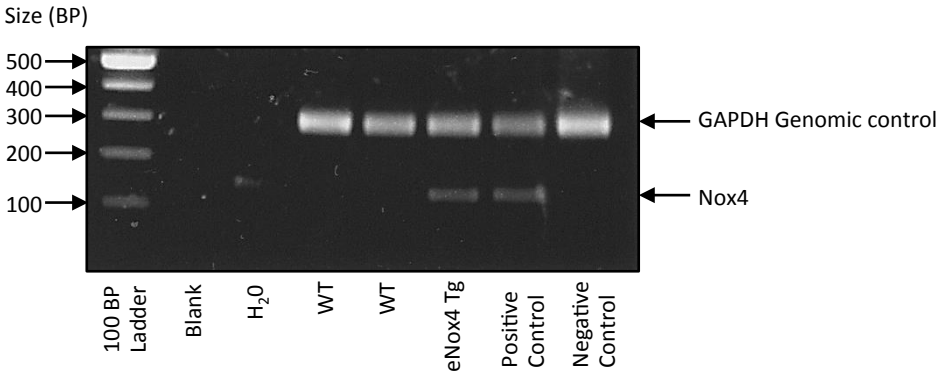

Figure 4.1: Genotyping eNox4 Tg Mice. A Representative genotyping result for eNox4 Tg mice. PCR analyses and subsequent gel electrophoresis of genomic DNA derived from an eNox4 Tg mouse litter. eNox4 Tg mice are identifiable by a band at ~120bp corresponding to the Nox4 transgene. GAPDH control primers generate a band at ~300bp and were used as a control to confirm successful PCR.

4.2.2 Determination of CSE mRNA Expression in eNox4 Tg Mice

In order to determine whether the Nox4-induced up-regulation in CSE mRNA and protein expression observed *in vitro* was recapitulated in endothelial cells *in vivo*, endothelial cells were isolated from the hearts of WT and eNox4 Tg mice.

4.2.3 Endothelial Cells were Enriched Following Isolation

To isolate endothelial cells from the hearts of WT and eNox4 Tg mice an affinity isolation method was developed that permitted the rapid and crude isolation of cardiac microvascular endothelial cells (CMEC) (Details of this protocol can be found in section 2.22). To determine whether endothelial cells were successfully isolated from the hearts of WT and eNox4 Tg mice, the relative expression of von

Willebrand Factor (vWF) mRNA (an endothelial-specific marker[174]) was determined in "input" (total cell isolate) and "output" samples (CD31-affinity-isolated endothelial cells). Figure 4.2A depicts a schematic flow diagram of the steps undertaken in this protocol highlighting when "input" and "output" samples were harvested. Figure 4.2B and C show that in both WT and eNox4 Tg isolations vWF mRNA was enriched in the "output" sample compared to the "input" sample.

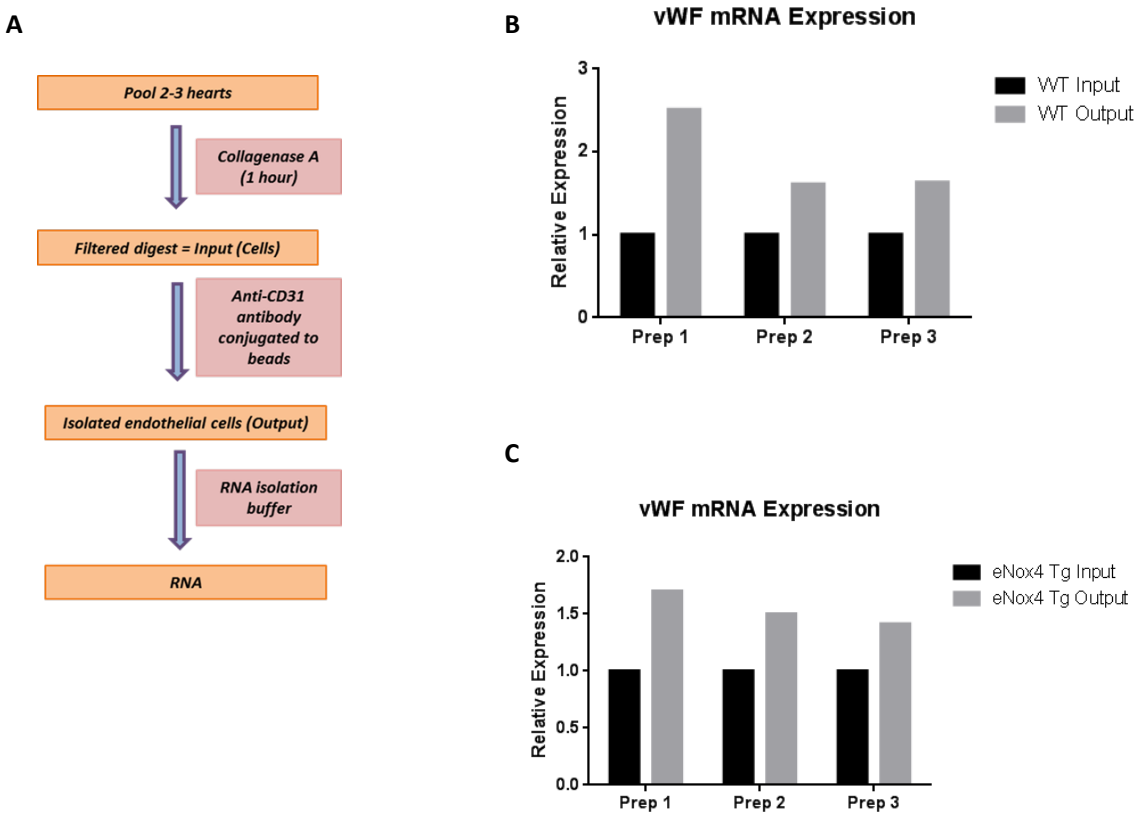

Figure 4.2: Enrichment for vWF Following Endothelial Cell Affinity-isolation. **A)** A flow diagram indicating the steps taken in the endothelial cell affinity isolation method. **B,C)** QPCR data comparing input and output samples for enrichment of vWF in **B)** WT and **C)** eNox4 Tg mouse lines before and after affinity isolation. All data normalised to β Actin mRNA expression. N=3 preparations, each preparation representing a pool of 2-3 hearts/genotype of mixed sexes.

4.2.4 Nox4 mRNA Expression is Potentially Increased in eNox4 Tg Mice

Endothelial cells isolated from WT and eNox4 Tg mice hearts were compared for expression of Nox4. Figure 4.3A and B show that Nox4 mRNA expression is greatly increased in the endothelium of eNox4 Tg mice compared to WT littermates.

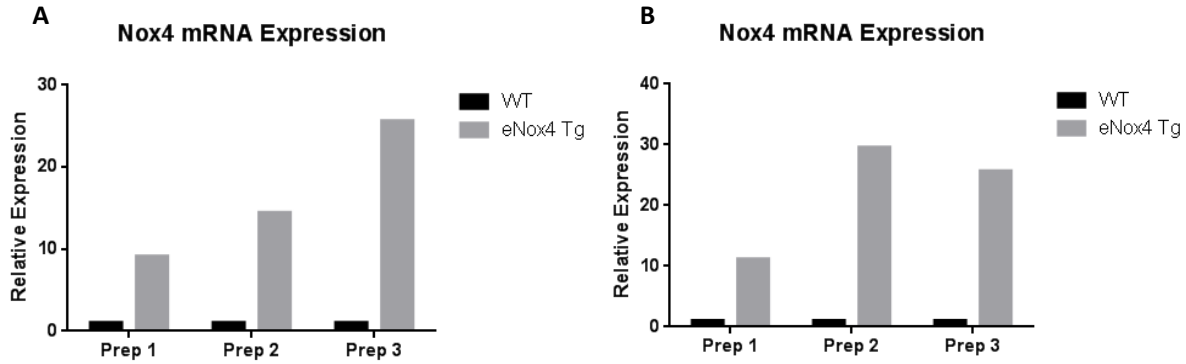

Figure 4.3: Endothelial Nox4 mRNA Expression is Increased in eNox4 Tg Mice. QPCR data comparing the endothelial expression of Nox4 mRNA between WT and eNox4 Tg lines. **A)** data normalised to vWF mRNA expression, **B)** data normalised to β Actin mRNA expression. N=3 preparations, each preparation representing a pool of 2-3 hearts/genotype of mixed sexes.

4.2.5 CSE mRNA Expression is Potentially Increased in eNox4 Tg Mice

To investigate whether CSE expression was increased in endothelial cells isolated from eNox4 Tg mice, compared with WT littermates, CSE mRNA expression was measured by QPCR. Figure 4.4A and B shows that CSE mRNA expression is increased in eNox4 Tg mice compared to WT littermates.

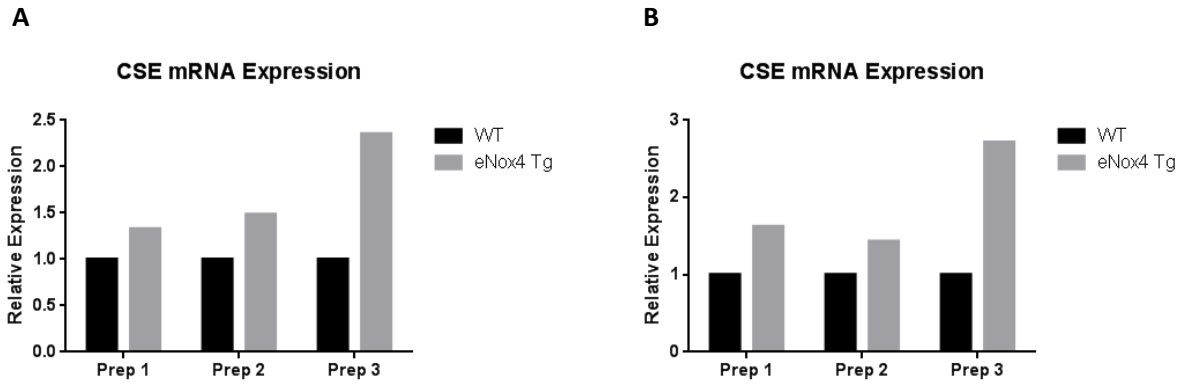

Figure 4.4: **Endothelial CSE mRNA Expression is Increased in eNox4 Tg Mice.** QPCR data comparing the endothelial expression of CSE mRNA between WT and eNox4 Tg lines. **A)** data normalised to vWF mRNA expression, **B)** data normalised to β Actin mRNA expression. N=3 preparations, each preparation representing a pool of 2-3 hearts/genotype of mixed sexes.

4.2.6 CSE Protein Expression is Significantly Increased in eNox4 Tg Mice

To determine whether the observed increase in CSE mRNA expression corresponded to a change in CSE protein expression, endothelial cell isolates from WT and eNox4 Tg mice were harvested for immunoblotting and CSE protein expression was compared. Figure 4.5A and B shows that CSE protein levels are significantly elevated in eNox4 Tg mice compared to WT littermates. Taken together with the mRNA data depicted above, these data demonstrate that Nox4 regulates CSE expression in the vascular endothelium, *in vivo*.

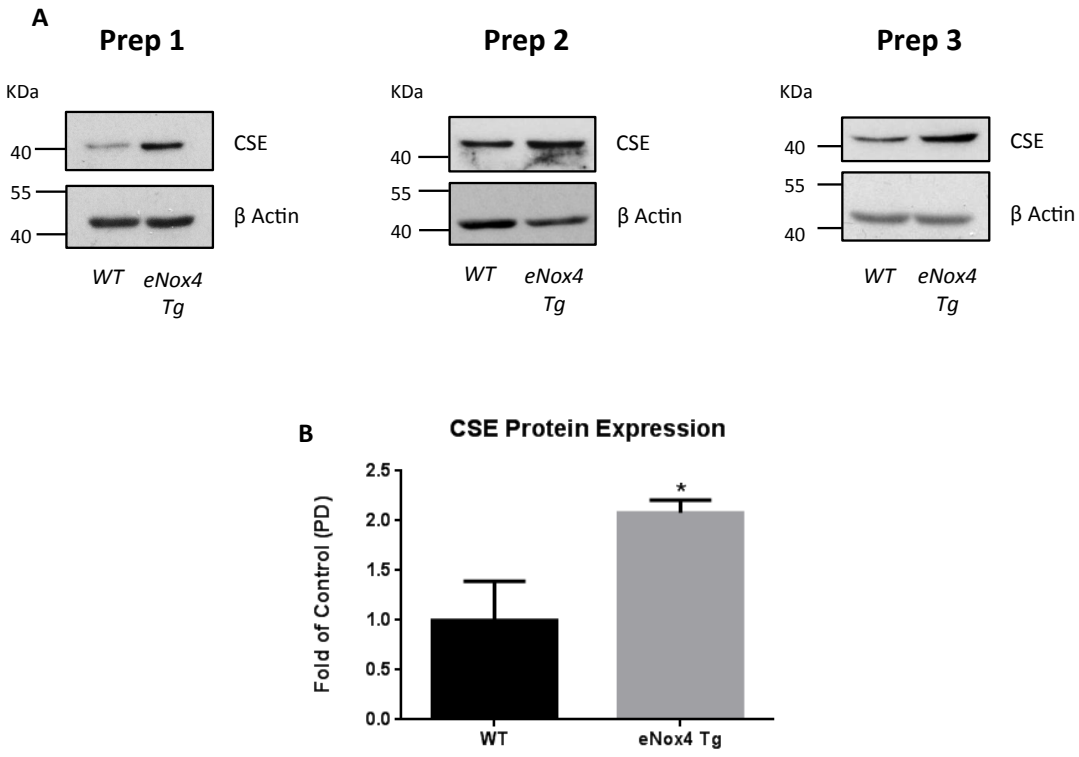

Figure 4.5: **Endothelial CSE Protein Expression is Significantly Increased in eNox4 Tg Mice. A)** Immunoblot data comparing CSE protein expression in the endothelium of WT and eNox4 Tg lines. **B)** Corresponding densitometric analysis of CSE protein expression. Data normalised to β Actin protein expression. N=3 preparations, each preparation representing a pool of 2-3 hearts/genotype of mixed sexes. * = $P<0.05$. Statistical analysis performed using an unpaired Students *t*-test.

4.2.7 Measuring H_2S Levels *ex vivo* using a Polarographic Sensor

To investigate whether the Nox4-induced increase in CSE expression observed in eNox4 Tg mice resulted in changes in tissue H_2S levels, a polarographic H_2S sensor probe based on that developed by Kraus *et al* [175] was utilised.

4.2.8 The Polarographic H_2S Sensor can Detect Increasing H_2S Concentrations in NaHS Standard Controls

In order to test the efficiency of the H_2S sensor, the probe was assessed for its ability to detect H_2S in known standard control solutions containing NaHS. Figure 4.6 shows that the probe detects H_2S levels in a dose-dependent manner confirming the manufacturers observations and guidelines.

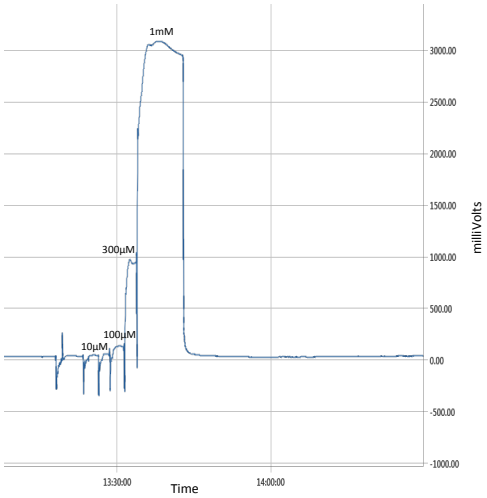

Figure 4.6: Dose-dependent Detection of H_2S using a Polarographic Micro-Sensor. A representative microsensor trace indicating a dose-dependent increase in detectable H_2S levels in solutions containing increasing NaHS concentrations (concentrations indicated on the trace).

4.2.9 H_2S Levels were Unchanged in the Livers of WT and eNox4 Tg Mice

The liver contains a high abundance of the H_2S-generating enzymes CBS and CSE, and therefore provides a useful positive control for the detection of endogenous H_2S. To test whether the probe was capable of detecting endogenously generated H_2S in the liver, the level of H_2S was compared between WT and eNox4 Tg isolated mouse liver pieces. Figure 4.7A shows a representative trace for these experiments indicating that H_2S levels could be detected in the liver when the substrate, L-cysteine was supplied. Figure 4.7B shows that no overall difference in H_2S levels were detectable between WT and eNox4 Tg livers when normalised to weight.

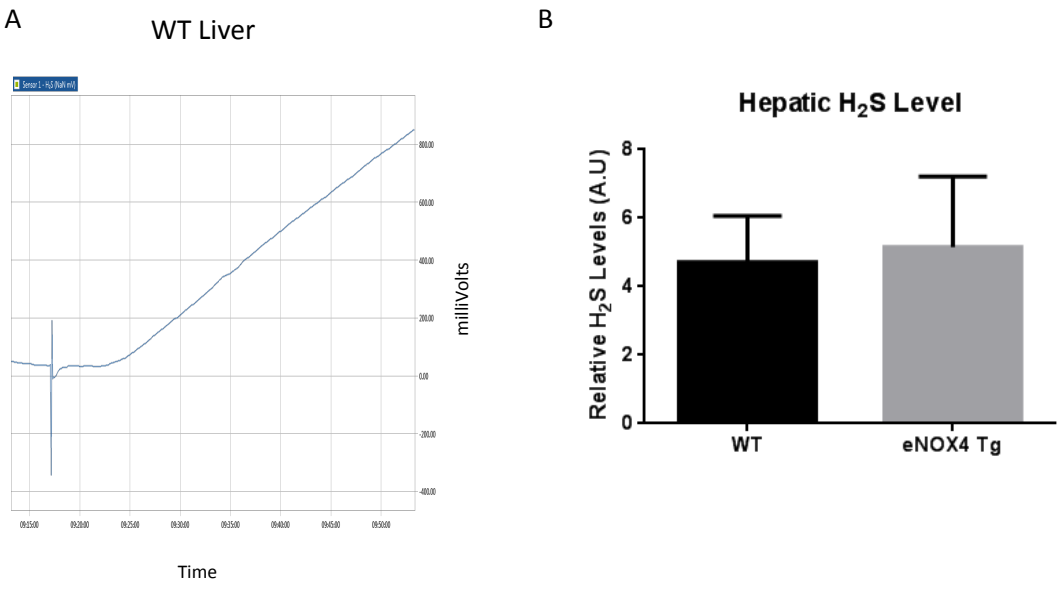

Figure 4.7: H_2S Levels are Unchanged between the Livers of WT and eNox4 Tg Mice. **A)** A representative microsensor trace for a WT liver sample. **B)** A comparison between WT and eNox4 Tg H_2S levels normalised to weight. Analysis was made by taking the millivolt reading obtained 30 minutes after initial H_2S detection for each sample and then normalising this value to the weight of the organ. WT N=6, eNox4 Tg N=7. Statistical analysis performed using an unpaired Students *t*-test.

4.2.10 H_2S was Undetectable in Lung and Heart Tissue

To determine whether differences in H_2S levels could be detected in more vascular tissues, the H_2S probe was used to measure H_2S in pieces of mouse lung and heart isolated from WT and eNox4 Tg mice. Figure 4.8A and B show that H_2S was undetectable in these organ samples even after prolonged incubation with the CSE substrate, L-cysteine, suggesting that the probe was not sensitive enough to detect the small levels of H_2S expected to be released from the vasculature.

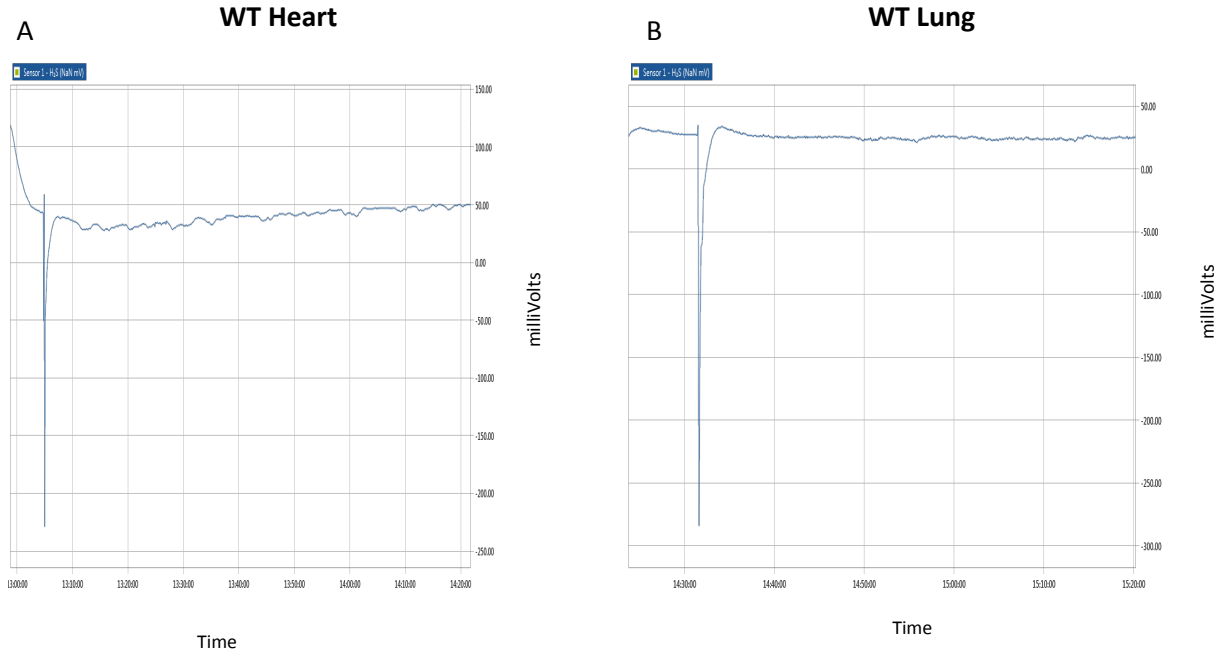

Figure 4.8: H_2S is Undetectable in Heart and Lung Tissue. Representative microsensor traces for **A)** WT heart and **B)** WT lung samples. Indicating no H_2S detection after a 1 hour incubation with L cysteine.

4.2.11 Vascular Contractility

CSE has been shown to have roles in regulating vascular tone[79]. To investigate whether the increase in endothelial CSE protein expression observed in the eNox4 Tg mouse impacted on vascular contractility, aortic vessel tension was compared between WT and eNox4 Tg mice using *ex vivo* wire myography.

4.2.12 Aortic Vessel Constriction to 60 mM KCl Remains Unchanged Between WT and eNox4 Tg mice

To begin to assess whether WT and eNox4 Tg aortae exhibit a difference in vasoconstriction, peak aortic constriction to the depolarising agent KCl was first measured. Figure 4.9 shows that no difference in the aortic contractility to KCl was apparent between the two genotypes.

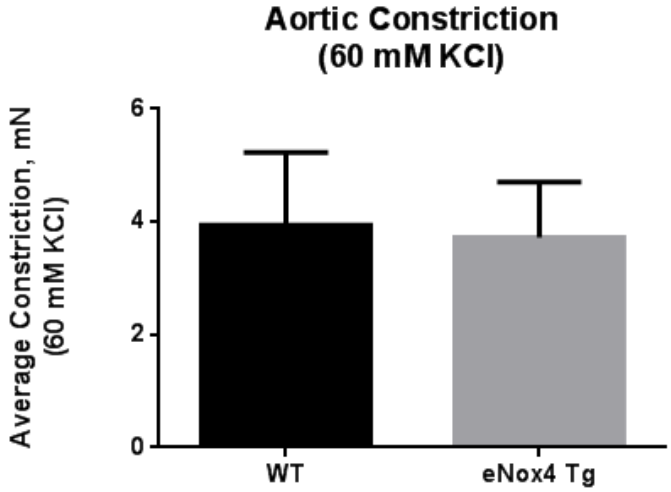

Figure 4.9: High KCl Induces Equivalent Constriction in WT and eNox4 Tg Aortae. A comparison of total aortic contraction to 60 mM KCl between WT and eNox4 Tg mice. WT N= 8 (12rings), eNox4 Tg N=6 (9 rings). Statistical analysis performed using an unpaired Students *t*-test.

4.2.13 eNox4 Tg Aortae are Hypo-contractile Compared to WT Littermates in Response to Phenylephrine (PE)

To further assess whether a difference in contractility exists between WT and eNox4 Tg aortae, vessels were constricted to increasing concentrations of the α1 adrenoreceptor agonist, phenylephrine (PE). Figure 4.10 shows that eNox4 Tg aortae are significantly less contractile in response to PE than WT littermates.

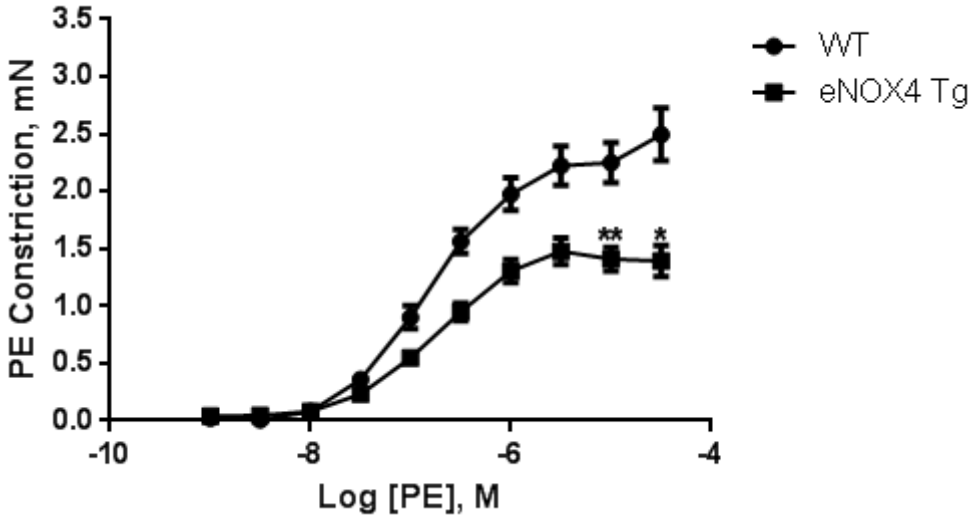

Figure 4.10: eNox4 Tg Aortae are Hypo-contractile compared to WT Controls. A comparison of PE-induced, dose-dependent aortic constriction (up to 30 μM) between WT and eNox4 Tg mice. WT N= 8 (12rings), eNox4 Tg N=6 (9 rings). * = $P<0.05$, ** = $P<0.01$. Statistical analysis performed using a 2 way ANOVA, followed by a Tukeys post-hoc test.

4.2.14 The eNox4 Tg Hypo-contractile Phenotype is H_2O_2-independent

To determine whether Nox4-derived H_2O_2 was responsible for the hypo-contractile phenotype observed in eNox4 Tg mice, aortae were pre-incubated with

PEG-catalase prior to PE-induced constriction. Figure 4.11 shows that PEG-catalase had no effect on the hypo-contractile phenotype observed in eNox4 Tg mouse aortae with respect to WT littermates, over the time scale of these experiments. These data suggest that Nox4-derived H_2O_2 is not involved in the hypo-contractile phenotype, at least in an acute manner.

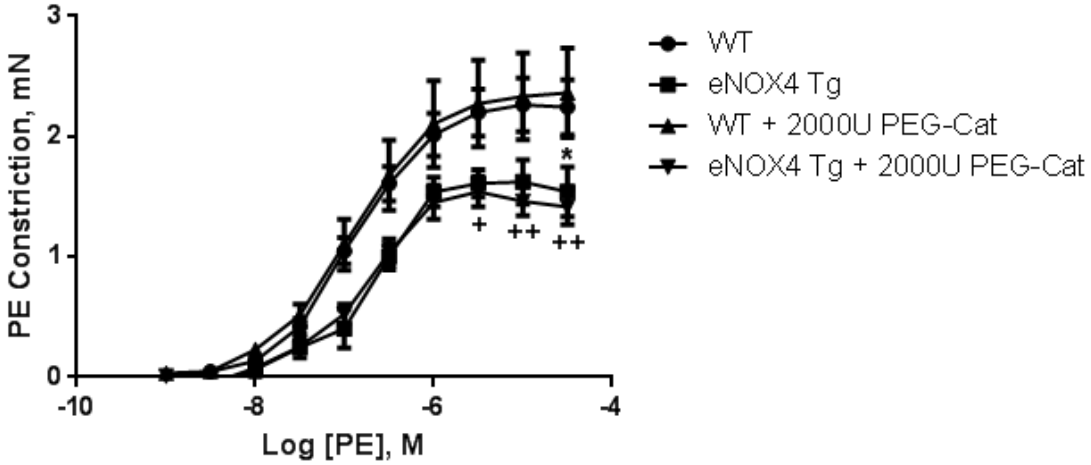

Figure 4.11: PEG-Catalase Does Not Affect the eNox4 Tg Hypo-contractile Phenotype. A comparison of PE-induced, dose-dependent aortic constriction (up to 30 μM) between WT and eNox4 Tg mice, with and without 20 minutes pre-incubation with 2000U/5 ml PEG-catalase (PEG-Cat). WT N= 7 (13rings), eNox4 Tg N=4 (5 rings), WT +PEG-Cat N=5 (8 rings), eNox4 Tg + PEG-Cat N=5 (8 rings). * = $P<0.05$ (* compares WT with eNox4 Tg), **+** = $P<0.05$, **++** = $P<0.01$ (**+** compares WT + PEG-Cat with eNox4 Tg + PEG-Cat). Statistical analyses performed using a 2 way ANOVA, followed by a Tukeys post-hoc test.

4.2.15 The eNox4 Tg Hypo-contractile Phenotype is Dependent on CSE Activity

To investigate whether the increased expression of CSE seen in the eNox4 Tg mouse was responsible for the observed hypo-contractile phenotype, aortae were

pre-incubated with the CSE inhibitor, propargylglycine (PPG), prior to PE-induced constriction. Figure 4.12 shows that administration of PPG normalises eNox4 Tg constriction to the same level as WT aortae treated with PPG, completely ablating the hypo-contractile phenotype observed in eNox4 Tg vessels. These data are consistent with a role for increased CSE expression in mediating the hypo-contractile phenotype observed in the eNox4 Tg mouse. WT vessels treated with PPG also showed an increase in contractility but this difference did not reach significance at the sample size assessed in these experiments.

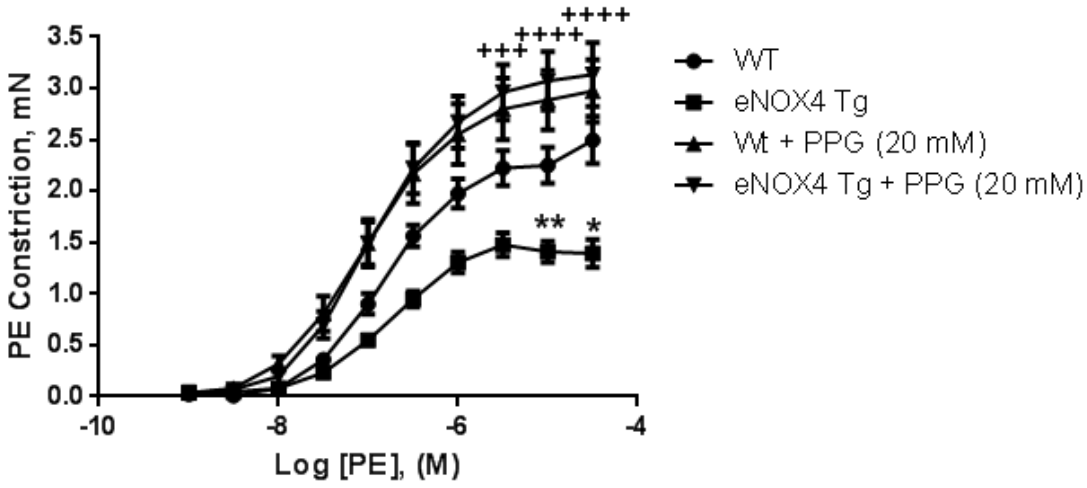

Figure 4.12: CSE Inhibition Ablates the eNox4 Tg Hypo-contractile Phenotype. A comparison of PE-induced, dose-dependent aortic constriction (up to 30 μM) between WT and eNox4 Tg mice, with and without 30 minutes pre-incubation with 20 mM PPG. WT N= 8 (12 rings), eNox4 Tg N=6 (9 rings), WT +PPG N=8 (13 rings), eNox4 Tg + PPG N=9 (16 rings). * = P<0.05, ** = P<0.01 (* compares WT with eNox4 Tg), **+++** = P<0.001, **++++** = P<0.0001 (**+** compares eNox4 Tg with eNox4 Tg + PPG). Statistical analyses performed using a 2 way ANOVA, followed by a Tukeys post-hoc test.

4.2.16 Endothelial-specific Nox4-Null Mice show no Difference in Contractility to PE at Baseline

The following studies involve the use of endothelial-specific Nox4-null mice (eNox4$^{-/-}$). These mice were generated by crossing Nox4$^{flox/flox}$ mice with endothelial-specific Tie2-Cre overexpressing transgenic mice (Nox4$^{flox/flox}$ Cre^{+})[173]. Nox4$^{flox/flox}$ females were crossed with Nox4$^{flox/flox}$ Cre^{+} males in order to generate equal numbers of control Nox4$^{flox/flox}$ and eNox4$^{-/-}$ mice. The presence or absence of the Cre-recombinase transgene was determined by genotyping. Figure 4.13 depicts a representative genotyping result for the eNox4$^{-/-}$ mouse line. Here one Nox4$^{flox/flox}$ and one eNox4$^{-/-}$ mouse are present among the litter. The eNox4$^{-/-}$ mouse can be identified by a band at ~200bp corresponding to the presence of Cre-recombinase. Primers which detect a genomic region corresponding to a GAPDH pseudogene were used as a positive control to confirm that the PCR reactions were successful.

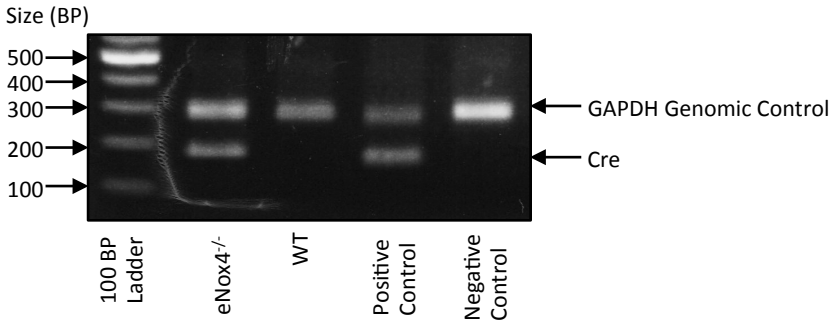

Figure 4.13: Genotyping eNox4$^{-/-}$ Mice. A Representative genotyping result for eNox4$^{-/-}$ mice. PCR analyses and subsequent gel electrophoresis of genomic DNA derived from an eNox4$^{-/-}$ mouse litter. eNox4$^{-/-}$ mice are identifiable by a band at ~200bp corresponding to the Cre-recombinase transgene. GAPDH control primers generate a band at ~300bp and were used as a control to confirm successful PCR.

To determine whether differences also exist between the contractility of eNox4$^{-/-}$ and Nox4$^{flox/flox}$ vessels, aortic vessel contractility was compared in response to KCl and PE. Figure 4.14A and B show that both contractile stimuli induced similar levels of response in vessels irrespective of genotype.

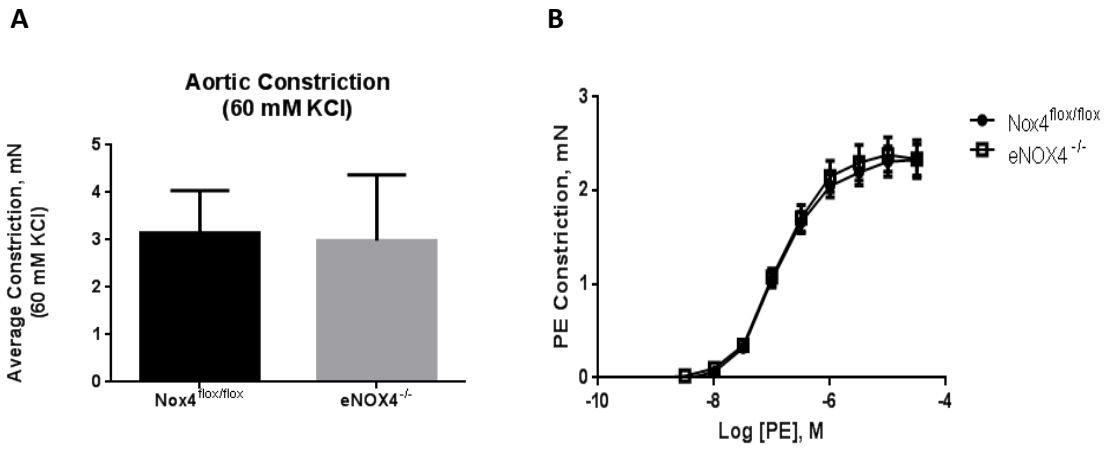

Figure 4.14: Nox4$^{flox/flox}$ and eNox4$^{-/-}$ Aortae Contract Similarly to Both KCl and PE treatments. A) A comparison of total aortic contraction to 60 mM KCl between WT and eNox4$^{-/-}$ mice. **B)** A comparison of PE-induced, dose-dependent aortic constriction between Nox4$^{flox/flox}$ and eNox4$^{-/-}$ mice. Nox4$^{flox/flox}$ N= 6 (12rings), eNox4$^{-/-}$ N=5 (13 rings). Statistical analysis performed using an unpaired Students *t*-test for total constriction to KCl and a 2 way ANOVA followed by Tukeys post-hoc test for PE-induced dose dependent constriction.

4.3 Discussion

4.3.1 Nox4 Regulates CSE Expression in Murine Endothelial Cells

Data presented in the previous chapter of this thesis demonstrate that endothelial Nox4 overexpression is capable of up-regulating CSE mRNA and protein expression *in vitro*. Consistent with these results, data described in this chapter demonstrate that CSE mRNA and protein expression are also up-regulated in endothelial cells isolated from the hearts of eNox4 Tg mice, compared to WT controls. Collectively, these data further support a role for Nox4 in the regulation of CSE transcriptional expression and contribute to the emerging literature surrounding a role for Nox proteins[100] as well as ROS[99] in the control of CSE transcription.

4.3.2 Nox4 and the Regulation of Vascular Tone

The endothelium regulates blood flow and tissue perfusion through its modulation of vascular tone[7]. This process is governed by a number of biomolecules and, of these, ROS are emerging as key mediators. Furthermore, it is thought that vasodilation and constriction are differentially regulated by both the type and source of ROS involved. Indeed, H_2O_2 is considered to play a physiological role as an EDHF[19 45] and can thus induce vasorelaxation. By contrast, O_2^- is involved in vasoconstriction[176] where, amongst other mechanisms, it can deplete NO bioavailability through the formation of peroxynitrite[177]. Accordingly, Nox4 has

been shown to have a number of vaso-protective effects, underscored by its ability to synthesise H_2O_2[47, 151]. Indeed, the eNox4 Tg mice utilised here were shown previously to have improved endothelial function, vasodilation and lower blood pressure when compared to WT controls[47]. Furthermore, Nox4 gene deletion models indicate that Nox4 contributes to vasorelaxation potentially through its regulation of eNOS[151]. In line with a role for Nox4 in the regulation of vascular tone, aortae isolated from eNox4 Tg mice were shown here to be significantly less contractile in response to PE than WT control vessels. These findings are perhaps not fully consistent with previously published data obtained from the same mouse model in which only a small (non-significant) reduction in PE-induced contractility was observed[47]. However, Craige *et al* demonstrated that VE-cadherin-driven endothelial-specific Nox4 overexpressing aortae also displayed significantly less contractility to PE, therefore supporting our observation[150]. These discrepancies in contractile function might be explained by differences in the methods and protocols employed to measure vascular tone. Thus Ray *et al* used an organ bath method[47] whereas a wire myograph, specially designed to detect subtle changes in resistance vessel tension, was utilised here. This could potentially lead to better delineation of contractile differences between genotypes, and account for the discrepancies apparent in these results. Furthermore, a number of experimental factors have been shown to influence vascular contractility, including dissection skills, optimal resting tension, age of the animals, composition of the buffer solutions, temperature of the dissecting medium, and vessel isolation time. Therefore subtle alterations in experimental protocol may account for the observed differences in contractility[178].

4.3.4 CSE Expression and Activity Leads to Hypo-contractility

To assess the potential involvement of the enhanced CSE expression, observed in eNox4 Tg endothelial cells, in mediating the hypo-contractile phenotype, vessels were pre-incubated with the CSE inhibitor, PPG, as previously reported[75]. Here, the addition of PPG normalised contractility between eNox4 Tg and WT vessels to PE, completely ablating the Nox4-induced hypo-contractile phenotype. These data strongly suggest that CSE is a key mediator of this phenotype and are potentially consistent with the emerging role of CSE in H_2S generation. Indeed, a number of studies have characterised CSE as a major vascular generator of H_2S that has been shown to induce endothelium-dependent vasodilation[75, 79, 83]. Furthermore, exogenous application of H_2S to vessels using NaS, NaHS or the slow-releasing H_2S donor drug, GYY4137, have previously been shown to induce vasorelaxation in aortae assessed by wire myogrpahy or in organ bath experiments[65 73, 75-77]. To support this, data demonstrating that incubation of (sub-maximally constricted) aortae with PPG exacerbated constriction, suggesting a role for CSE in the regulation of basal tone[75]. This is further corroborated by data derived from a study in rats showing that PPG alone could increase blood pressure[179], an effect consistent with the hypertensive phenotype observed in $CSE^{-/-}$ mice[79]. Thus, it is apparent from these studies that CSE is a contributor to both basal and inducible vascular tone. Furthermore, it appears that the Nox4-induced hypo-contractile phenotype observed here, is likely due to the enhanced expression and activity of CSE in the endothelium of the eNox4 Tg mouse.

4.3.5 Acute Nox4-induced Hypo-contractility is H_2O_2-independent

The mechanisms that underscore the biochemical actions of H_2S remain contentious. At physiological pH levels, H_2S is predominantly deprotonated (HS^-), and is therefore membrane-impermeable. In this state its cell-cell signalling potential is possibly limited to its transmission through intercellular junctions. Recently it has been suggested that ROS, such as H_2O_2, can oxidise H_2S leading to its conversion into polysulfide species that are relatively membrane-permeable. In this state, polysulphides can enter adjacent smooth muscle to modify muscle dynamics without the need for cell-cell junctions[73 57].

Previous reports by Ray *et al* demonstrated that the enhanced endothelium dependent vasodilation to ACh, observed in eNox4 Tg mice, *was* catalase-inhibitable. This suggests an acute involvement of Nox4-derived H_2O_2 in this process[47], perhaps consistent with a role for H_2O_2 in the oxidation of H_2S to promote its signalling capabilites. To elaborate on these findings and further assess whether Nox4-derived H_2O_2 was also acutely involved in mediating the hypo-contractile phenotype, potentially through a reaction with H_2S and subsequent polysulphide formation, aortae were pre-incubated with the peroxidase enzyme, PEG-catalase. Here, short-term administration of PEG-catalase failed to normalise the Nox4-induced hypo-contractile phenotype, suggesting a H_2O_2-independent mechanism (at least in an acute manner). These data indicate that the hypo-contractile phenotype is likely due to the Nox4-induced increase in CSE expression and subsequent actions of H_2S, which do not involve its ROS-dependent conversion to polysulphide.

Taking these observations together, it appears that Nox4 may act both to promote the endothelial-expression of CSE and H_2S production, and additionally to enable endothelial-derived H_2S to signal within VSMCs upon cholinergic stimulation through the generation of polysulphides. In this setting, scavenging by catalase would act acutely to prevent endothelium-derived H_2S signalling by diminishing polysulphide formation. However, the role of gap junctional intercellular communication, both among and between endothelial cells and VSMCs, is known to be involved in the regulation of vascular tone[180]. Gap junctions provide partial cytoplasmic continuity between cells, allowing the intercellular flux of second messenger molecules between cell types. Pharmacological evaluations have demonstrated the importance of gap junctions in the modulation of contractile responses elicited by α1-adrenergic stimulation[181]. It is therefore possible that stimulation by PE acts to promote gap junction formation resulting in the free intercellular movement of HS^- without the necessity for oxidation by H_2O_2 (and hence the lack of inhibition by catalase in this process). Therefore differences in agonist induced signalling may account for the apparent phenotypic discrepancies discussed above.

To further assess the involvement of endothelial Nox4 in vascular constriction, $Nox4^{flox/flox}$ and $eNox4^{-/-}$ mice aortae were analysed using wire myography as described above. No difference in contractility to KCl or PE was observed between genotypes. Nox4 is thought to be stress-inducible at the level of transcription and therefore the loss of Nox4 may not confer an effect under unstressed conditions. Indeed, studies performed in global Nox4-null mice revealed the requirement for a

stress stimulus (angiotensin II) in order to observe a phenotypic difference in aortic relaxation[151].

An assessment of CSE expression in eNox4$^{-/-}$ endothelial cells was not performed here. However, based on data presented in this thesis in which Nox4 was ablated in HUVEC, *in vitro*, the removal of endogenous Nox4 might also be expected to reduce CSE levels in endothelial cells in *vivo*. However, differences in complexity between *in vitro* and *in vivo* systems may mean that CSE expression remains unchanged in these animals. An assessment of CSE expression in eNox4$^{-/-}$ endothelial cells will therefore be considered for future work, together with an assessment of aortic contractility when eNox4$^{-/-}$ mice are placed under a physiological or pathophysiological stress.

To conclude, Nox4 has been shown to regulate CSE expression in murine endothelial cells at both the mRNA and protein level, resulting in a hypo-contractile phenotype, in response to PE. This phenotype was ablated by the CSE inhibitor PPG and appears to be H_2O_2-independent at an acute level. Collectively these data contribute to existing reports detailing a functional role for both Nox4 and CSE in the regulation of vascular tone, and further implicate Nox4 as a regulator of the production of the gasotransmitter, H_2S in the endothelium.

4.3.6 Experimental Limitations

4.3.6.1 Measuring H_2S levels ex vivo

CSE protein expression was increased in the endothelium of eNox4 Tg mice. Attempts were therefore made to assess H_2S levels in these animals using a polarographic H_2S microsensor[175]. H_2S levels in the liver, an organ known to express high levels of CBS and CSE[182], were detectable, but showed no apparent differences between genotypes. This is likely due to the relatively small contribution of the endothelium to H_2S generation in this organ. Unfortunately, H_2S production was undetectable using the aforementioned probe, in tissues other than the liver, including highly vascularised tissues such as the lung and heart. Previous studies, using different H_2S detection methods, have successfully quantified vascular H_2S levels[79] albeit at low levels[179]. Therefore, the results described here may reflect the sensitivity of the probe used, which may be insufficient to detected the small amounts of H_2S that are expected to be released from the endothelial cell monolayer.

4.3.6.2 Endothelial Cell Affinity Isolation Caveats.

Endothelial cell isolations were performed on the basis of their affinity to an anti-CD31 antibody. CD31 is commonly used as an endothelial cell marker[174], and immunoprecipitation with antiCD31 antibodies should therefore lead to selective affinity isolation of endothelial cells. It should be noted, however, that other cell types, such as leucocytes (monocytes and neutrophils[183]), also express CD31 and may therefore lead to cellular contamination of endothelial isolates. This is a

caveat inherent to the crude isolation method used here. To overcome this, vWF mRNA expression was used as a comparative marker before, and after, affinity isolation. All "output" samples were successfully enriched for vWF indicating preferential isolation of endothelial cells using this method.

4.3.6.3 Wire Myography and Aortic Vessel Tension.

Ex vivo wire myography has been used extensively to assess vascular tone in a number of different vessel types[178]. Here, this technique was implemented in order to measure vascular tone in the aorta. Although the use of aortae provide proof of principle that the Nox4-induced increase in CSE expression affected vascular tone, its physiological implications are limited, as large conduit vessels do not affect blood pressure to the same extent as smaller vessels such as resistance vessels. Thus, a more appropriate vessel type for analysis might be mesenteric resistance vessels which are more integral to blood pressure regulation. Another limitation arising from these experiments involves the use of PPG. While PPG has been used by other groups as a CSE inhibitor, non-specific off-target effects cannot be excluded. To overcome this, and to directly confirm the involvement of CSE in the hypo-contractile phenotype, the effect of endothelial-specific overexpression of Nox4 in a CSE-null genetic background would prove valuable.

Chapter 5: Results 3

5.1 Introduction

The data presented in the previous two chapters suggest that Nox4 is a positive, physiological regulator of CSE transcriptional expression *in vitro* and *in vivo*, an effect that appears to be important for H_2S biosynthesis. The molecular mechanisms underscoring this transcriptional regulation were therefore investigated.

5.1.1 General Transcriptional Control

Eukaryotic gene expression is a highly complex and stringently-regulated event involving the collective activity of numerous proteins[184]. The process involves the binding of transcription factors to cognate binding sequences present at either proximal or distal DNA regions, relative to the core promoter. The transcriptional pre-initiation complex (PIC); composed of multiple proteins with varied functions such as promoter recognition, histone modification and nucleosome unwinding is assembled at the core promoter. A central component of this complex is RNA polymerase II (Pol II)[185], an enzyme that is responsible for mediating the transcription of genomic DNA into messenger RNA (mRNA). Transcription by Pol II proceeds in a processive manner through three stages; initiation, elongation and termination during which mRNA is capped and modified co-transcriptionally to form a mature, spliced and polyadenylated mRNA product. Of these events, the binding of transcriptional activators to their cognate enhancer element represents

the point at which specific cellular signals converge to promote the transcription of a defined set of genes[184, 186].

5.1.2 Transcriptional Regulation of CSE Gene Expression

A number of signalling pathways and transcription factors have previously been suggested to regulate CSE gene expression[187]. Studies conducted in human hepatocellular carcinoma cell lines have demonstrated that CSE expression can be regulated through the phosphatidylinositol-3-kinase (PI3K)-Akt-Specific Protein 1 (SP1) transcription factor-signalling network[188]. Here, it was shown that the inhibition of PI3K or deletion of Akt resulted in a reduction in CSE expression. By contrast, experimentally-induced activation of Akt increased CSE expression. It was also found that the -592/+139bp region of the human CSE gene (relative to the cap site) represented the CSE core promoter, and luciferase reporter assays further confirmed the involvement of the PI3K/Akt/Sp1 pathway in CSE transcriptional regulation. Consistent with this, SP1 was shown to bind directly to the CSE promoter in chromatin immunoprecipitation (ChIP) assays[189].

In addition to SP1, studies performed in rat mesangial cells have suggested a role for the known redox-sensitive transcription factor, Nrf2, in the regulation of CSE expression[100]. Here it was shown that platelet-derived growth factor-BB was capable of inducing Nrf2 activation and its translocation to the nucleus, with a subsequent increase in CSE transcription. This observed increase in CSE expression was abolished in response to NADPH oxidase inhibition, or ROS

scavenging by DPI and NAC respectively. Furthermore, mesangial cells from Nrf2-null mice displayed reduced CSE expression that failed to increase in response to PDGF[100].

The integrated stress response (ISR) has a number of signalling arms, one of which involves the phosphorylation of eukaryotic translation initiation factor 2α (eIF2α) by 4 eIF2α kinases[190]; PKR-like ER Kinase (PERK), protein kinase double-stranded RNA-dependent kinase (PKR), general control non-derepressible-2 Kinase (GCN2) and haem-regulated inhibitor kinase (HRI) leading to the subsequent protein expression of the basic leucine-zipper transcription factor, activating transcription factor 4 (ATF4)[191] (Figure 5.1). This pathway has been shown to regulate CSE expression in a number of studies. Thus mouse embryonic fibroblasts (MEFs) with a genetic deletion in ATF4 ($ATF4^{-/-}$ MEFs) exhibited a dramatic baseline reduction in CSE protein expression. To further demonstrate that CSE was regulated by the ISR, ISR inducing agents, tunicamycin and thapsigargin, were shown to increase CSE protein expression in wild type MEFs[192]. To support this, data obtained by Han *et al* demonstrated that the mRNA expression of CSE was increased in response to tunicamycin, and that this effect was abolished in the absence of ATF4[193]. Taken together, these findings suggest that CSE is a key transcriptional target activated by the ISR.

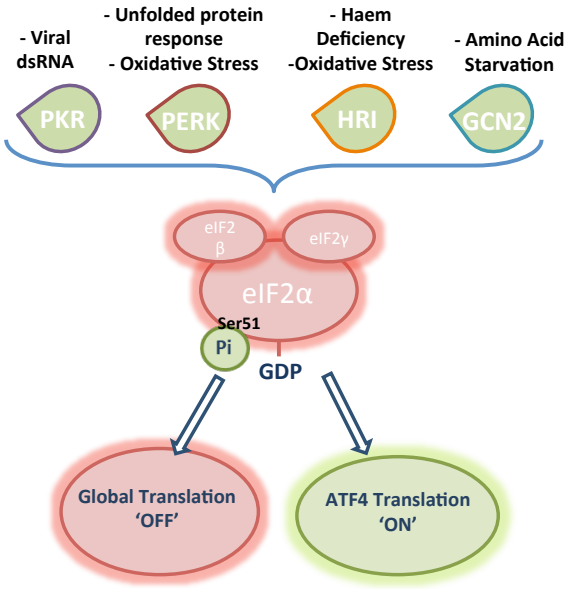

Figure 5.1: Regulation of Translation by eIF2α Phosphorylation. A schematic illustration of the ATF4 arm of the integrated stress response. Different stresses activate 4 distinct eIF2α kinases that phosphorylate eIF2α on serine 51. This results in the attenuation of global translation but permits ATF4 translation. ATF4 can then drive target gene expression.

In separate studies, NfκB, JNK and p38 MAP kinases have also been implicated in the regulation of CSE expression *in vitro*[194, 195]. To add to this, other putative transcription-factor-binding consensus sequences have been identified in the mouse CSE promoter using the Transfac 4.0 database[187]. Collectively, these data suggest that CSE transcriptional expression is complex and mediated by a number of distinct and defined signalling pathways and transcription factors which are likely to be cell-type specific.

5.1.3 Nox4 Signalling and the Regulation of Transcription

At the physiological and molecular level, Nox4 has been shown to have pleiotropic effects in the cardiovascular system[148]. An integral component underscoring its ability to induce this diverse array of phenotypes stems from its ability to generate the secondary messenger molecule, H_2O_2[148]. At the cellular level, Nox4 is involved in the activation and inhibition of numerous signalling pathways and can exert control over specific transcriptional responses[151]. The Kelch-like ECH-associated protein1 (KEAP1)/Nrf2 transcriptional signalling module represents a well-characterised ROS-induced system that (as discussed previously) has previously been shown to regulate CSE expression[100] (Figure 5.2). In unstressed conditions, KEAP1 sequesters Nrf2 in the cytoplasm where it is targeted for ubiquitin-mediated degradation. However under oxidative stress, critical cysteine residues in KEAP1 are oxidised resulting in the liberation of Nrf2 and its subsequent translocation to the nucleus where it drives the expression of a battery of antioxidant and detoxifying genes[196]. Nox4 has been shown to regulate Nrf2-dependent gene expression in the hearts of mice with cardiac-specific Nox4 overexpression (csNox4 Tg)[158]. Here, a microarray screen of csNox4 Tg hearts revealed that a number of Nrf2 target genes were up-regulated, compared to WT littermates, resulting in higher levels of GSH. This effect was attributed to an increase in the expression of Nrf2-target genes, since this change in GSH did not occur in an Nrf2-null background[158]. In support of these findings, Schroder *et al* demonstrated that endothelial Nox4 controls basal Nrf2 activity[151]. Here, tamoxifen-induced global Nox4 deletion resulted in a reduction in Nrf2 protein expression and reporter gene activity. HO-1, a known Nrf2 target, was also

reduced in its expression when Nox4 was deleted[151]. Taken together, Nox4 appears to play a role in the regulation of cellular antioxidant gene expression through Nrf2 and could potentially regulate CSE expression through this pathway.

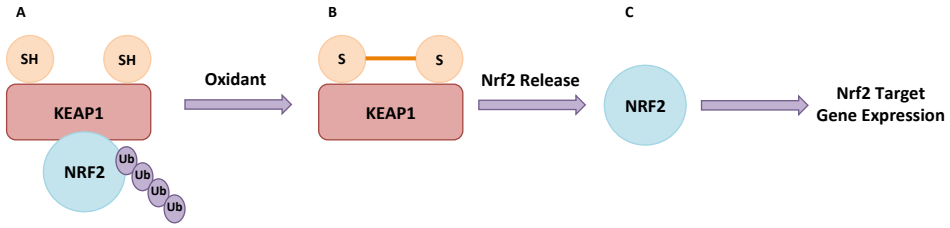

Figure 5.2: **Oxidant-induced Nrf2 Activation.** A schematic illustration of Nrf2 activation. A) Nrf2 is sequestered in the cytosol by KEAP1 and targeted for proteosomal degradation. B) The presence of oxidants causes the formation of a disulphide bond in KEAP1 that releases Nrf2. C) Liberated Nrf2 enters the nucleus where it drives the expression of its target genes.

Nox4 is a stress-inducible protein and as such plays a role in mediating cellular stress responses. The ISR outlined above has been shown, in cardiomyocytes, to involve Nox4[197]. Here, energy deprivation induced by glucose depletion resulted in the increased expression and activation of Nox4 in the endoplasmic reticulum (ER). This subsequently activated the eIF2α/ATF4 signalling cascade, an effect that was lost upon Nox4 depletion. Interestingly, Nox4 was suggested to activate this pathway through the inhibition of the ER-localised prolyl hydroxylase 4 protein (PHD4), since PHD4 knockdown in Nox4-depleted cells rescued ATF4 expression. This mechanism is thought to be important in mediating autophagy during ischemia and nutrient deprivation in the heart and, importantly, it points to a role for Nox4 in the regulation and activation of ATF4[197].

Collectively, these data provide evidence that CSE transcription may be regulated by multiple signalling pathways and transcription factors that are also associated with Nox4 activity. It is tempting to speculate that the previously-defined role for Nox4 in the regulation of CSE transcription described in this thesis may involve the activation of one or more of these pathways.

Aim

To determine the components of the molecular signalling pathways and transcription factors that drives the Nox4-induced increase in CSE expression in endothelial cells.

5.2 Results

5.2.1 The Regulation of CSE Transcription

As stated previously, a number of transcription factors have been shown to regulate CSE expression. In order to investigate which transcription factor(s) was responsible for the Nox4-induced up-regulation of CSE mRNA expression in endothelial cells several previously-characterised transcription factors were silenced in the presence of Nox4 overexpression. Figure 5.3A-F shows the results of this screen. Here, all three transcription factors; Nrf2, Sp1 and ATF4 were successfully silenced at the mRNA level in HUVECs (A,C,E). Figure 5.3E and F shows that the silencing of ATF4 results in a complete ablation of the Nox4-induced up-regulation in CSE mRNA expression, an effect that was not observed upon Nrf2 or SP1 silencing.

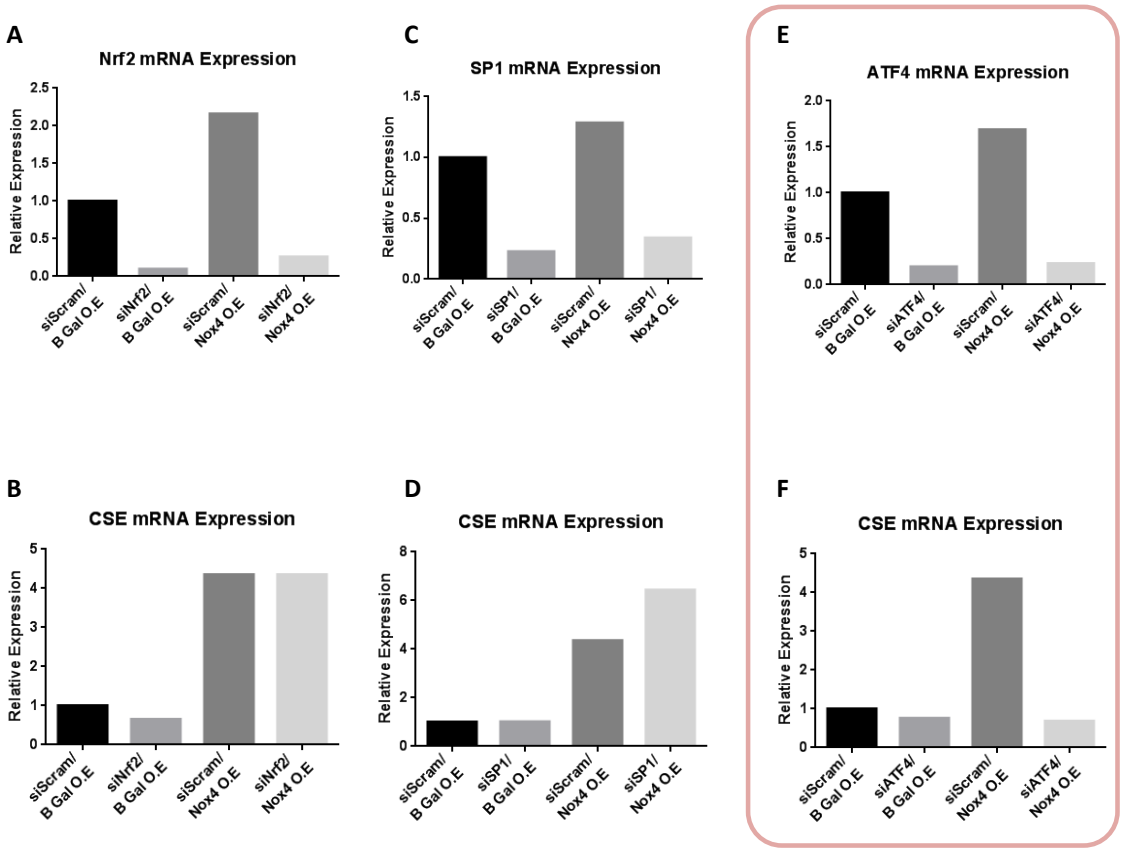

Figure 5.3: Nox4 Activates CSE Expression in HUVEC *via* ATF4. A,C,E) QPCR data showing that Nrf2, SP1 and ATF4 were successfully silenced following a 48 hour targeted a siRNA treatment compared to scrambled siRNA controls in HUVECs. **B,D,F)** shows the effect of 48 hour Nrf2, SP1 and ATF4 silencing on the Nox4-induced up-regulation in CSE expression in HUVEC overexpressing B Gal (B Gal O.E) or Nox4 (Nox4 O.E) for 24 hours. The red box highlights the observation that ATF4 silencing ablates the Nox4-induced increase in CSE expression. All data normalised to β Actin mRNA expression. N=1.

5.2.2 ATF4 Drives CSE Expression in HUVECs

In the transcription factor screen depicted above, ATF4 was identified as a strong candidate for driving CSE expression in Nox4-overexpressing HUVECs. To confirm a role for ATF4 in this process the experiment was repeated to determine

statistical significance. Figure 5.4A-C shows the results of this experiment. Figure 5.4B demonstrates that ATF4 can be successfully silenced at the mRNA level by siRNA-mediated ablation and that upon Nox4 overexpression ATF4 mRNA expression is significantly increased. Figure 5.4C further shows that this silencing of ATF4 completely ablates the Nox4-induced up-regulation in CSE mRNA expression.

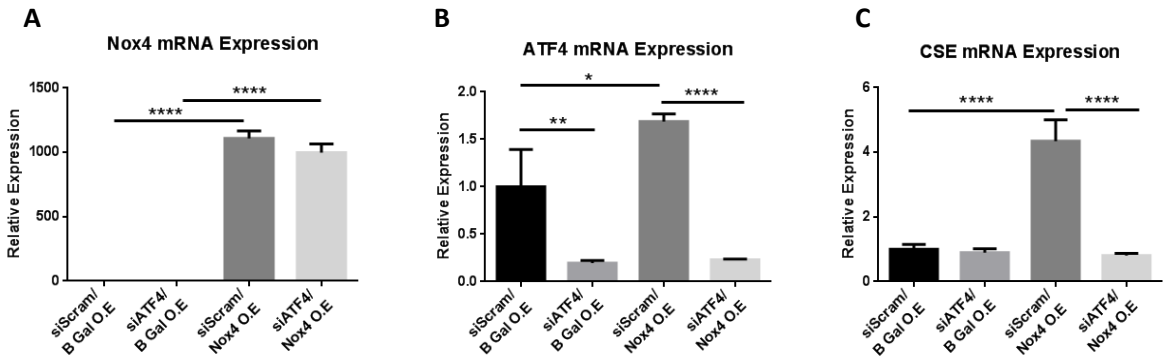

Figure 5.4: **ATF4 Silencing Ablates Nox4-induced CSE Expression**: QPCR data for **A)** Nox4, **B)** ATF4 and **C)** CSE mRNA expression following 48 hours ATF4 silencing (siATF4) or scrambled siRNA controls (siScram) with or without a 24 hour Nox4 overexpression (Nox4 O.E) or B Gal overexpression (B Gal O.E) in HUVECs. All data normalised to β Actin mRNA expression. O.E = Overexpression. N=3, *=<0.05, ** = P<0.01, **** = P=<0.0001. Statistical analysis performed using one-way ANOVA using a Tukeys post-hoc test.

To determine whether the Nox4-induced increase in ATF4 mRNA expression resulted in a concomitant increase in ATF4 protein expression, immunoblots were performed on HUVECs overexpressing Nox4 in the presence or absence of siRNA targeted to ATF4. Figure 5.5 shows that Nox4 overexpression significantly increased ATF4 protein expression and that this effect was lost upon ATF4 silencing.

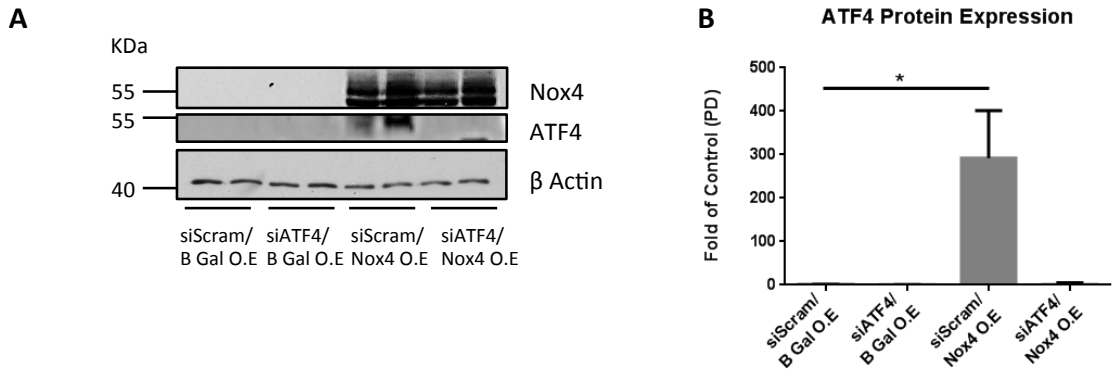

Figure 5.5: ATF4 Protein Expression is Increased in Response to Nox4 Overexpression. A) A representative immunoblot for ATF4 and Nox4 protein expression following 48 hours ATF4 silencing (siATF4) or scrambled siRNA controls (siScram) with either a 24 hour Nox4 overexpression (Nox4 O.E) or B Gal overexpression (B Gal O.E) in HUVECs. **B)** Corresponding densitometric analysis for ATF4 protein expression normalised to β Actin protein levels. N=3, *=<0.05. Statistical analysis performed using one-way ANOVA using a Tukeys post-hoc test.

5.2.3 ATF4 and CSE mRNA Expression Increase in a Time Dependent Manner with Nox4 Overexpression

To further investigate the relationship between Nox4-induced ATF4 and CSE expression, a time-course of Nox4 overexpression was performed. Here, Nox4 was overexpressed for 6, 12 and 24 hours and the mRNA expression levels of ATF4 and CSE were analysed using QPCR. Figure 5.6 shows the results of these experiments. Nox4 expression increased progressively over this time period and this was accompanied by a time-dependent increase in ATF4 and CSE mRNA expression, indicating that a temporal relationship exists between the expression of Nox4, ATF4 and CSE.

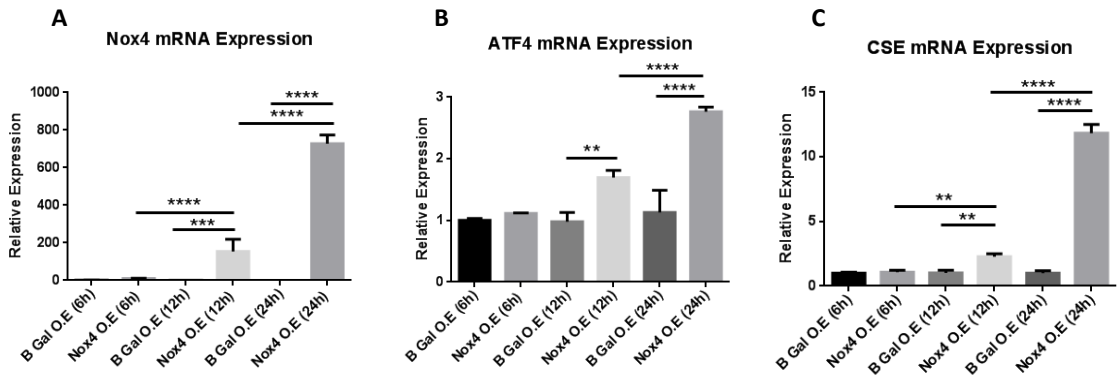

Figure 5.6: Nox4 Induces A Time-dependent Increase in ATF4 and CSE mRNA Expression. **A-C)** QPCR data for **A)** Nox4, **B)** ATF4 and **C)** CSE mRNA expression following Nox4 overexpression (Nox4 O.E) for 6, 12 and 24 hours compared to B Gal overexpressing (B Gal O.E) control HUVECs. Data normalised to β Actin mRNA expression. O.E = Overexpression. N=3, ** = P≤0.01, *** = P<0.01 **** = P=<0.0001. Statistical analysis performed using one-way ANOVA using a Tukeys post-hoc test.

To further assess the involvement of ATF4 in the regulation of CSE transcription, ATF4 overexpression experiments were performed. Figure 5.7A and B show that ATF4 was successfully overexpressed in HUVECs. Figure 5.7C demonstrates that CSE mRNA expression was significantly up-regulated upon ATF4 overexpression. Taken together with ATF4 silencing data depicted above, these data suggest that ATF4 expression is necessary to increase CSE transcription in endothelial cells upon Nox4 overexpression, and is sufficient in itself to up-regulate this expression.

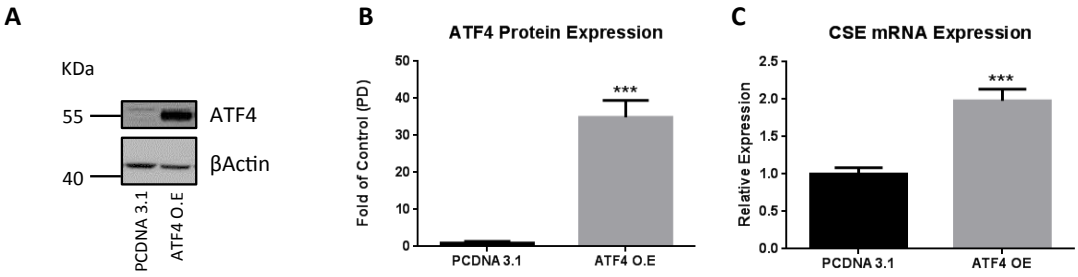

Figure 5.7: ATF4 Overexpression Significantly Increases CSE mRNA Expression. A) A representative immunoblot demonstrating ATF4 protein expression following 24 hours ATF4 (ATF4 O.E) or empty vector control PCDNA3.1 overexpression (PCDNA3.1) in HUVECs. **B)** Corresponding densitometric analysis for ATF4 protein expression normalised to β Actin protein levels. **C)** QPCR data showing CSE mRNA expression for the same experiment normalised to β Actin mRNA expression. N=3, ***=<0.001. Statistical analysis performed using an unpaired Students *t*-test. O.E = Overexpression.

5.2.4 ATF4 Activates CSE Transcription *via cis*-regulatory Sequence(s) Within Intron One of the CSE Gene

ATF4 has been shown here to increase CSE mRNA expression. To investigate whether this had a direct effect on CSE promoter activity, human CSE promoter constructs were cloned into a promotorless luciferase reporter gene vector (PGL4.22). The promoter constructs generated included a 764bp region of the CSE proximal promoter *(-764bp-luc*), that contained the previously identified upstream human CSE core promoter[188], and a 6415bp promoter construct that comprised a large region of the proximal upstream CSE promoter (*-6415bp-luc*) (See Figure 5.8A for promoter construct schematics). To assess the ability of these fragments to mediate transcriptional transactivation by ATF4, transient transfections into HEK293 cells, which (by contrast to HUVECs) are readily and efficiently transfected, were performed. Initial investigations were undertaken to determine

whether either of the proximal upstream promoter regions described above were involved in mediating the ATF4-induced increase in CSE expression. Thus HEK293 cells were transfected with the promoter constructs; *-764bp-luc* and *-6415bp-luc* in the presence or absence of ATF4 overexpression. Figure 5.8A schematically depicts the constructs used in these experiments and shows where they map to on the human CSE gene. Figure 5.8B shows that both *-764bp-luc* and *-6415bp-luc* were greatly increased in their promoter activity compared to empty vector (PGL4.22) controls. This demonstrates that both reporter constructs were successfully cloned, transfected and active in HEK293 cells. However, upon ATF4 overexpression the *-764bp-luc* construct was significantly *reduced* in its luciferase activity, while the *-6415bp-luc* construct showed no significant change in activity, although this also trended toward a reduction. These data demonstrate that sequences upstream of the CSE core promoter are not likely to be involved in the ATF4-induced increase in CSE transcription.

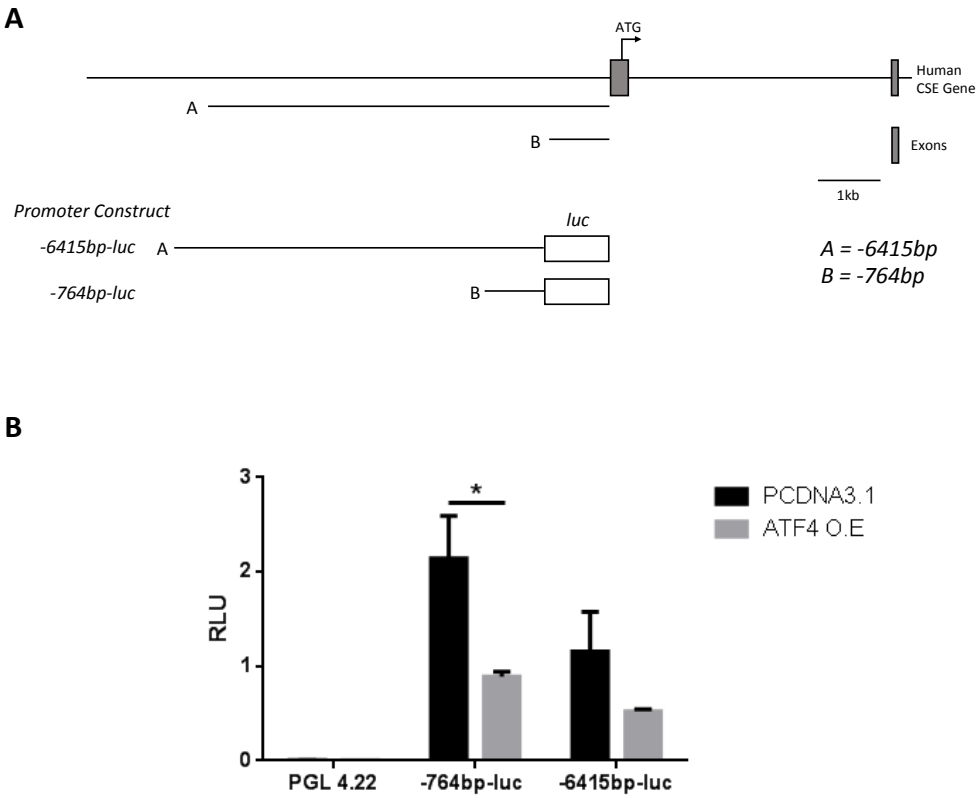

Figure 5.8: ATF4 Overexpression does not Increase the Luciferase Activity of CSE Proximal Promoter Constructs. A) A schematic illustration of the reporter constructs used in this experiment; *-6415bp-luc* and *-764bp-luc* respectively, showing where they map to on the human CSE gene. **B)** Luciferase reporter assay data for empty vector *PGL4.22*, *-764bp-luc* and *-6415bp-luc* in the presence of ATF4 overexpression (ATF4 O.E) or PCDNA3.1 overexpression (PCDNA 3.1) for 24 hours in HEK293 cells. Data are normalised to luciferase activity resulting from a thymidine kinase (TK) co-transfected reference plasmid (TK-PRL). ATG: Translational start site, RLU: Relative Light Units. Luc: luciferase gene. N=4, *=P<0.05. Statistical analysis performed using an unpaired Students *t*-test.

A genome-wide chromatin immunoprecipitation-sequencing (ChIP-Seq) analysis of ATF4 binding sites within MEF cells treated with the ER-stress inducing agent, tunicamycin, has recently been reported[193]. The data from this study were examined and one of the sites identified maps to the mouse CSE gene locus, at

position +938, (relative to the transcriptional start site) within intron one. Intriguingly, although ATF4 ChIP-Seq data for the human genome has not been reported, sequences within the first intron of CSE are indicated as being potentially regulatory due to sequence and/or altered chromatin structure on the Ensemble genome-browser;

http://www.ensembl.org/Homo_sapiens/Gene/Regulation?db=otherfeatures;g=1491;r=1:70411218-70440114.

To assess whether these sequences were involved in mediating the ATF4 transcriptional transactivation of CSE, a 2.4Kb genomic fragment, comprising this (potentially regulatory) intronic sequence was cloned downstream of the polyadenylation site of the luciferase gene (Figure 5.9A, fragment C), within the "basal" promoter construct -*764bp-luc*, to generate -*764bp-luc-IE*. HEK293 cells were transfected with the promoter constructs; -*764bp-luc* and -*764bp-luc-IE* in the presence or absence of ATF4 overexpression. Figure 5.9A schematically depicts the constructs used in this experiment showing how they map to the human CSE gene. Figure 5.9B shows that the -*764bp-luc* construct was significantly reduced in its luciferase activity upon ATF4 overexpression consistent with previous findings. However, the -*764bp-luc-IE* construct showed a dramatic and significant increase in its luciferase activity upon ATF4 overexpression. Taken together, these data suggest that ATF4 acts to increase CSE expression through a downstream *cis*-acting intronic enhancer region present within intron one of the human CSE gene.

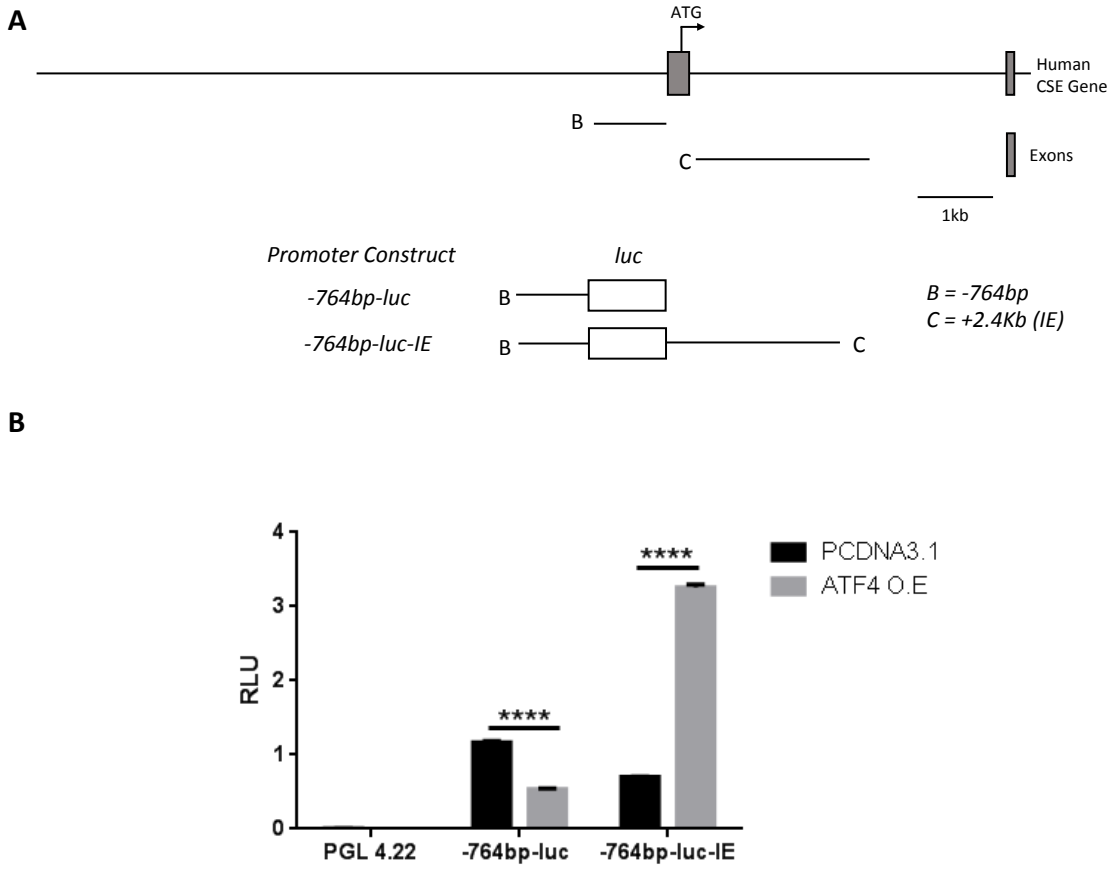

Figure 5.9: ATF4 Regulates CSE Expression Through an Intronic Enhancer. A) A schematic illustration of the reporter constructs used in this experiment; *-764bp-luc* and *-764bp-luc-IE* respectively, showing where they map to on the human CSE gene. **B)** Luciferase reporter assay data for empty vector *PGL4.22*, *-764bp-luc* and *-764bp-luc-IE* in the presence of ATF4 overexpression (ATF4 O.E) or PCDNA3.1 overexpression (PCDNA3.1) for 24 hours in HEK293 cells. Data are normalised to luciferase activity resulting from a thymidine kinase (TK) co-transfected reference plasmid (TK-PRL). ATG: Translational start site. RLU: relative light units. Luc: luciferase gene. N=4, **** = P<0.0001. Statistical analysis performed using an unpaired *t*-test.

5.2.5 ATF4 Binds Directly to the Intronic Enhancer Element in the CSE Gene

In order to determine whether the transcriptional up-regulation of CSE mediated by ATF4 results from the direct binding of ATF4 to sequences within the identified intronic enhancer, ChIP analyses were performed. The ATF4-binding region, previously identified by ChIP-seq, within the first intron of the mouse CSE gene does not comprise a canonical ATF4 binding motif. To determine the likely ATF4-binding site within the human intronic sequence, a short 60bp sequence comprising the previously identified mouse ATF4-binding element was compared to the 2.4Kb human intronic enhancer sequence using an online alignment tool (www.ebi.ac.uk/Tools/msa/clustalo/). This identified a short region of significant homology (12/14bp identity) that mapped between 822bp to 835bp of intron one (Figure 5.10A). Primers were thus designed to span this region and test for ATF4 binding using ChIP analyses (Primer site A). HEK293 cells were transfected with the *-764bp-luc-IE* construct, with or without co-transfected ATF4-overexpressing plasmids, and chromatin was prepared from this for analysis. Figure 5.10B demonstrates specific binding of ATF4 to this region of the human CSE intron upon ATF4 overexpression. By contrast, a region within the endogenous human exon 3 (RLP30) as well as a region downstream of the previously-identified ATF4 binding site (Primer site B) served as negative controls and did not bind ATF4 in control or ATF4-overexpressing HEK cells (Figure 5.10C). As expected, both genomic regions were shown to bind to histone H3. Specificity of binding was further demonstrated since neither region bound to normal rabbit IgG. (Figure 5.10B).

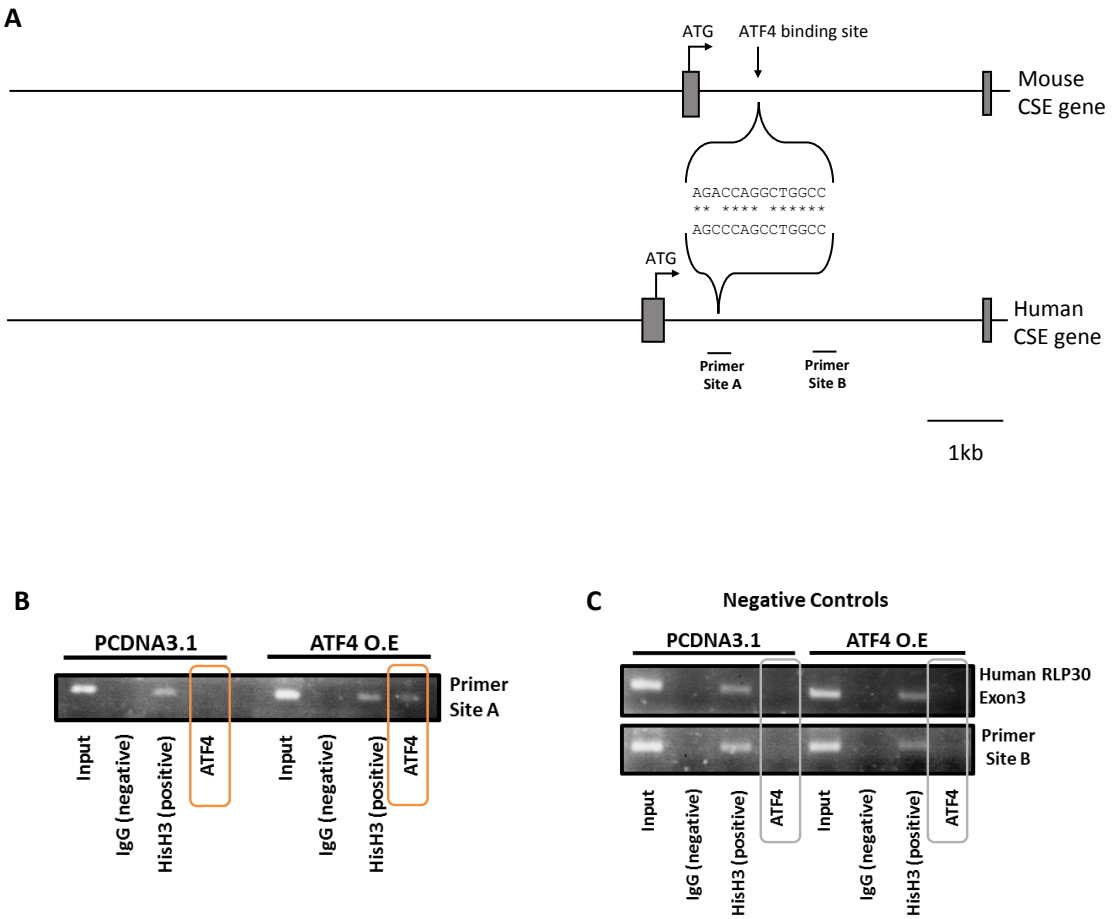

Figure 5.10: ATF4 Regulates CSE Transcription *via* Direct Binding to a *cis*-regulatory Intronic Site. A) A Schematic illustration showing the alignment of putative ATF4 binding sites within intron 1 of mouse and human CSE gene loci. **B, C)** Formaldehyde cross-linked chromatin prepared from HEK cells transfected with PCDNA3.1 or ATF4 incubated with normal rabbit IgG (negative control), anti acetyl-histone H3 (positive control), or anti-ATF4 as indicated. Aliquots of chromatin before immunoprecipitation served as a positive control (input). Purified DNA was analysed using primers specific for site A or site B, as indicated in schematic **A**, or exon 3 of Human RLP30. The results presented are representative of 3 separate experiments (N=3).

5.2.6 Nox4 Overexpression Induces eIF2α Phosphorylation Leading to ATF4 Protein Expression

Upstream of ATF4 is the eIF2α signalling module. In conditions of cellular stress, eIF2α becomes phosphorylated at serine 51, leading to increases in ATF4 protein levels. To investigate whether the Nox4-induced increase in ATF4 protein expression was preceded by an increase in eIF2α phosphorylation, HUVECs-overexpressing Nox4 were harvested for immunoblotting and the levels of total and phosphorylated eIF2α were analysed. Figure 5.11A and B show that eIF2α phosphorylation at serine 51 is significantly increased following Nox4 overexpression, whilst total eIF2α expression remains unchanged (Figure 5.11C). Figure 5.11D shows that the Nox4-induced increase in eIF2α phosphorylation correlates with a significant increase in ATF4 protein expression.

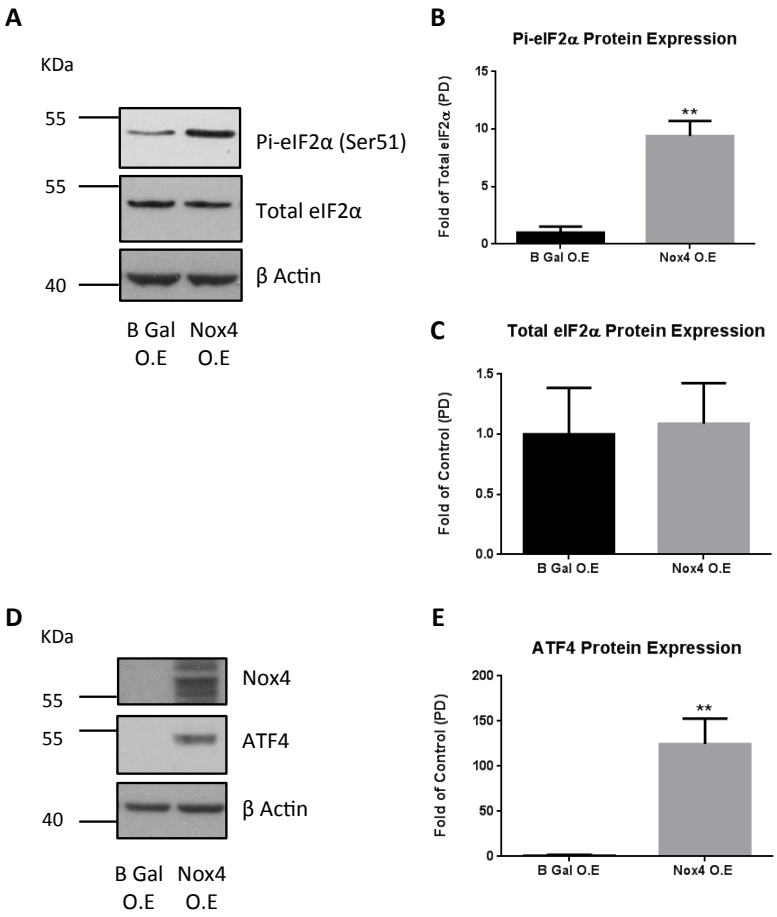

Figure 5.11: Nox4 Overexpression Increases eIF2α Phosphorylation and ATF4 Protein Expression. A, D) Representative immunoblots for phosphorylated eIF2α (Pi-eIF2α (Ser51)), total eIF2α, ATF4 and Nox4 protein expression following 24 hours Nox4 (Nox4 O.E) or B Gal control overexpression (B Gal O.E) in HUVECs. Corresponding densitometric analyses for **B)** Pi-eIF2α, **C)** total eIF2α and **E)** ATF4 and total eIF2α protein expression is normalised to β Actin protein levels (**C**, **E**), Pi-eIF2α expression normalised to total-eIF2α levels (**C**). O.E = Overexpression. N=3, **=P<0.001. Statistical analysis performed using an unpaired Students *t*-test.

5.2.7 Silencing HRI Significantly Blunts the Nox4-induced Increase in CSE Expression.

The control of eIF2α phosphorylation is elicited by 4 upstream eIF2α kinases that are activated in response to different stress stimuli[190, 198]. The activities of two of

these kinases; PERK and HRI, have been shown previously to be up-regulated in response to ROS[199, 200]. To assess the involvement of these two kinases in the Nox4-induced up-regulation in CSE transcription, they were systematically silenced in the presence of Nox4 overexpression. Figure 5.12A and C shows that both PERK and HRI were successfully silenced at the mRNA level. Interestingly, the silencing of PERK led to a further enhancement in CSE expression upon Nox4 overexpression (Figure 5.12 B). The silencing of HRI, however, resulted in a highly significant decrease in CSE mRNA levels following Nox4 overexpression (Figure 5.12D).

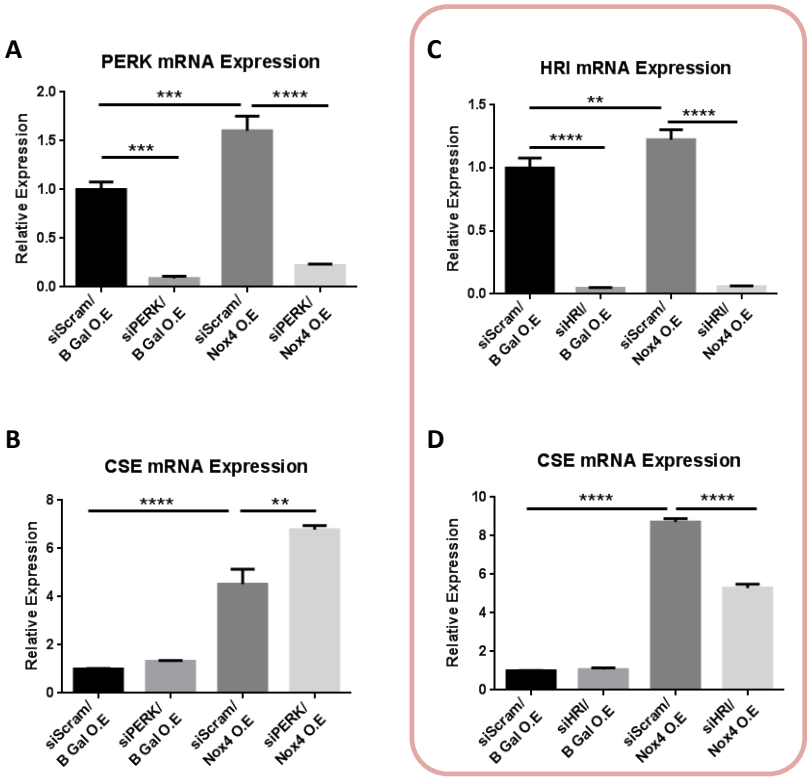

Figure 5.12: Silencing HRI Decreases Nox4-induced CSE mRNA Expression. A-D) An assessment of two redox-regulated eIF2α kinases in the Nox4-induced regulation of CSE expression in HUVECs. **A,C)** QPCR data showing the silencing of PERK and HRI respectively (48hours) in the presence or absence of either Nox4 overexpression (Nox4 O.E) or B Gal overexpression (B Gal O.E) for 24 hours. **B,D)** show the effect of PERK and HRI silencing on the Nox4-induced up-regulation in CSE expression respectively. All data normalised to β Actin mRNA expression. Red box shows that HRI silencing significantly blunts the Nox4-induced increase in CSE expression. N=3. ** = P<0.01, *** = P<0.01 **** = P=<0.0001. Statistical analysis performed using one-way ANOVA and a Tukeys post-hoc test.

5.2.8 siRNA-mediated Ablation of HRI Reduces eIF2α Phosphorylation and ATF4 Protein Expression Upon Nox4 Overexpression

siRNA-mediated ablation of HRI expression decreases the Nox4-induced increase in CSE expression. Thus to determine whether this effect involves a corresponding decrease in eIF2α phosphorylation and ATF4 protein expression, HRI expression

was silenced in the presence of Nox4 overexpression in HUVECs. Immunoblotting of protein extracts harvested from these cells shows that Nox4 overexpression significantly increases eIF2α phosphorylation and that this is significantly reduced when HRI is silenced (Figure 5.13A and B).

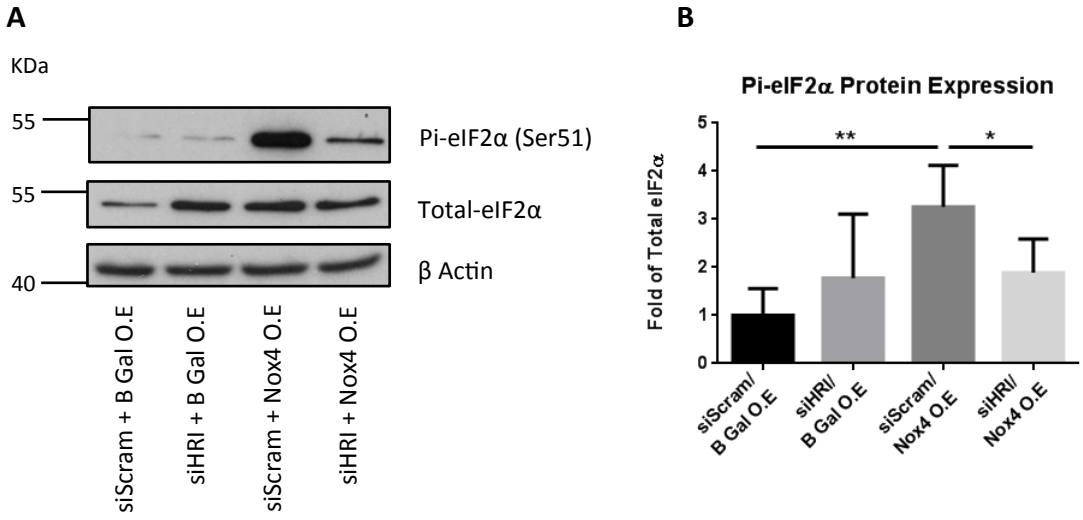

Figure 5.13: **Silencing HRI Reduces Nox4-induced eIF2α Phosphorylation. A)** A representative immunoblot for Pi-eIF2α and Total-eIF2α protein expression following 48 hours HRI silencing (siHRI) or scrambled siRNA controls (siScram) with either a 24 hour Nox4 overexpression (Nox4 O.E) or B Gal overexpression (B Gal O.E) in HUVECs. **B)** Corresponding densitometric analysis for Pi-eIF2α protein expression normalised to total eIF2α levels. N=4, * = P<0.05, ** = P<0.01. Statistical analysis performed using unpaired Students *t*-test.

ATF4 expression was also analysed in the same experiment and Figure 5.14 shows that Nox4 overexpression increased ATF4 protein expression and that this was significantly reduced upon silencing of HRI expression. Taken together these data indicate that Nox4 regulates CSE expression, in part, through the HRI/eIF2α/ATF4 signalling cascade.

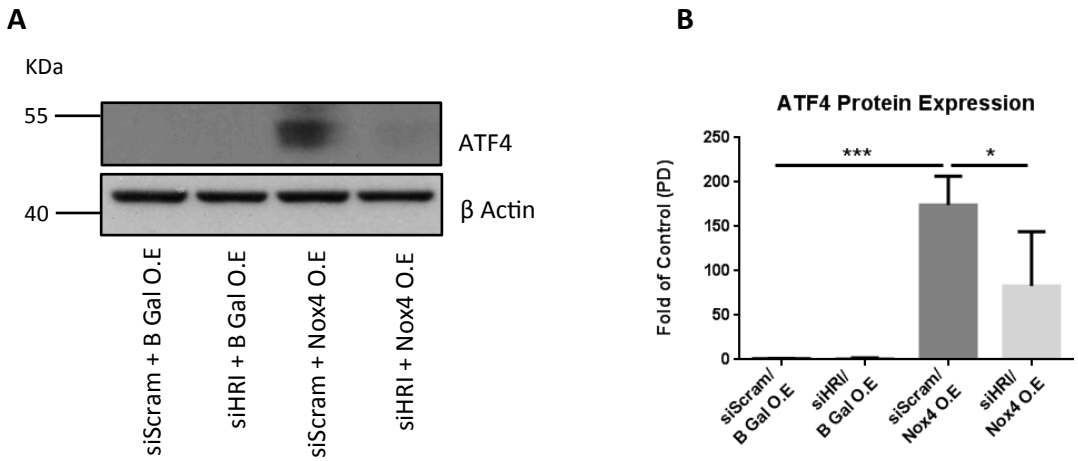

Figure 5.14: **siRNA-mediated Silencing of HRI Decreases Nox4-induced ATF4 Protein Expression. A)** A representative immunoblot for ATF4 protein expression following 48 hours HRI silencing (SiHRI) or scrambled siRNA controls (siScram) with either a 24 hour Nox4 overexpression (Nox4 O.E) or B Gal overexpression (B Gal O.E) in HUVECs. **B)** Corresponding densitometric analysis for ATF4 protein expression normalised to β Actin protein levels. N=5, * P = <0.05, *** P = <0.001. Statistical analysis performed using unpaired Students *t*-test.

5.3 Discussion

A role for Nox4 in the regulation of CSE gene expression was previously characterised in chapters 3 and 4. Here an investigation into the molecular mechanisms underscoring this observation was performed.

5.3.1 ATF4 Regulates CSE Expression in HUVECs

Previous studies have shown that CSE transcription can be regulated by multiple transcription factors, some of which, such as Nrf2[100] and ATF4[193], have also been shown to be associated with Nox4 signalling responses[158, 197]. Data shown here indicate that Nox4 overexpression enhanced ATF4 mRNA and protein expression, an effect that occurred in a time-dependent manner at the mRNA level. This increase in ATF4 expression correlated with an increase in CSE mRNA expression. Indeed, siRNA-mediated silencing of ATF4, upon Nox4 overexpression, resulted in a complete ablation in the Nox4-induced increase in CSE transcriptional expression. Furthermore, ATF4 overexpression was shown to enhance CSE mRNA levels significantly. Taken together, these data collectively demonstrate a definitive role for ATF4 in the Nox4-induced regulation of CSE expression in HUVECs, and are consistent with previous reports showing that ATF4 can regulate CSE expression. Thus two activators of ATF4, tunicamycin and thapsigargin, were shown to increase CSE protein expression in WT MEFs[192]. Consistent with these findings, CSE mRNA levels were shown to increase in response to tunicamycin, but failed to do so in an ATF4-null background[193]. Furthermore, Lee *et al*

demonstrated using a micro-array screen that cysteine deprivation, a known activator of the eIF2α/ATF4 cascade, increased the expression of a number of genes involved in sulphur metabolism and oxidative stress (such as CSE) in human hepatoma cells[201].

In line with a role for ATF4 in the regulation of CSE expression, luciferase reporter assays performed here demonstrated that ATF4 overexpression enhanced the luciferase activity of a CSE reporter construct containing a 2.4Kb intronic region of the CSE gene. This region contains sequences that are indicated as being potentially regulatory due to sequence and/or altered chromatin structure on the Ensemble genome browser. Consistent with this, data shown here demonstrate that this intronic region confers enhancer activity in response to ATF4 overexpression. Moreover, previous reports using ChiP Seq analyses revealed that ATF4 could directly bind to a homologous region within the mouse CSE gene, but this was not functionally validated[193]. Consistent with this, ChIP analyses performed here revealed that ATF4 could bind directly to the human intronic enhancer (IE) of the CSE gene, therefore corroborating these previous reports[193]. Taken together, the functional validation of the IE using luciferase reporter assays, as well as ChIP data showing the direct binding of ATF4 to this region, indicate that CSE is a direct transcriptional target of ATF4.

5.3.2 EIF2α Phosphorylation is Increased in Response to Nox4 Overexpression

ATF4 is a basic lucine-zipper transcription factor whose expression is regulated *via* the ISR[191]. It has long been known that cellular stresses, such as the unfolded protein response (UPR), attenuate global translation but permit ATF4 translation. The control of this process is governed by the phosphorylation of eIF2α at serine 51(Figure 5.15)[202].

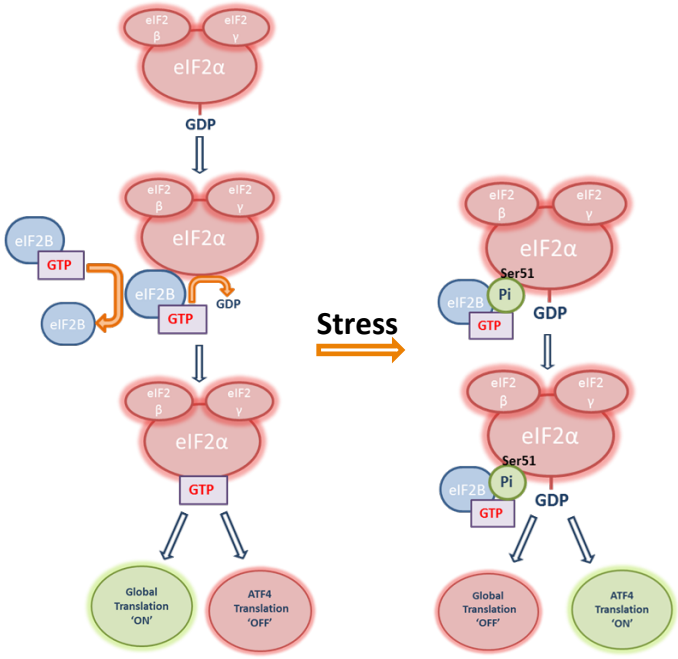

Figure 5.15: Stress-induced eIF2α Phosphorylation. A schematic illustration depicting eIF2α inhibition upon phosphorylation. In unstressed conditions eIF2α becomes GTP-bound, an effect mediated by the guanine nucleotide exchange factor, eIF2B. In this state, global translation is permitted but ATF4 translation is inhibited. Upon stress induction, eIF2α becomes phosphorylated at serine 51 leading to eIF2B sequestering and subsequent loss in its GTP exchange activity. EIF2α therefore remains GDP-bound and inactive, attenuating global translation but permitting ATF4 translation.

EIF2α phosphorylation at serine 51 results in the reduced assembly rate of the cell's translational machinery, therefore decreasing global protein synthesis. By contrast, ATF4 translation is enhanced under these conditions. ATF4 mRNA has 2 untranslated open reading frames (uORFs). The second uORF overlaps with the open reading frame (ORF) responsible for ATF4 protein coding. During stress, a lag in translational reinitiation at uORF2 results in its bypass and subsequent translational reinitiation at the ORF encoding full-length ATF4 protein[203] (Figure 5.16). Here it was shown that Nox4 overexpression increased ATF4 protein expression and that this subsequently correlated with a significant increase in eIF2α phosphorylation at serine 51. This is consistent with the classical mechanism of ATF4 activation discussed above. It should also be noted that ATF4 mRNA expression also increased with Nox4 overexpression suggesting that in addition to the classic mechanism of ATF4 activation, other modes of action may also facilitate this process, such as mRNA stabilisation.

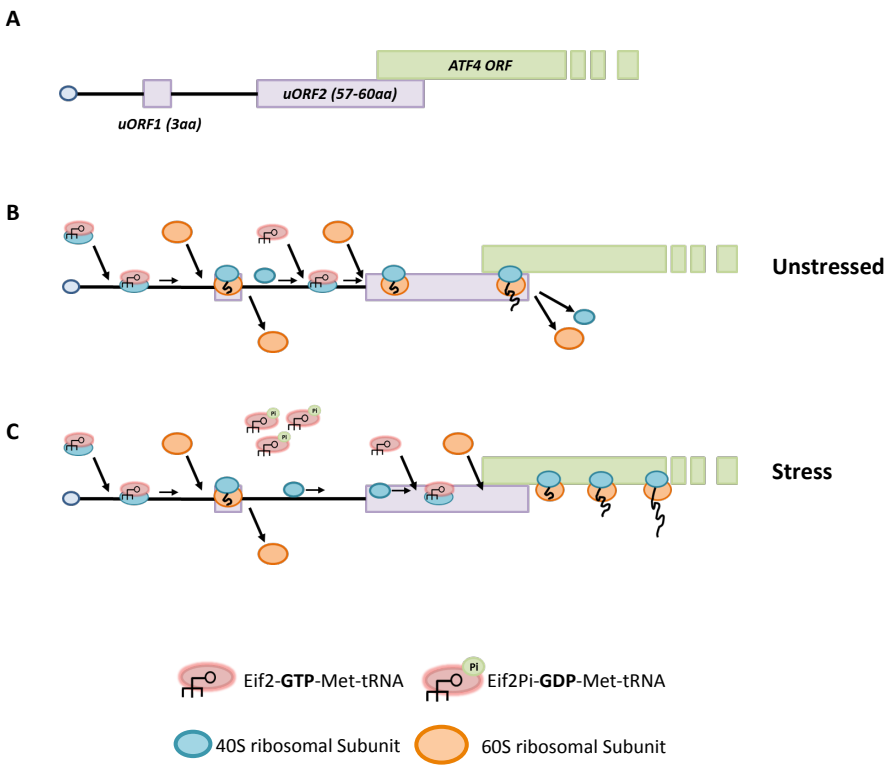

Figure 5.16: The Mechanism of ATF4 Translation. A schematic illustration depicting ATF4 translation. **A)** ATF4 mRNA structure containing 2 untranslated open reading frames (uORF). **B)** In unstressed conditions eIF2α-GTP bound associates with the 40S and 60S ribosomal subunits and translates a short polypeptide at uORF1. This then dissociates and reinitiates translation at uORF2, translation proceeds past the ORF for ATF4 and is then prematurely terminated preventing ATF4 protein expression. **C)** Upon stress induction, eIF2α phosphorylation at serine 51 leads to a lag in translational reinitiation at uORF2 resulting in it being bypassed and initiation subsequently reinitiating at the ORF for ATF4, thus permitting ATF4 translation and protein expression[203].

5.3.3 HRI Mediates eIF2α Phosphorylation, ATF4 Activation and CSE Expression in Response to Nox4 Overexpression

The eIF2α kinase family is composed of four serine-threonine kinases that have well-established roles in attenuating global translation in response to various

stress signals. The four family members include; PERK, PKR, GCN2 and HRI[190]. Of these, the activities of PERK and HRI have been shown to be up-regulated in response to ROS[199, 200].

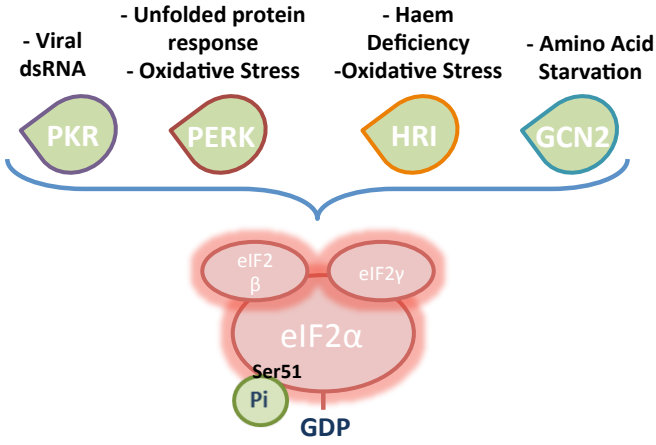

Figure 5.17: eIF2α Phosphorylation is Mediated by Four eIF2α Kinases. A schematic illustration depicting the four eIF2a kinases and their respective stress stimuli. PKR: Protein kinase double-stranded RNA-dependent kinase. PERK: PKR-like ER Kinase. HRI: Haem-regulated inhibitor kinase. GCN2: General control non-derepressible-2 Kinase.

The silencing of PERK and HRI revealed that the HRI kinase was involved in the Nox4-induced regulation of CSE expression in HUVECs, as HRI silencing significantly reduced the Nox4-induced increase in CSE mRNA expression. Indeed, HRI silencing was also shown to regulate eIF2α phosphorylation and ATF4 activation in response to Nox4 overexpression. The identification of the involvement of HRI in the regulation of CSE expression is novel. Indeed, reports of HRI function in the endothelium have not yet been made, nor has Nox4 been shown to regulate this kinase. The observation that Nox4 can induce HRI activity, as determined by eIF2α phosphorylation, is intriguing when considered alongside its emerging activation mechanisms.

5.3.4 HRI Activation and Regulation

Classical HRI activation occurs under conditions of haem depletion in red blood cells where it ensures that globin mRNA translation is only permissible when sufficient haem is available to be incorporated into the final haemoglobin protein product[200]. The HRI protein is composed of 5 domains; an N- and C-terminal domain, 2 kinase domains and a central kinase insert domain. Consistent with other eIF2α kinase family members, the C-terminal kinase domain is highly conserved and is responsible for the phosphorylation of serine 51 on eIF2α. However the N-terminal domain is distinctly different between eIF2α kinase family members and represents the regulatory region. In the case of HRI, the N-terminus contains a stable haem-binding site as well as a reversible haem-binding pocket located in the kinase insert domain, which is responsible for governing HRI activation and inhibition[190].

A number of studies have been devoted to elucidating the mechanisms that underpin HRI activation. As a result, Chen *et al* have subsequently proposed a three-stage activation scheme to explain this process. Stage one involves newly-synthesised HRI monomers rapidly associating to form a dimer that is bound at its N-termini by stable haem. This dimer then autophosphorylates to from a ProHRI complex. ProHRI subsequently enters stage 2 of its activation that involves further autophosphorylation events and the acquisition of its ability to reversibly bind to haem in its kinase insert domain. In the final stage, complete HRI activation is governed by the presence of haem. When haem is in abundance, it binds to the haem-binding pockets present in the kinase insert domain resulting in its

inactivation. By contrast, under conditions where haem is limiting, haem is lost from its binding pocket and a conformational change in the protein subsequently elicits further autophosphorylation events leading to the phosphorylation of Threonine 485 in the activation loop of the C-terminal kinase domain. This results in full kinase activity, subsequent phosphorylation of eIF2α and a halt in global translation. Fully active HRI is then thought to be 'switched off' *via* its degradation in the proteasome [204, 205]. Although many studies have focused on the haem-induced regulation of HRI, it has also become apparent that other stressors can permit its activation including oxidative stress [200, 204]. These observations are interesting when considered in light of data presented here demonstrating that Nox4 regulates eIF2α phosphorylation through HRI.

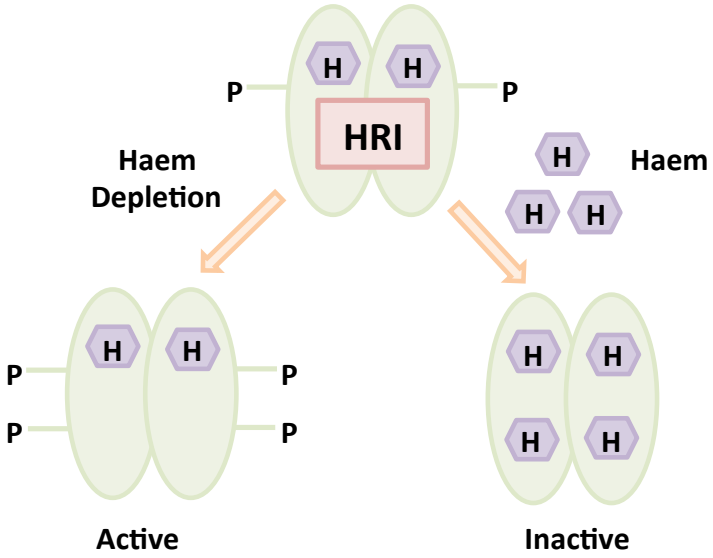

Figure 5.18: The Mechanism of Haem-dependent HRI Activation. A schematic illustration depicting the classical HRI activation mechanism. In conditions of haem (H) abundance, haem binds to the reversible haem-binding sites in the kinase insert domain resulting in HRI inactivation. Upon haem depletion, haem is lost from the kinase insert domain leading to autophosphorylation and a conformational change in the protein resulting in HRI activation.

Arsenite is a compound that has been shown to activate HRI independently of haem depletion. Incubation of mouse reticulocytes with increasing concentrations of sodium arsenite or exposure of reticulocytes to 200 μM sodium arsenite over a time course of 90 minutes increased HRI activation as indexed by an increase in its electrophoretic mobility using SDS PAGE. Furthermore, eIF2α phosphorylation was increased in arsenite-treated cells. The enhanced eIF2α phosphorylation induced by arsenite was shown to be solely dependent on the activation of HRI, because $HRI^{-/-}$ cells were unable to phosphorylate eIF2α in response to arsenite treatment. Although the mechanism of arsenite-induced HRI activation is still unclear it was suggested that ROS might play a role. Indeed, incubation of mouse reticulocytes with 20 mM NAC in combination with sodium arsenite prevented HRI

activation and eIF2α phosphorylation[200]. Furthermore, arsenite has been shown to promote O_2^- and H_2O_2 production, as well as NADPH oxidase activation in endothelial cells *in vitro*[206, 207]. This collectively suggests a role for ROS in the oxidative regulation of HRI. Another explanation for the Nox4-induced activation of HRI observed in this study comes from reports suggesting that H_2O_2 is involved in the non-enzymatic degradation of haem, where it is thought to split haem rings chemically[208, 209]. It is therefore tempting to speculate that Nox4-derived H_2O_2 may enhance the degradation and hence the depletion of haem, subsequently leading to HRI activation *via* the classical mechanism outlined above.

To conclude endothelial Nox4 regulates CSE expression through the HRI/eIF2α/ATF4 signalling module.

Chapter 6: General Discussion

6.1 Introduction

The data collected together in this thesis begin to define a physiological role for endothelial Nox4 in the regulation of CSE expression. It was demonstrated that Nox4 induces the transcriptional transactivation of CSE through the activation of the HRI/eIF2α/ATF4 signalling module in HUVECs (Figure 6.1). Furthermore, the Nox4-induced regulation of CSE was shown to function in the regulation of vascular contractility in isolated aortae. The broader implications of these findings will now be discussed.

6.2 Endothelial Nox4 as a Source of ROS in the Regulation of Gasotransmitter Production.

Endothelial dysfunction has repeatedly been recognised as a common factor in a number of CVD states such as hypertension[3]. Indeed, the endothelium has well-documented, homeostatic roles in the control of blood flow and tissue perfusion through its modulation of vascular tone[11, 210]. This process is highly complex and involves the interaction of many extracellular and intracellular vasoactive mediators that collectively regulate vasodilation and vasoconstriction. Perturbations in the levels or activities of these mediators can be a cause or consequence of endothelial dysfunction that can subsequently lead to impaired tonal regulation[11]. Thus, an impetus toward gaining a further understanding of the molecular mechanisms that underscore the endothelium-dependent regulation of vascular tone has been established.

Much research attention has focused on the importance of gasotransmitter signalling in the regulation of vascular tone[16, 20, 54, 79]. Unlike peptide signalling molecules, gasotransmitters are highly reactive gases (at least in the case of NO and H_2S) that are not readily stored in vesicles. Accordingly, they must be synthesised as needed, close to their specific sites of action[49]. Consequently, both the expression and the activity of their biosynthetic enzymes must be tightly controlled. Within the endothelium, the relevant enzymes involved in the generation of these gases are eNOS (for NO)[211], HO-1 (for CO)[212] and CSE (for H_2S)[213]. The rapid turnover of gaseous signalling molecules presents a number of difficulties in the development of therapeutics. Firstly, gaseous molecules are volatile and readily reactive, reducing their pharmacokinetic properties. To overcome this, donor compounds have been developed which release their respective gases slowly. Unfortunately, the ubiquitous release of these gases makes them difficult to target to specific sites of action. As such, novel approaches involving the manipulation of the endogenous signalling pathways that regulate the expression and/or activity of gasotransmitter-producing enzymes may prove fruitful. For this to become a viable therapeutic option, a better understanding of the endogenous regulation of gasotransmitter signalling is first required.

It has become apparent that ROS may play a significant role in the regulation of gasotransmitter production and it would appear that Nox4 is an important source of ROS in this process. Indeed, Nox4-null mice display decreased eNOS expression and a subsequent reduction in NO formation[151] and possibly consistent with this, H_2O_2 can promote vasodilation of rabbit aortae in an eNOS-dependent manner[153]. Furthermore, Nox4 has been shown to regulate Nrf2 and induce HO-1 expression

in cardiac-specific Nox4-overexpressing hearts[158]. Moreover, *in vitro* simulation of hemodynamic stress, using phenylephrine-stimulated neonatal rat ventricular myocytes, resulted in an increase in Nox4 and Nrf2 protein expression, and a subsequent up-regulation in HO-1 mRNA expression. This effect was ablated when either Nox4 or Nrf2 were silenced[214]. Consistent with these observations, global Nox4-null mice display reduced HO-1 expression in isolated lung endothelial cells, leading to enhanced apoptosis. This has been attributed to perturbed CO production[151]. Interestingly, data compiled in this thesis demonstrate a further physiological role for endothelial Nox4 in the transcriptional regulation of CSE, an endogenous generator of the third gasotransmitter, H_2S. Nox4 overexpression, which has been shown previously to generate significantly-enhanced levels of H_2O_2 in endothelial cells[47], as well as Nox4 silencing using siRNA, were shown to regulate both the mRNA and protein expression of CSE in HUVECs.

The Nox4-induced increase in CSE expression was found to correlate with a small increase in H_2S levels. Indeed, these data are further supported by the apparent lack of canonical transsulfuration activity in HUVECs, which suggests that CSE may be functioning instead in H_2S biosynthesis. These findings support previous reports that suggest that H_2O_2 regulates CSE gene expression[99] and activity[101], and demonstrate that Nox4 acts a physiological cellular source of ROS in this process. Taken together with previously published data surrounding a role for Nox4 in gasotransmitter signalling, it appears that Nox4 may be a master regulator of gasotransmitter production within the endothelium.

6.3 Nox4, CSE and Vascular Tone

ROS are emerging as novel signalling molecules involved in the control of vascular tone and it is thought that vasodilation and constriction are differentially regulated by both the type and source of ROS involved. Indeed, H_2O_2 is considered to play a physiological role as an EDHF[19 45] and can thus induce vasorelaxation. By contrast, O_2^- is involved in vasoconstriction[176], where it can deplete NO bioavailability through the formation of peroxynitrite[177]. Accordingly, Nox4 has been shown to have a number of vaso-protective effects, underscored by its ability to synthesise H_2O_2[47, 151, 215, 216]. Perhaps consistent with this, endothelial Nox4 has been shown to participate in the regulation of vascular tone, in a mouse model in which its overexpression improved endothelial function, vasodilation and lowered blood pressure compared to WT littermate controls[47]. By contrast, Nox4 deletion resulted in reduced endothelium-dependent vasodilation following *in vivo* AngII infusion[151]. These effects differ markedly from the endothelial dysfunction associated with the expression and activity of vascular Nox1 and Nox2[138, 217].

The Nox4-induced regulation of gasotransmitter production has previously been associated with preserved endothelial and vascular function[151]. Data shown in this thesis support these observations by demonstrating that eNox4 Tg mice have a vascular hypo-contractile phenotype when constricted with PE, a finding consistent with data obtained by Craige *et al* who observed the same phenotype in VE-cadherin-mediated endothelial-specific Nox4-overexpressing mice[150]. Moreover, CSE mRNA and protein expression were shown to be up-regulated in endothelial cells, isolated from the hearts eNox4 Tg mice. This is potentially

responsible for the hypo-contractile phenotype, since this phenotype was completely ablated when vessels were incubated with the CSE inhibitor, PPG. Interestingly, it would appear that this Nox4-induced effect occurred due to a chronic change in CSE gene expression, rather than the acute action of Nox4 signalling, since short-term administration of PEG-catalase failed to ablate the hypo-contractile phenotype.

A number of studies have characterised CSE as a major vascular generator of H_2S that regulates vascular tone[75, 79, 83]. Exogenous application of H_2S to vessels using NaS, NaHS and the slow-releasing H_2S donor, GYY4137 have previously been shown to induce vasorelaxation in *ex vivo*, wire myography models[65 73, 75-77]. Moreover, *in vivo* data obtained using PPG[179], as well as in $CSE^{-/-}$ mice[79], have highlighted a crucial role for CSE in regulating both basal and inducible vascular tone. Data shown in this thesis attribute the pro-relaxatory, hypo-contractile phenotype to the endogenous up-regulation of CSE induced by Nox4 overexpression. Although H_2S levels were not successfully measured *in vivo*, it is tempting to hypothesise, based on the wealth of data surrounding the vasodilatory actions of H_2S and CSE, that H_2S and/or an associated derivative (such as polysulphides) are involved in this process.

6.4 Nox4, ATF4 and the ISR.

Nox4 is a stress-inducible protein whose activity is predominantly regulated at the gene expression level[133]. Many studies have demonstrated that Nox4 expression

can be induced by a diverse array of cellular stresses including nutritional stress, pressure overload-induced cardiac hypertrophy and hypoxia[216, 218, 219]. The well-defined involvement of Nox4 in stress-associated responses is further highlighted by its signalling activity in the regulation of stress-associated transcription factors. In cardiac-specific Nox4-overexpressing transgenic hearts, Nox4 has been shown to regulate Nrf2 activity[158]. Furthermore, this regulation is lost in the endothelium of Nox4-null mice[151]. In addition to Nrf2, Nox4 also regulates the activity of the ISR transcription factor, ATF4 in cardiomyocytes[197]. Previous reports have suggested that CSE is a transcriptional target of both of these transcription factors[100, 193]. Here, the Nox4-induced regulation of CSE and its potential dependence upon either Nrf2 or ATF4 were interrogated in HUVECs and it was shown that the Nox4-induced expression of CSE occurred in an ATF4- dependent manner. Indeed, ATF4 silencing upon Nox4 overexpression resulted in a complete ablation of the Nox4-induced increase in CSE transcriptional expression, and this was reversed by ATF4 overexpression. Furthermore, a 2.4Kb region of human CSE intron 1 was shown to function as an enhancer in response to ATF4 overexpression, and ChIP analyses revealed that ATF4 could bind directly to this region. Taken together these data indicate that Nox4 regulates CSE expression through ATF4, which functions to increase CSE expression by binding (and functionally activating) an intronic enhancer element in intron 1 of the CSE gene.

The ATF4 arm of the ISR is mediated by the activation of four up-stream eIF2α kinases; PERK, PKR, GCN2 and HRI[190]. Previous studies in cardiomyocytes have shown that Nox4 is induced in response to glucose deprivation and acts to promote autophagy through the activation of PERK. The oxidant target in this

study was suggested to be PHD4, an ER resident PHD isoform[197]. Interestingly, the action of Nox4 described here in endothelial cells was found not to be dependent on PERK but was significantly ablated by siRNA-mediated silencing of the haem-dependent kinase, HRI. Indeed, Nox4 was shown to promote the activation of HRI leading to an increase in eIF2α phosphorylation, ATF4 protein expression and subsequent CSE transcription. It is apparent from these studies that Nox4 can differentially regulate ATF4 activation through either PHD4 and PERK or HRI. These discrepancies in Nox4-medicated ATF4 activation may arise from differences in the cell type used. Nox4 is found in the ER of cardiomyocytes[197], consistent with its activation of ER-localised PHD4 and PERK. However, in endothelial cells Nox4 is present in a number of locations including the ER and the nucleus[129, 132]. It is thought that the subcellular localisation of Nox4 may influence its signalling potential and therefore lead to differential activation of specific cellular signalling pathways[131]. Accordingly, Nox4 may induce ATF4 activation through HRI in the endothelium, and through PHD4 and PERK in cardiomyocytes. Alternatively, the relative levels of PHD4 in cardiomyocytes and endothelial cells may be a factor in determining the target of Nox4 in each cell type. Thus, if cardiomyocytes possess more PHD4 than endothelial cells, this may lead to preferential Nox4-induced PHD4/PERK activation in cardiomyocytes.

The redox-dependent mechanisms that underlie HRI activation are not currently understood, although previous studies in both erythroid cells and MEFs have reported its activation *via* "oxidative stress" induced by exposure to the heavy metal, arsenite[200, 207, 220]. Although a redox-driven mechanism for HRI activation was not investigated here, some hypothetical explanations can be drawn. For

example, it is possible that Nox4-derived H_2O_2 is involved in the non-enzymatic degradation of haem[208, 209] leading to haem depletion and subsequent HRI activation. Alternatively, the oxidation status of haem iron may play a role. In oxidising conditions, such as those induced by Nox4 activation, ferrous iron (Fe^{2+}) is oxidised to ferric iron (Fe^{3+}) which may subsequently lead to changes in the structure of haem, preventing it from allosterically inhibiting HRI. In addition, as mentioned above, HO-1 is a well-established transcriptional target of Nrf2 that has previously been shown to become activated in response to Nox4[214]. Indeed, Nox4 may promote HO-1 expression and thus the enzymatic degradation of haem, which could potentially lead to the indirect activation of HRI. However, data shown here suggest that Nrf2 is not involved, as its silencing had no effect on the Nox4-induced increase in CSE expression. Finally, one cannot rule out the possibility that HRI contains redox-sensitive cysteine residues that can be modified by Nox4-derived ROS in order to elicit a functional change in the protein.

The silencing of HRI in the presence of Nox4 overexpression in HUVECs led to only a partial reduction in the activity of the eIF2α/ATF4/CSE pathway. This might suggest that other kinases might also be able to regulate the pathway in response to Nox4 activation. Indeed, PKR and GCN2 represent two eIF2α kinases that were not tested in this study. It is possible that these kinases may also become active in response to Nox4 overexpression, and could therefore account for the residual activation of the eIF2α/ATF4/CSE pathway when HRI is silenced. In order to investigate this, experiments involving the silencing of these two kinases using siRNA followed by Nox4 overexpression would need to be performed. Another possibility is that HRI was not completely silenced at the protein level, and

although the mRNA of HRI was highly reduced upon siRNA treatment, its corresponding protein expression may not have been completely ablated.

Taken together, these data define a role for Nox4 in the activation of the HRI/eIF2α/ATF4 stress-induced signalling module in endothelial cells. Figure 6.1 depicts a schematic illustration of the proposed mechanism underlying the Nox4-induced regulation of CSE through a mechanism that potentially involves haem homeostasis or signalling.

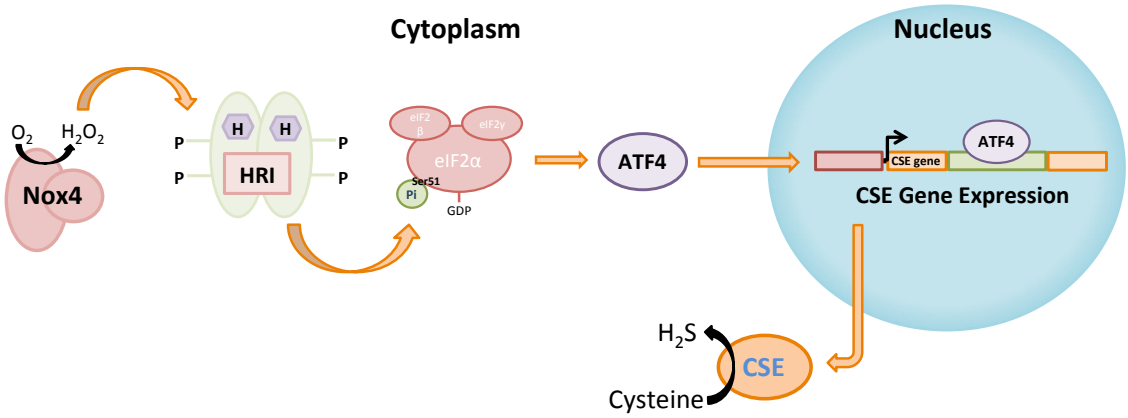

Figure 6.1: The Mechanism of the Nox4-induced Increase in CSE Expression in Endothelial Cells. A schematic illustration of the mechanism underscoring the Nox4-induced increase in CSE expression in endothelial cells. Nox4 activates HRI leading to the phosphorylation of eIF2α on serine 51. EIF2α phosphorylation attenuates global translation but permits ATF4 protein expression. ATF4 then binds to an intronic enhancer element in intron 1 of the CSE gene and subsequently promotes CSE expression. Enhanced CSE expression results in reduced PE-induced aortic constriction as a consequence of increased H_2S production.

6.5 Haem as an Integral Component in Gasotransmitter Signalling

The finding that haem levels might regulate CSE expression and hence H_2S production in endothelial cells is intriguing when considered alongside the other gasotransmitters (NO and CO), which are both generated within the endothelium to regulate vascular tone, and require haem for their synthesis. eNOS binds haem within its oxygenase domain[221], and HO-1 requires haem as its obligatory substrate[222]. Interestingly, considerable functional and regulatory cross-talk has between shown to exist between the three gasotransmitters at multiple levels[83, 223]. It is therefore possible that down-regulated eNOS or HO-1 activity, due to haem deficiency, may result in the activation of Nox4 and subsequent CSE/H_2S production, through HRI signalling. Thus, when haem becomes limiting H_2S production may increase to compensate for the reduced bioavailability of NO and CO, with Nox4 acting as a regulatory switch in this process. Here, the contribution of haem to the Nox4-induced regulation of CSE expression could be interrogated by supplying hemin (a haem donor) in the presence of Nox4 overexpression. Thus if low haem bioavailability is a factor in regulating this pathway, haem repletion should reduce the Nox4-induced increase in CSE expression. Alternatively, the use of HO-1 inhibitors (that would increase cellular haem bioavailability) may lead to similar effects. In addition, experiments involving the inhibition of haem biosynthesis may prove useful in helping do decipher whether haem deficiency is up-stream or down-stream of Nox4.

6.6 Regulation of Nox4 by Hypoxia

Hypoxia occurs in conditions such as ischemia, where blood flow is restricted and tissue oxygen levels are reduced to a point where normal cellular metabolism and function become compromised. Previous studies have shown that the transcription of Nox4 can be induced in response to ischemia, *in vivo*[224, 225], and hypoxia[218] *in vitro*. Furthermore, at the molecular level, hypoxic induction of Nox4 has been shown to be regulated by the binding of hypoxia-inducible factor 1α (HIF1α) to a proximal promoter region in the Nox4 gene, which led to an enhancement in the expression of a linked luciferase reporter[218]. In addition to HIF, previous work conducted in our group, demonstrated that the Nox4 promoter is positively regulated by E2F transcription factor family members[226], which are also known to play a role in hypoxia-mediated induction of transcription[227].

Interestingly, in addition to driving Nox4 expression[218], hypoxia also regulates the expression of CSE[228]. Based on the data presented here, as well as that published previously, it is tempting to hypothesise that hypoxic stress may represent an up-stream physiological activator of Nox4 that subsequently stimulates CSE expression and H_2S production through the HRI/eIF2α/ATF4 signalling module. Indeed, it is also known that CSE/H_2S can dilate vessels[65, 79] and that both Nox4 and CSE are positively implicated in angiogenesis[67, 150], two processes that would prove beneficial in the recovery from conditions such as ischemic hypoxia. Thus it will be of potential importance to determine whether hypoxia or chemical inducers of hypoxia such as dimethyloxalylglycine (DMOG) or cobalt chloride are activators of this pathway.

6.7 Angiogenesis and Future Directions

Much attention has been focussed upon the importance of all three gasotransmitters; NO[211], CO[229] and (most recently) H_2S[213] in the regulation of angiogenesis. In all cases the angiogenic properties of endothelial cells have been demonstrated *in vitro* to be promoted by the addition of donors of these gasotransmitters[83, 212, 213]. Consistent with their potential roles in promoting angiogenesis after ischemia, genetic depletion of each of these enzymes has been shown to result in impaired revascularisation following tissue ischemia[230-232]. The expression and/or activities of these enzymes might also be expected to be up-regulated by hypoxia/ischemia. Indeed, the transcriptional expression of both HO-1 and CSE are robustly up-regulated in response to hypoxia. Thus, exposure of rats to hypoxia acts to increase HO-1 mRNA expression in several tissues, while in VSMCs hypoxia similarly acts to up-regulate HO-1 transcription[233]. Moreover, CSE mRNA expression was shown to increase in ischemic tissue following femoral artery ligation in mice[230]. In addition, H_2S production by CSE within rodent carotid bodies has been shown to be greatly increased in response to hypoxia[234], although in this case CSE mRNA/protein levels were not assessed. The data presented here further demonstrate a role for ROS-associated signalling in gasotransmitter production and strongly implicate Nox4 as a physiological source of ROS in this process. As stated previously, Nox4 expression is induced in response to hypoxia[218]. There is therefore a compelling case for the involvement of Nox4 in the regulation of gasotransmitter-dependent signalling in hypoxia-induced angiongenic responses both *in vitro* and *in vivo*.

6.8 Summary

To conclude, data shown in this thesis demonstrate that endothelial Nox4 is a physiological regulator of CSE expression *in vitro* and *in vivo* and that this effect is mediated by the HRI/eIF2α/ATF4 signalling module (Figure 6.1). The Nox4-induced regulation of CSE was also shown to have functional consequences in the regulation of vascular contractility elicited in response to PE. These findings provide a novel mechanism for the regulation of vascular tone by Nox4, that may be of potential therapeutic benefit. For example the identification and use of endogenous activators of CSE expression may lead to improved vascular function in endothelial dysfunction-induced hypertension, where increased H_2S bioavailability would prove beneficial. This work would also suggest that Nox4 can act as a beneficial Nox isoform, a finding consistent with a number of other studies[47, 151, 154, 158, 216], and might caution against potential therapeutic pitfalls that could arise from the development of pharmaceutical inhibitors of Nox4.

References

1. Leal J, Luengo-Fernandez R, Gray A, Petersen S, Rayner M. Economic burden of cardiovascular diseases in the enlarged European union. *European heart journal*. 2006;27:1610-1619
2. Kearney PM, Whelton M, Reynolds K, Muntner P, Whelton PK, He J. Global burden of hypertension: Analysis of worldwide data. *Lancet*. 2005;365:217-223
3. Dharmashankar K, Widlansky ME. Vascular endothelial function and hypertension: Insights and directions. *Current hypertension reports*. 2010;12:448-455
4. Hadi HA, Carr CS, Al Suwaidi J. Endothelial dysfunction: Cardiovascular risk factors, therapy, and outcome. *Vascular health and risk management*. 2005;1:183-198
5. Halcox JP, Schenke WH, Zalos G, Mincemoyer R, Prasad A, Waclawiw MA, Nour KR, Quyyumi AA. Prognostic value of coronary vascular endothelial dysfunction. *Circulation*. 2002;106:653-658
6. Vito RP, Dixon SA. Blood vessel constitutive models-1995-2002. *Annual review of biomedical engineering*. 2003;5:413-439
7. Sumpio BE, Riley JT, Dardik A. Cells in focus: Endothelial cell. *The international journal of biochemistry & cell biology*. 2002;34:1508-1512
8. Aird WC. Phenotypic heterogeneity of the endothelium: I. Structure, function, and mechanisms. *Circulation research*. 2007;100:158-173
9. Aird WC. Phenotypic heterogeneity of the endothelium: II. Representative vascular beds. *Circulation research*. 2007;100:174-190
10. Galley HF, Webster NR. Physiology of the endothelium. *British journal of anaesthesia*. 2004;93:105-113
11. Sandoo A, van Zanten JJ, Metsios GS, Carroll D, Kitas GD. The endothelium and its role in regulating vascular tone. *The open cardiovascular medicine journal*. 2010;4:302-312
12. Deanfield JE, Halcox JP, Rabelink TJ. Endothelial function and dysfunction: Testing and clinical relevance. *Circulation*. 2007;115:1285-1295
13. Pober JS, Sessa WC. Evolving functions of endothelial cells in inflammation. *Nature reviews. Immunology*. 2007;7:803-815
14. Munoz-Chapuli R, Quesada AR, Angel Medina M. Angiogenesis and signal transduction in endothelial cells. *Cellular and molecular life sciences : CMLS*. 2004;61:2224-2243
15. Korthuis RJ. *Skeletal muscle circulation*. San Rafael (CA); 2011.
16. Palmer RM, Ferrige AG, Moncada S. Nitric oxide release accounts for the biological activity of endothelium-derived relaxing factor. *Nature*. 1987;327:524-526
17. Bos CL, Richel DJ, Ritsema T, Peppelenbosch MP, Versteeg HH. Prostanoids and prostanoid receptors in signal transduction. *The international journal of biochemistry & cell biology*. 2004;36:1187-1205
18. Feletou M, Vanhoutte PM. Endothelium-derived hyperpolarizing factor: Where are we now? *Arteriosclerosis, thrombosis, and vascular biology*. 2006;26:1215-1225
19. Matoba T, Shimokawa H, Kubota H, Morikawa K, Fujiki T, Kunihiro I, Mukai Y, Hirakawa Y, Takeshita A. Hydrogen peroxide is an endothelium-derived

hyperpolarizing factor in human mesenteric arteries. *Biochemical and biophysical research communications*. 2002;290:909-913
20. Mustafa AK, Sikka G, Gazi SK, Steppan J, Jung SM, Bhunia AK, Barodka VM, Gazi FK, Barrow RK, Wang R, Amzel LM, Berkowitz DE, Snyder SH. Hydrogen sulfide as endothelium-derived hyperpolarizing factor sulfhydrates potassium channels. *Circulation research*. 2011;109:1259-1268
21. Bellomo R, Giantomasso DD. Noradrenaline and the kidney: Friends or foes? *Crit Care*. 2001;5:294-298
22. Kim S, Iwao H. Molecular and cellular mechanisms of angiotensin II-mediated cardiovascular and renal diseases. *Pharmacological reviews*. 2000;52:11-34
23. Feletou M, Huang Y, Vanhoutte PM. Vasoconstrictor prostanoids. *Pflugers Archiv : European journal of physiology*. 2010;459:941-950
24. La M, Reid JJ. Endothelin-1 and the regulation of vascular tone. *Clinical and experimental pharmacology & physiology*. 1995;22:315-323
25. Henderson AH. St cyres lecture. Endothelium in control. *British heart journal*. 1991;65:116-125
26. McGuire JJ, Ding H, Triggle CR. Endothelium-derived relaxing factors: A focus on endothelium-derived hyperpolarizing factor(s). *Canadian journal of physiology and pharmacology*. 2001;79:443-470
27. Furchgott RF, Zawadzki JV. The obligatory role of endothelial cells in the relaxation of arterial smooth muscle by acetylcholine. *Nature*. 1980;288:373-376
28. Pacher P, Beckman JS, Liaudet L. Nitric oxide and peroxynitrite in health and disease. *Physiological reviews*. 2007;87:315-424
29. Alderton WK, Cooper CE, Knowles RG. Nitric oxide synthases: Structure, function and inhibition. *The Biochemical journal*. 2001;357:593-615
30. Palmer RM, Rees DD, Ashton DS, Moncada S. L-arginine is the physiological precursor for the formation of nitric oxide in endothelium-dependent relaxation. *Biochemical and biophysical research communications*. 1988;153:1251-1256
31. Palmer RM, Ashton DS, Moncada S. Vascular endothelial cells synthesize nitric oxide from L-arginine. *Nature*. 1988;333:664-666
32. Govers R, Rabelink TJ. Cellular regulation of endothelial nitric oxide synthase. *American journal of physiology. Renal physiology*. 2001;280:F193-206
33. Fleming I, Busse R. Signal transduction of enos activation. *Cardiovascular research*. 1999;43:532-541
34. Hobbs AJ, Ignarro LJ. Nitric oxide-cyclic GMP signal transduction system. *Methods in enzymology*. 1996;269:134-148
35. Cosentino F, Luscher TF. Maintenance of vascular integrity: Role of nitric oxide and other bradykinin mediators. *European heart journal*. 1995;16 Suppl K:4-12
36. Huang PL, Huang Z, Mashimo H, Bloch KD, Moskowitz MA, Bevan JA, Fishman MC. Hypertension in mice lacking the gene for endothelial nitric oxide synthase. *Nature*. 1995;377:239-242
37. De Nucci G, Gryglewski RJ, Warner TD, Vane JR. Receptor-mediated release of endothelium-derived relaxing factor and prostacyclin from bovine aortic

endothelial cells is coupled. *Proceedings of the National Academy of Sciences of the United States of America*. 1988;85:2334-2338
38. Ingerman-Wojenski C, Silver MJ, Smith JB, Macarak E. Bovine endothelial cells in culture produce thromboxane as well as prostacyclin. *The Journal of clinical investigation*. 1981;67:1292-1296
39. Majed BH, Khalil RA. Molecular mechanisms regulating the vascular prostacyclin pathways and their adaptation during pregnancy and in the newborn. *Pharmacological reviews*. 2012;64:540-582
40. Chen G, Suzuki H, Weston AH. Acetylcholine releases endothelium-derived hyperpolarizing factor and EDHF from rat blood vessels. *British journal of pharmacology*. 1988;95:1165-1174
41. Busse R, Edwards G, Feletou M, Fleming I, Vanhoutte PM, Weston AH. EDHF: Bringing the concepts together. *Trends in pharmacological sciences*. 2002;23:374-380
42. Brandes RP, Schmitz-Winnenthal FH, Feletou M, Godecke A, Huang PL, Vanhoutte PM, Fleming I, Busse R. An endothelium-derived hyperpolarizing factor distinct from no and prostacyclin is a major endothelium-dependent vasodilator in resistance vessels of wild-type and endothelial no synthase knockout mice. *Proceedings of the National Academy of Sciences of the United States of America*. 2000;97:9747-9752
43. Scotland RS, Madhani M, Chauhan S, Moncada S, Andresen J, Nilsson H, Hobbs AJ, Ahluwalia A. Investigation of vascular responses in endothelial nitric oxide synthase/cyclooxygenase-1 double-knockout mice: Key role for endothelium-derived hyperpolarizing factor in the regulation of blood pressure in vivo. *Circulation*. 2005;111:796-803
44. Edwards G, Dora KA, Gardener MJ, Garland CJ, Weston AH. K^+ is an endothelium-derived hyperpolarizing factor in rat arteries. *Nature*. 1998;396:269-272
45. Matoba T, Shimokawa H, Nakashima M, Hirakawa Y, Mukai Y, Hirano K, Kanaide H, Takeshita A. Hydrogen peroxide is an endothelium-derived hyperpolarizing factor in mice. *The Journal of clinical investigation*. 2000;106:1521-1530
46. Cosentino F, Barker JE, Brand MP, Heales SJ, Werner ER, Tippins JR, West N, Channon KM, Volpe M, Luscher TF. Reactive oxygen species mediate endothelium-dependent relaxations in tetrahydrobiopterin-deficient mice. *Arteriosclerosis, thrombosis, and vascular biology*. 2001;21:496-502
47. Ray R, Murdoch CE, Wang M, Santos CX, Zhang M, Alom-Ruiz S, Anilkumar N, Ouattara A, Cave AC, Walker SJ, Grieve DJ, Charles RL, Eaton P, Brewer AC, Shah AM. Endothelial Nox4 NADPH oxidase enhances vasodilatation and reduces blood pressure in vivo. *Arteriosclerosis, thrombosis, and vascular biology*. 2011;31:1368-1376
48. Wang R. Gasotransmitters: Growing pains and joys. *Trends in biochemical sciences*. 2014;39:227-232
49. Mustafa AK, Gadalla MM, Snyder SH. Signaling by gasotransmitters. *Science signaling*. 2009;2:re2
50. *Gasotransmitters - physiology and pathophysiology*. New York: Springer; 2012.

51. Stein A, Bailey SM. Redox biology of hydrogen sulfide: Implications for physiology, pathophysiology, and pharmacology. *Redox biology*. 2013;1:32-39
52. Maines MD. The heme oxygenase system: A regulator of second messenger gases. *Annual review of pharmacology and toxicology*. 1997;37:517-554
53. Wu L, Wang R. Carbon monoxide: Endogenous production, physiological functions, and pharmacological applications. *Pharmacological reviews*. 2005;57:585-630
54. Wang R, Wang Z, Wu L. Carbon monoxide-induced vasorelaxation and the underlying mechanisms. *British journal of pharmacology*. 1997;121:927-934
55. Zakhary R, Gaine SP, Dinerman JL, Ruat M, Flavahan NA, Snyder SH. Heme oxygenase 2: Endothelial and neuronal localization and role in endothelium-dependent relaxation. *Proceedings of the National Academy of Sciences of the United States of America*. 1996;93:795-798
56. Abe K, Kimura H. The possible role of hydrogen sulfide as an endogenous neuromodulator. *The Journal of neuroscience : the official journal of the Society for Neuroscience*. 1996;16:1066-1071
57. Kimura H. Hydrogen sulfide and polysulfides as biological mediators. *Molecules*. 2014;19:16146-16157
58. Kabil O, Banerjee R. Redox biochemistry of hydrogen sulfide. *The Journal of biological chemistry*. 2010;285:21903-21907
59. Lowicka E, Beltowski J. Hydrogen sulfide H_2S - the third gas of interest for pharmacologists. *Pharmacological reports : PR*. 2007;59:4-24
60. Kolluru GK, Shen X, Bir SC, Kevil CG. Hydrogen sulfide chemical biology: Pathophysiological roles and detection. *Nitric oxide : biology and chemistry / official journal of the Nitric Oxide Society*. 2013;35:5-20
61. Kimura H. Hydrogen sulfide as a neuromodulator. *Molecular neurobiology*. 2002;26:13-19
62. Nagahara N, Ito T, Kitamura H, Nishino T. Tissue and subcellular distribution of mercaptopyruvate sulfurtransferase in the rat: Confocal laser fluorescence and immunoelectron microscopic studies combined with biochemical analysis. *Histochemistry and cell biology*. 1998;110:243-250
63. Shibuya N, Mikami Y, Kimura Y, Nagahara N, Kimura H. Vascular endothelium expresses 3-mercaptopyruvate sulfurtransferase and produces hydrogen sulfide. *Journal of biochemistry*. 2009;146:623-626
64. Zhao W, Zhang J, Lu Y, Wang R. The vasorelaxant effect of H_2S as a novel endogenous gaseous k(atp) channel opener. *The EMBO journal*. 2001;20:6008-6016
65. Kohn C, Schleifenbaum J, Szijarto IA, Marko L, Dubrovska G, Huang Y, Gollasch M. Differential effects of cystathionine-gamma-lyase-dependent vasodilatory h2s in periadventitial vasoregulation of rat and mouse aortas. *PloS one*. 2012;7:e41951
66. Altaany Z, Yang G, Wang R. Crosstalk between hydrogen sulfide and nitric oxide in endothelial cells. *Journal of cellular and molecular medicine*. 2013;17:879-888
67. Wang K, Ahmad S, Cai M, Rennie J, Fujisawa T, Crispi F, Baily J, Miller MR, Cudmore M, Hadoke PW, Wang R, Gratacos E, Buhimschi IA, Buhimschi CS, Ahmed A. Dysregulation of hydrogen sulfide producing enzyme

cystathionine gamma-lyase contributes to maternal hypertension and placental abnormalities in preeclampsia. *Circulation*. 2013;127:2514-2522
68. Kraus JP, Hasek J, Kozich V, Collard R, Venezia S, Janosikova B, Wang J, Stabler SP, Allen RH, Jakobs C, Finn CT, Chien YH, Hwu WL, Hegele RA, Mudd SH. Cystathionine gamma-lyase: Clinical, metabolic, genetic, and structural studies. *Molecular genetics and metabolism*. 2009;97:250-259
69. Chiku T, Padovani D, Zhu W, Singh S, Vitvitsky V, Banerjee R. H_2S biogenesis by human cystathionine gamma-lyase leads to the novel sulfur metabolites lanthionine and homolanthionine and is responsive to the grade of hyperhomocysteinemia. *The Journal of biological chemistry*. 2009;284:11601-11612
70. Paul BD, Snyder SH. H_2S signalling through protein sulfhydration and beyond. *Nature reviews. Molecular cell biology*. 2012;13:499-507
71. Mustafa AK, Gadalla MM, Sen N, Kim S, Mu W, Gazi SK, Barrow RK, Yang G, Wang R, Snyder SH. H_2S signals through protein s-sulfhydration. *Science signaling*. 2009;2:ra72
72. Greiner R, Palinkas Z, Basell K, Becher D, Antelmann H, Nagy P, Dick TP. Polysulfides link h2s to protein thiol oxidation. *Antioxidants & redox signaling*. 2013;19:1749-1765
73. Stubbert D, Prysyazhna O, Rudyk O, Scotcher J, Burgoyne JR, Eaton P. Protein kinase G1 alpha oxidation paradoxically underlies blood pressure lowering by the reductant hydrogen sulfide. *Hypertension*. 2014;64:1344-1351
74. Hosoki R, Matsuki N, Kimura H. The possible role of hydrogen sulfide as an endogenous smooth muscle relaxant in synergy with nitric oxide. *Biochemical and biophysical research communications*. 1997;237:527-531
75. Al-Magableh MR, Hart JL. Mechanism of vasorelaxation and role of endogenous hydrogen sulfide production in mouse aorta. *Naunyn-Schmiedeberg's archives of pharmacology*. 2011;383:403-413
76. Al-Magableh MR, Kemp-Harper BK, Hart JL. Hydrogen sulfide treatment reduces blood pressure and oxidative stress in angiotensin II-induced hypertensive mice. *Hypertension research : official journal of the Japanese Society of Hypertension*. 2015;38:13-20
77. Chitnis MK, Njie-Mbye YF, Opere CA, Wood ME, Whiteman M, Ohia SE. Pharmacological actions of the slow release hydrogen sulfide donor gyy4137 on phenylephrine-induced tone in isolated bovine ciliary artery. *Experimental eye research*. 2013;116:350-354
78. Bucci M, Papapetropoulos A, Vellecco V, Zhou Z, Pyriochou A, Roussos C, Roviezzo F, Brancaleone V, Cirino G. Hydrogen sulfide is an endogenous inhibitor of phosphodiesterase activity. *Arteriosclerosis, thrombosis, and vascular biology*. 2010;30:1998-2004
79. Yang G, Wu L, Jiang B, Yang W, Qi J, Cao K, Meng Q, Mustafa AK, Mu W, Zhang S, Snyder SH, Wang R. H_2S as a physiologic vasorelaxant: Hypertension in mice with deletion of cystathionine gamma-lyase. *Science*. 2008;322:587-590
80. Tang G, Wu L, Liang W, Wang R. Direct stimulation of K_{ATP} channels by exogenous and endogenous hydrogen sulfide in vascular smooth muscle cells. *Molecular pharmacology*. 2005;68:1757-1764

81. Tang G, Yang G, Jiang B, Ju Y, Wu L, Wang R. H_2S is an endothelium-derived hyperpolarizing factor. *Antioxidants & redox signaling*. 2013;19:1634-1646
82. Predmore BL, Julian D, Cardounel AJ. Hydrogen sulfide increases nitric oxide production from endothelial cells by an akt-dependent mechanism. *Frontiers in physiology*. 2011;2:104
83. Coletta C, Papapetropoulos A, Erdelyi K, Olah G, Modis K, Panopoulos P, Asimakopoulou A, Gero D, Sharina I, Martin E, Szabo C. Hydrogen sulfide and nitric oxide are mutually dependent in the regulation of angiogenesis and endothelium-dependent vasorelaxation. *Proceedings of the National Academy of Sciences of the United States of America*. 2012;109:9161-9166
84. Olszewski AJ, McCully KS. Homocysteine metabolism and the oxidative modification of proteins and lipids. *Free radical biology & medicine*. 1993;14:683-693
85. Selhub J. Homocysteine metabolism. *Annual review of nutrition*. 1999;19:217-246
86. Nygard O, Vollset SE, Refsum H, Stensvold I, Tverdal A, Nordrehaug JE, Ueland M, Kvale G. Total plasma homocysteine and cardiovascular risk profile. The hordaland homocysteine study. *JAMA : the journal of the American Medical Association*. 1995;274:1526-1533
87. Araki A, Sako Y, Fukushima Y, Matsumoto M, Asada T, Kita T. Plasma sulfhydryl-containing amino acids in patients with cerebral infarction and in hypertensive subjects. *Atherosclerosis*. 1989;79:139-146
88. Malinow MR, Levenson J, Giral P, Nieto FJ, Razavian M, Segond P, Simon A. Role of blood pressure, uric acid, and hemorheological parameters on plasma homocyst(e)ine concentration. *Atherosclerosis*. 1995;114:175-183
89. Bearden SE, Beard RS, Jr., Pfau JC. Extracellular transsulfuration generates hydrogen sulfide from homocysteine and protects endothelium from redox stress. *American journal of physiology. Heart and circulatory physiology*. 2010;299:H1568-1576
90. Lentz SR, Sobey CG, Piegors DJ, Bhopatkar MY, Faraci FM, Malinow MR, Heistad DD. Vascular dysfunction in monkeys with diet-induced hyperhomocyst(e)inemia. *The Journal of clinical investigation*. 1996;98:24-29
91. Zhang C, Cai Y, Adachi MT, Oshiro S, Aso T, Kaufman RJ, Kitajima S. Homocysteine induces programmed cell death in human vascular endothelial cells through activation of the unfolded protein response. *The Journal of biological chemistry*. 2001;276:35867-35874
92. Mosharov E, Cranford MR, Banerjee R. The quantitatively important relationship between homocysteine metabolism and glutathione synthesis by the transsulfuration pathway and its regulation by redox changes. *Biochemistry*. 2000;39:13005-13011
93. Austin RC, Lentz SR, Werstuck GH. Role of hyperhomocysteinemia in endothelial dysfunction and atherothrombotic disease. *Cell death and differentiation*. 2004;11 Suppl 1:S56-64
94. Sen U, Mishra PK, Tyagi N, Tyagi SC. Homocysteine to hydrogen sulfide or hypertension. *Cell biochemistry and biophysics*. 2010;57:49-58
95. Chen Z, Chakraborty S, Banerjee R. Demonstration that mammalian methionine synthases are predominantly cobalamin-loaded. *The Journal of biological chemistry*. 1995;270:19246-19249

96. Banerjee R, Zou CG. Redox regulation and reaction mechanism of human cystathionine-beta-synthase: A PLP-dependent hemesensor protein. *Archives of biochemistry and biophysics*. 2005;433:144-156
97. Vitvitsky V, Thomas M, Ghorpade A, Gendelman HE, Banerjee R. A functional transsulfuration pathway in the brain links to glutathione homeostasis. *Journal of Biological Chemistry*. 2006;281:35785-35793
98. Garg SK, Yan Z, Vitvitsky V, Banerjee R. Differential dependence on cysteine from transsulfuration versus transport during t cell activation. *Antioxidants & redox signaling*. 2011;15:39-47
99. Wang M, Guo Z, Wang S. Cystathionine gamma-lyase expression is regulated by exogenous hydrogen peroxide in the mammalian cells. *Gene expression*. 2012;15:235-241
100. Hassan MI, Boosen M, Schaefer L, Kozlowska J, Eisel F, von Knethen A, Beck M, Hemeida RA, El-Moselhy MA, Hamada FM, Beck KF, Pfeilschifter J. Platelet-derived growth factor-bb induces cystathionine gamma-lyase expression in rat mesangial cells via a redox-dependent mechanism. *British journal of pharmacology*. 2012;166:2231-2242
101. Lin VS, Lippert AR, Chang CJ. Cell-trappable fluorescent probes for endogenous hydrogen sulfide signaling and imaging H_2O_2-dependent H_2S production. *Proceedings of the National Academy of Sciences of the United States of America*. 2013;110:7131-7135
102. Perry SF, Spinelli Oliveira E. Respiration in a changing environment. *Respiratory physiology & neurobiology*. 2010;173 Suppl:S20-25
103. Valko M, Leibfritz D, Moncol J, Cronin MT, Mazur M, Telser J. Free radicals and antioxidants in normal physiological functions and human disease. *The international journal of biochemistry & cell biology*. 2007;39:44-84
104. Brieger K, Schiavone S, Miller FJ, Jr., Krause KH. Reactive oxygen species: From health to disease. *Swiss medical weekly*. 2012;142:w13659
105. Winterbourn CC. Reconciling the chemistry and biology of reactive oxygen species. *Nature chemical biology*. 2008;4:278-286
106. Griendling KK, Sorescu D, Ushio-Fukai M. NADPH oxidase: Role in cardiovascular biology and disease. *Circulation research*. 2000;86:494-501
107. Brown DI, Griendling KK. Nox proteins in signal transduction. *Free radical biology & medicine*. 2009;47:1239-1253
108. Galli S, Antico Arciuch VG, Poderoso C, Converso DP, Zhou Q, Bal de Kier Joffe E, Cadenas E, Boczkowski J, Carreras MC, Poderoso JJ. Tumor cell phenotype is sustained by selective mapk oxidation in mitochondria. *PloS one*. 2008;3:e2379
109. D'Autreaux B, Toledano MB. ROS as signalling molecules: Mechanisms that generate specificity in ros homeostasis. *Nature reviews. Molecular cell biology*. 2007;8:813-824
110. Finkel T. Signal transduction by reactive oxygen species. *The Journal of cell biology*. 2011;194:7-15
111. Halliwell B, Gutteridge JMC. *Free radicals in biology and medicine*. Oxford ; New York: Oxford University Press; 2007.
112. Rhee SG, Chang TS, Bae YS, Lee SR, Kang SW. Cellular regulation by hydrogen peroxide. *Journal of the American Society of Nephrology : JASN*. 2003;14:S211-215

113. Stadtman ER, Levine RL. Free radical-mediated oxidation of free amino acids and amino acid residues in proteins. *Amino acids*. 2003;25:207-218
114. Chung HS, Wang SB, Venkatraman V, Murray CI, Van Eyk JE. Cysteine oxidative posttranslational modifications: Emerging regulation in the cardiovascular system. *Circulation research*. 2013;112:382-392
115. Burgoyne JR, Eaton P. Contemporary techniques for detecting and identifying proteins susceptible to reversible thiol oxidation. *Biochemical Society transactions*. 2011;39:1260-1267
116. Veal EA, Day AM, Morgan BA. Hydrogen peroxide sensing and signaling. *Molecular cell*. 2007;26:1-14
117. Burgoyne JR, Madhani M, Cuello F, Charles RL, Brennan JP, Schroder E, Browning DD, Eaton P. Cysteine redox sensor in PKG1alpha enables oxidant-induced activation. *Science*. 2007;317:1393-1397
118. Burgoyne JR, Eaton P. Oxidant sensing by protein kinases a and g enables integration of cell redox state with phosphoregulation. *Sensors (Basel)*. 2010;10:2731-2751
119. Pham-Huy LA, He H, Pham-Huy C. Free radicals, antioxidants in disease and health. *International journal of biomedical science : IJBS*. 2008;4:89-96
120. Murphy MP. How mitochondria produce reactive oxygen species. *The Biochemical journal*. 2009;417:1-13
121. Meneshian A, Bulkley GB. The physiology of endothelial xanthine oxidase: From urate catabolism to reperfusion injury to inflammatory signal transduction. *Microcirculation*. 2002;9:161-175
122. Bedard K, Krause KH. The Nox family of ROS-generating NADPH oxidases: Physiology and pathophysiology. *Physiological reviews*. 2007;87:245-313
123. Sheppard FR, Kelher MR, Moore EE, McLaughlin NJ, Banerjee A, Silliman CC. Structural organization of the neutrophil NADPH oxidase: Phosphorylation and translocation during priming and activation. *Journal of leukocyte biology*. 2005;78:1025-1042
124. Lambeth JD. Nox enzymes and the biology of reactive oxygen. *Nature reviews. Immunology*. 2004;4:181-189
125. Liu L, Rodriguez-Belmonte EM, Mazloum N, Xie B, Lee MY. Identification of a novel protein, pdip38, that interacts with the p50 subunit of DNA polymerase delta and proliferating cell nuclear antigen. *The Journal of biological chemistry*. 2003;278:10041-10047
126. Lyle AN, Deshpande NN, Taniyama Y, Seidel-Rogol B, Pounkova L, Du P, Papaharalambus C, Lassegue B, Griendling KK. Poldip2, a novel regulator of Nox4 and cytoskeletal integrity in vascular smooth muscle cells. *Circulation research*. 2009;105:249-259
127. Drummond GR, Selemidis S, Griendling KK, Sobey CG. Combating oxidative stress in vascular disease: NADPH oxidases as therapeutic targets. *Nature reviews. Drug discovery*. 2011;10:453-471
128. Clark RA, Leidal KG, Pearson DW, Nauseef WM. NADPH oxidase of human neutrophils. Subcellular localization and characterization of an arachidonate-activatable superoxide-generating system. *The Journal of biological chemistry*. 1987;262:4065-4074
129. Van Buul JD, Fernandez-Borja M, Anthony EC, Hordijk PL. Expression and localization of Nox2 and Nox4 in primary human endothelial cells. *Antioxidants & redox signaling*. 2005;7:308-317

130. Anilkumar N, Weber R, Zhang M, Brewer A, Shah AM. Nox4 and Nox2 NADPH oxidases mediate distinct cellular redox signaling responses to agonist stimulation. *Arteriosclerosis, thrombosis, and vascular biology*. 2008;28:1347-1354
131. Chen K, Kirber MT, Xiao H, Yang Y, Keaney JF, Jr. Regulation of ROS signal transduction by NADPH oxidase 4 localization. *The Journal of cell biology*. 2008;181:1129-1139
132. Kuroda J, Nakagawa K, Yamasaki T, Nakamura K, Takeya R, Kuribayashi F, Imajoh-Ohmi S, Igarashi K, Shibata Y, Sueishi K, Sumimoto H. The superoxide-producing NADPH oxidase Nox4 in the nucleus of human vascular endothelial cells. *Genes to cells : devoted to molecular & cellular mechanisms*. 2005;10:1139-1151
133. Serrander L, Cartier L, Bedard K, Banfi B, Lardy B, Plastre O, Sienkiewicz A, Forro L, Schlegel W, Krause KH. Nox4 activity is determined by mRNA levels and reveals a unique pattern of ROS generation. *The Biochemical journal*. 2007;406:105-114
134. Xi G, Shen XC, Wai C, Clemmons DR. Recruitment of Nox4 to a plasma membrane scaffold is required for localized reactive oxygen species generation and sustained src activation in response to insulin-like growth factor-i. *The Journal of biological chemistry*. 2013;288:15641-15653
135. Cave AC, Brewer AC, Narayanapanicker A, Ray R, Grieve DJ, Walker S, Shah AM. NADPH oxidases in cardiovascular health and disease. *Antioxidants & redox signaling*. 2006;8:691-728
136. Hilenski LL, Clempus RE, Quinn MT, Lambeth JD, Griendling KK. Distinct subcellular localizations of Nox1 and Nox4 in vascular smooth muscle cells. *Arteriosclerosis, thrombosis, and vascular biology*. 2004;24:677-683
137. Drummond GR, Sobey CG. Endothelial NADPH oxidases: Which Nox to target in vascular disease? *Trends in endocrinology and metabolism: TEM*. 2014;25:452-463
138. Judkins CP, Diep H, Broughton BR, Mast AE, Hooker EU, Miller AA, Selemidis S, Dusting GJ, Sobey CG, Drummond GR. Direct evidence of a role for Nox2 in superoxide production, reduced nitric oxide bioavailability, and early atherosclerotic plaque formation in apoe-/- mice. *American journal of physiology. Heart and circulatory physiology*. 2010;298:H24-32
139. Barry-Lane PA, Patterson C, van der Merwe M, Hu Z, Holland SM, Yeh ET, Runge MS. P47phox is required for atherosclerotic lesion progression in apoe(-/-) mice. *The Journal of clinical investigation*. 2001;108:1513-1522
140. Jung O, Schreiber JG, Geiger H, Pedrazzini T, Busse R, Brandes RP. Gp91phox-containing NADPH oxidase mediates endothelial dysfunction in renovascular hypertension. *Circulation*. 2004;109:1795-1801
141. Landmesser U, Cai H, Dikalov S, McCann L, Hwang J, Jo H, Holland SM, Harrison DG. Role of p47(phox) in vascular oxidative stress and hypertension caused by angiotensin II. *Hypertension*. 2002;40:511-515
142. Matsuno K, Yamada H, Iwata K, Jin D, Katsuyama M, Matsuki M, Takai S, Yamanishi K, Miyazaki M, Matsubara H, Yabe-Nishimura C. Nox1 is involved in angiotensin II-mediated hypertension: A study in Nox1-deficient mice. *Circulation*. 2005;112:2677-2685
143. Dikalova A, Clempus R, Lassegue B, Cheng G, McCoy J, Dikalov S, San Martin A, Lyle A, Weber DS, Weiss D, Taylor WR, Schmidt HH, Owens GK, Lambeth

JD, Griendling KK. Nox1 overexpression potentiates angiotensin II-induced hypertension and vascular smooth muscle hypertrophy in transgenic mice. *Circulation*. 2005;112:2668-2676
144. Brandes RP, Weissmann N, Schroder K. NADPH oxidases in cardiovascular disease. *Free radical biology & medicine*. 2010;49:687-706
145. Rueckschloss U, Quinn MT, Holtz J, Morawietz H. Dose-dependent regulation of NADPH oxidase expression by angiotensin II in human endothelial cells: Protective effect of angiotensin II type 1 receptor blockade in patients with coronary artery disease. *Arteriosclerosis, thrombosis, and vascular biology*. 2002;22:1845-1851
146. Murdoch CE, Alom-Ruiz SP, Wang M, Zhang M, Walker S, Yu B, Brewer A, Shah AM. Role of endothelial Nox2 NADPH oxidase in angiotensin II-induced hypertension and vasomotor dysfunction. *Basic research in cardiology*. 2011;106:527-538
147. Gavazzi G, Banfi B, Deffert C, Fiette L, Schappi M, Herrmann F, Krause KH. Decreased blood pressure in Nox1-deficient mice. *FEBS letters*. 2006;580:497-504
148. Chen F, Haigh S, Barman S, Fulton DJ. From form to function: The role of Nox4 in the cardiovascular system. *Frontiers in physiology*. 2012;3:412
149. Touyz RM, Montezano AC. Vascular Nox4: A multifarious NADPH oxidase. *Circulation research*. 2012;110:1159-1161
150. Craige SM, Chen K, Pei Y, Li C, Huang X, Chen C, Shibata R, Sato K, Walsh K, Keaney JF, Jr. NADPH oxidase 4 promotes endothelial angiogenesis through endothelial nitric oxide synthase activation. *Circulation*. 2011;124:731-740
151. Schroder K, Zhang M, Benkhoff S, Mieth A, Pliquett R, Kosowski J, Kruse C, Luedike P, Michaelis UR, Weissmann N, Dimmeler S, Shah AM, Brandes RP. Nox4 is a protective reactive oxygen species generating vascular NADPH oxidase. *Circulation research*. 2012;110:1217-1225
152. Frey RS, Ushio-Fukai M, Malik AB. NADPH oxidase-dependent signaling in endothelial cells: Role in physiology and pathophysiology. *Antioxidants & redox signaling*. 2009;11:791-810
153. Zembowicz A, Hatchett RJ, Jakubowski AM, Gryglewski RJ. Involvement of nitric oxide in the endothelium-dependent relaxation induced by hydrogen peroxide in the rabbit aorta. *British journal of pharmacology*. 1993;110:151-158
154. Vogel J, Kruse C, Zhang M, Schroder K. Nox4 supports proper capillary growth in exercise and retina neo-vascularization. *The Journal of physiology*. 2015;593:2145-2154
155. Zhu YZ, Wang ZJ, Ho P, Loke YY, Zhu YC, Huang SH, Tan CS, Whiteman M, Lu J, Moore PK. Hydrogen sulfide and its possible roles in myocardial ischemia in experimental rats. *J Appl Physiol (1985)*. 2007;102:261-268
156. Meier M, Janosik M, Kery V, Kraus JP, Burkhard P. Structure of human cystathionine beta-synthase: A unique pyridoxal 5'-phosphate-dependent heme protein. *The EMBO journal*. 2001;20:3910-3916
157. Pare G, Chasman DI, Parker AN, Zee RR, Malarstig A, Seedorf U, Collins R, Watkins H, Hamsten A, Miletich JP, Ridker PM. Novel associations of cps1, mut, Nox4, and dpep1 with plasma homocysteine in a healthy population: A genome-wide evaluation of 13 974 participants in the women's genome health study. *Circulation. Cardiovascular genetics*. 2009;2:142-150

158. Brewer AC, Murray TV, Arno M, Zhang M, Anilkumar NP, Mann GE, Shah AM. Nox4 regulates Nrf2 and glutathione redox in cardiomyocytes in vivo. *Free radical biology & medicine*. 2011;51:205-215
159. Von Lohneysen K, Noack D, Jesaitis AJ, Dinauer MC, Knaus UG. Mutational analysis reveals distinct features of the nox4-p22 phox complex. *The Journal of biological chemistry*. 2008;283:35273-35282
160. Miles EW, Kraus JP. Cystathionine beta-synthase: Structure, function, regulation, and location of homocystinuria-causing mutations. *The Journal of biological chemistry*. 2004;279:29871-29874
161. Forman HJ. Use and abuse of exogenous h2o2 in studies of signal transduction. *Free Radical Bio Med*. 2007;42:926-932
162. Forman HJ. The use and abuse of exogenous electrophiles and hydroperoxides in studies of signal transduction. *Free Radical Res*. 2006;40:S58-S58
163. Altenhofer S, Kleikers PW, Radermacher KA, Scheurer P, Rob Hermans JJ, Schiffers P, Ho H, Wingler K, Schmidt HH. The nox toolbox: Validating the role of NADPH oxidases in physiology and disease. *Cellular and molecular life sciences : CMLS*. 2012;69:2327-2343
164. Pullar JM, Hampton MB. Diphenyleneiodonium triggers the efflux of glutathione from cultured cells. *Journal of Biological Chemistry*. 2002;277:19402-19407
165. Carlsson J, Berglin EH, Claesson R, Edlund MB, Persson S. Catalase inhibition by sulfide and hydrogen peroxide-induced mutagenicity in salmonella typhimurium strain ta102. *Mutation research*. 1988;202:59-64
166. Kabil O, Vitvitsky V, Xie P, Banerjee R. The quantitative significance of the transsulfuration enzymes for H_2S production in murine tissues. *Antioxidants & redox signaling*. 2011;15:363-372
167. Ishigami M, Hiraki K, Umemura K, Ogasawara Y, Ishii K, Kimura H. A source of hydrogen sulfide and a mechanism of its release in the brain. *Antioxidants & redox signaling*. 2009;11:205-214
168. Shen X, Peter EA, Bir S, Wang R, Kevil CG. Analytical measurement of discrete hydrogen sulfide pools in biological specimens. *Free radical biology & medicine*. 2012;52:2276-2283
169. Hughes MN, Centelles MN, Moore KP. Making and working with hydrogen sulfide: The chemistry and generation of hydrogen sulfide in vitro and its measurement in vivo: A review. *Free radical biology & medicine*. 2009;47:1346-1353
170. Shen X, Pattillo CB, Pardue S, Bir SC, Wang R, Kevil CG. Measurement of plasma hydrogen sulfide in vivo and in vitro. *Free radical biology & medicine*. 2011;50:1021-1031
171. Bartholomew TC, Powell GM, Dodgson KS, Curtis CG. Oxidation of sodium sulphide by rat liver, lungs and kidney. *Biochemical pharmacology*. 1980;29:2431-2437
172. Matlin AJ, Clark F, Smith CW. Understanding alternative splicing: Towards a cellular code. *Nature reviews. Molecular cell biology*. 2005;6:386-398
173. Schlaeger TM, Bartunkova S, Lawitts JA, Teichmann G, Risau W, Deutsch U, Sato TN. Uniform vascular-endothelial-cell-specific gene expression in both embryonic and adult transgenic mice. *Proceedings of the National Academy of Sciences of the United States of America*. 1997;94:3058-3063

174. Pusztaszeri MP, Seelentag W, Bosman FT. Immunohistochemical expression of endothelial markers cd31, cd34, von willebrand factor, and fli-1 in normal human tissues. *The journal of histochemistry and cytochemistry : official journal of the Histochemistry Society*. 2006;54:385-395
175. Doeller JE, Isbell TS, Benavides G, Koenitzer J, Patel H, Patel RP, Lancaster JR, Jr., Darley-Usmar VM, Kraus DW. Polarographic measurement of hydrogen sulfide production and consumption by mammalian tissues. *Analytical biochemistry*. 2005;341:40-51
176. Loomis ED, Sullivan JC, Osmond DA, Pollock DM, Pollock JS. Endothelin mediates superoxide production and vasoconstriction through activation of NADPH oxidase and uncoupled nitric-oxide synthase in the rat aorta. *The Journal of pharmacology and experimental therapeutics*. 2005;315:1058-1064
177. Beckman JS, Koppenol WH. Nitric oxide, superoxide, and peroxynitrite: The good, the bad, and ugly. *The American journal of physiology*. 1996;271:C1424-1437
178. Ko EA, Song MY, Donthamsetty R, Makino A, Yuan JX. Tension measurement in isolated rat and mouse pulmonary artery. *Drug discovery today. Disease models*. 2010;7:123-130
179. Zhao W, Ndisang JF, Wang R. Modulation of endogenous production of H_2S in rat tissues. *Canadian journal of physiology and pharmacology*. 2003;81:848-853
180. Christ GJ, Spray DC, el-Sabban M, Moore LK, Brink PR. Gap junctions in vascular tissues. Evaluating the role of intercellular communication in the modulation of vasomotor tone. *Circulation research*. 1996;79:631-646
181. Christ GJ. Modulation of alpha 1-adrenergic contractility in isolated vascular tissues by heptanol: A functional demonstration of the potential importance of intercellular communication to vascular response generation. *Life sciences*. 1995;56:709-721
182. Stipanuk MH, Beck PW. Characterization of the enzymic capacity for cysteine desulphhydration in liver and kidney of the rat. *The Biochemical journal*. 1982;206:267-277
183. Muller WA. The role of pecam-1 (CD31) in leukocyte emigration: Studies in vitro and in vivo. *Journal of leukocyte biology*. 1995;57:523-528
184. Alberts B, Wilson JH, Hunt T. *Molecular biology of the cell*. New York: Garland Science; 2008.
185. Nikolov DB, Burley SK. Rna polymerase II transcription initiation: A structural view. *Proceedings of the National Academy of Sciences of the United States of America*. 1997;94:15-22
186. Shandilya J, Roberts SG. The transcription cycle in eukaryotes: From productive initiation to RNA polymerase II recycling. *Biochimica et biophysica acta*. 2012;1819:391-400
187. Ishii I, Akahoshi N, Yu XN, Kobayashi Y, Namekata K, Komaki G, Kimura H. Murine cystathionine gamma-lyase: Complete cdna and genomic sequences, promoter activity, tissue distribution and developmental expression. *The Biochemical journal*. 2004;381:113-123
188. Yin P, Zhao C, Li Z, Mei C, Yao W, Liu Y, Li N, Qi J, Wang L, Shi Y, Qiu S, Fan J, Zha X. Sp1 is involved in regulation of cystathionine gamma-lyase gene

expression and biological function by PI3K/AKT pathway in human hepatocellular carcinoma cell lines. *Cellular signalling*. 2012
189. Yin P, Zhao C, Li Z, Mei C, Yao W, Liu Y, Li N, Qi J, Wang L, Shi Y, Qiu S, Fan J, Zha X. Sp1 is involved in regulation of cystathionine gamma-lyase gene expression and biological function by PI3K/AKT pathway in human hepatocellular carcinoma cell lines. *Cellular signalling*. 2012;24:1229-1240
190. Donnelly N, Gorman AM, Gupta S, Samali A. The EIFalpha kinases: Their structures and functions. *Cellular and molecular life sciences : CMLS*. 2013;70:3493-3511
191. Ameri K, Harris AL. Activating transcription factor 4. *The international journal of biochemistry & cell biology*. 2008;40:14-21
192. Dickhout JG, Carlisle RE, Jerome DE, Mohammed-Ali Z, Jiang H, Yang G, Mani S, Garg SK, Banerjee R, Kaufman RJ, Maclean KN, Wang R, Austin RC. Integrated stress response modulates cellular redox state via induction of cystathionine gamma-lyase: Cross-talk between integrated stress response and thiol metabolism. *The Journal of biological chemistry*. 2012;287:7603-7614
193. Han J, Back SH, Hur J, Lin YH, Gildersleeve R, Shan J, Yuan CL, Krokowski D, Wang S, Hatzoglou M, Kilberg MS, Sartor MA, Kaufman RJ. ER-stress-induced transcriptional regulation increases protein synthesis leading to cell death. *Nature cell biology*. 2013;15:481-490
194. Wang M, Guo Z, Wang S. The binding site for the transcription factor, nf-kappab, on the cystathionine gamma-lyase promoter is critical for lps-induced cystathionine gamma-lyase expression. *International journal of molecular medicine*. 2014;34:639-645
195. Kandil S, Brennan L, McBean GJ. Glutathione depletion causes a jnk and p38mapk-mediated increase in expression of cystathionine-gamma-lyase and upregulation of the transsulfuration pathway in c6 glioma cells. *Neurochemistry international*. 2010;56:611-619
196. Kaspar JW, Niture SK, Jaiswal AK. Nrf2:Inrf2 (keap1) signaling in oxidative stress. *Free radical biology & medicine*. 2009;47:1304-1309
197. Sciarretta S, Zhai P, Shao D, Zablocki D, Nagarajan N, Terada LS, Volpe M, Sadoshima J. Activation of NADPH oxidase 4 in the endoplasmic reticulum promotes cardiomyocyte autophagy and survival during energy stress through the protein kinase rna-activated-like endoplasmic reticulum kinase/eukaryotic initiation factor 2alpha/activating transcription factor 4 pathway. *Circulation research*. 2013;113:1253-1264
198. Lu PD, Harding HP, Ron D. Translation reinitiation at alternative open reading frames regulates gene expression in an integrated stress response. *The Journal of cell biology*. 2004;167:27-33
199. Avivar-Valderas A, Salas E, Bobrovnikova-Marjon E, Diehl JA, Nagi C, Debnath J, Aguirre-Ghiso JA. Perk integrates autophagy and oxidative stress responses to promote survival during extracellular matrix detachment. *Molecular and cellular biology*. 2011;31:3616-3629
200. Lu L, Han AP, Chen JJ. Translation initiation control by heme-regulated eukaryotic initiation factor 2alpha kinase in erythroid cells under cytoplasmic stresses. *Molecular and cellular biology*. 2001;21:7971-7980
201. Lee JI, Dominy JE, Jr., Sikalidis AK, Hirschberger LL, Wang W, Stipanuk MH. Hepg2/c3a cells respond to cysteine deprivation by induction of the amino

acid deprivation/integrated stress response pathway. *Physiological genomics*. 2008;33:218-229
202. Harding HP, Zhang Y, Ron D. Protein translation and folding are coupled by an endoplasmic-reticulum-resident kinase. *Nature*. 1999;397:271-274
203. Jackson RJ, Hellen CU, Pestova TV. The mechanism of eukaryotic translation initiation and principles of its regulation. *Nature reviews. Molecular cell biology*. 2010;11:113-127
204. Rafie-Kolpin M, Han AP, Chen JJ. Autophosphorylation of threonine 485 in the activation loop is essential for attaining EIF2alpha kinase activity of hri. *Biochemistry*. 2003;42:6536-6544
205. Bauer BN, Rafie-Kolpin M, Lu L, Han A, Chen JJ. Multiple autophosphorylation is essential for the formation of the active and stable homodimer of heme-regulated EIF2 alpha kinase. *Biochemistry*. 2001;40:11543-11551
206. Smith KR, Klei LR, Barchowsky A. Arsenite stimulates plasma membrane NADPH oxidase in vascular endothelial cells. *American journal of physiology. Lung cellular and molecular physiology*. 2001;280:L442-449
207. Barchowsky A, Klei LR, Dudek EJ, Swartz HM, James PE. Stimulation of reactive oxygen, but not reactive nitrogen species, in vascular endothelial cells exposed to low levels of arsenite. *Free radical biology & medicine*. 1999;27:1405-1412
208. Nagababu E, Rifkind JM. Heme degradation by reactive oxygen species. *Antioxidants & redox signaling*. 2004;6:967-978
209. Belcher JD, Beckman JD, Balla G, Balla J, Vercellotti G. Heme degradation and vascular injury. *Antioxidants & redox signaling*. 2010;12:233-248
210. Busse R, Fleming I. Vascular endothelium and blood flow. *Handbook of experimental pharmacology*. 2006:43-78
211. Cooke JP. No and angiogenesis. *Atherosclerosis. Supplements*. 2003;4:53-60
212. Li Volti G, Sacerdoti D, Sangras B, Vanella A, Mezentsev A, Scapagnini G, Falck JR, Abraham NG. Carbon monoxide signaling in promoting angiogenesis in human microvessel endothelial cells. *Antioxidants & redox signaling*. 2005;7:704-710
213. Papapetropoulos A, Pyriochou A, Altaany Z, Yang G, Marazioti A, Zhou Z, Jeschke MG, Branski LK, Herndon DN, Wang R, Szabo C. Hydrogen sulfide is an endogenous stimulator of angiogenesis. *Proceedings of the National Academy of Sciences of the United States of America*. 2009;106:21972-21977
214. Smyrnias I, Zhang X, Zhang M, Murray TV, Brandes RP, Schroder K, Brewer AC, Shah AM. Nicotinamide adenine dinucleotide phosphate oxidase-4-dependent upregulation of nuclear factor erythroid-derived 2-like 2 protects the heart during chronic pressure overload. *Hypertension*. 2015;65:547-553
215. Wu RF, Ma Z, Liu Z, Terada LS. Nox4-derived H_2O_2 mediates endoplasmic reticulum signaling through local ras activation. *Molecular and cellular biology*. 2010;30:3553-3568
216. Zhang M, Brewer AC, Schroder K, Santos CX, Grieve DJ, Wang M, Anilkumar N, Yu B, Dong X, Walker SJ, Brandes RP, Shah AM. NADPH oxidase-4 mediates protection against chronic load-induced stress in mouse hearts by enhancing angiogenesis. *Proceedings of the National Academy of Sciences of the United States of America*. 2010;107:18121-18126

217. Wind S, Beuerlein K, Armitage ME, Taye A, Kumar AH, Janowitz D, Neff C, Shah AM, Wingler K, Schmidt HH. Oxidative stress and endothelial dysfunction in aortas of aged spontaneously hypertensive rats by Nox1/2 is reversed by NADPH oxidase inhibition. *Hypertension*. 2010;56:490-497
218. Diebold I, Petry A, Hess J, Gorlach A. The NADPH oxidase subunit Nox4 is a new target gene of the hypoxia-inducible factor-1. *Molecular biology of the cell*. 2010;21:2087-2096
219. Sciarretta S, Volpe M, Sadoshima J. Nox4 regulates autophagy during energy deprivation. *Autophagy*. 2014;10:699-701
220. McEwen E, Kedersha N, Song B, Scheuner D, Gilks N, Han A, Chen JJ, Anderson P, Kaufman RJ. Heme-regulated inhibitor kinase-mediated phosphorylation of eukaryotic translation initiation factor 2 inhibits translation, induces stress granule formation, and mediates survival upon arsenite exposure. *The Journal of biological chemistry*. 2005;280:16925-16933
221. Chen PF, Tsai AL, Wu KK. Cysteine 184 of endothelial nitric oxide synthase is involved in heme coordination and catalytic activity. *The Journal of biological chemistry*. 1994;269:25062-25066
222. Ryter SW, Alam J, Choi AM. Heme oxygenase-1/carbon monoxide: From basic science to therapeutic applications. *Physiological reviews*. 2006;86:583-650
223. Leffler CW, Parfenova H, Jaggar JH, Wang R. Carbon monoxide and hydrogen sulfide: Gaseous messengers in cerebrovascular circulation. *Journal of applied physiology*. 2006;100:1065-1076
224. McCann SK, Dusting GJ, Roulston CL. Early increase of Nox4 NADPH oxidase and superoxide generation following endothelin-1-induced stroke in conscious rats. *Journal of neuroscience research*. 2008;86:2524-2534
225. Vallet P, Charnay Y, Steger K, Ogier-Denis E, Kovari E, Herrmann F, Michel JP, Szanto I. Neuronal expression of the nadph oxidase Nox4, and its regulation in mouse experimental brain ischemia. *Neuroscience*. 2005;132:233-238
226. Zhang L, Sheppard OR, Shah AM, Brewer AC. Positive regulation of the NADPH oxidase Nox4 promoter in vascular smooth muscle cells by e2f. *Free radical biology & medicine*. 2008;45:679-685
227. Qin G, Kishore R, Dolan CM, Silver M, Wecker A, Luedemann CN, Thorne T, Hanley A, Curry C, Heyd L, Dinesh D, Kearney M, Martelli F, Murayama T, Goukassian DA, Zhu Y, Losordo DW. Cell cycle regulator E2F1 modulates angiogenesis via p53-dependent transcriptional control of vegf. *Proceedings of the National Academy of Sciences of the United States of America*. 2006;103:11015-11020
228. Wang M, Guo Z, Wang S. Regulation of cystathionine gamma-lyase in mammalian cells by hypoxia. *Biochemical genetics*. 2014;52:29-37
229. Dulak J, Deshane J, Jozkowicz A, Agarwal A. Heme oxygenase-1 and carbon monoxide in vascular pathobiology: Focus on angiogenesis. *Circulation*. 2008;117:231-241
230. Kolluru GK, Bir SC, Yuan S, Shen X, Pardue S, Wang R, Kevil CG. Cystathionine gamma-lyase regulates arteriogenesis through NO dependent monocyte recruitment. *Cardiovascular research*. 2015

231. Murohara T, Asahara T, Silver M, Bauters C, Masuda H, Kalka C, Kearney M, Chen D, Symes JF, Fishman MC, Huang PL, Isner JM. Nitric oxide synthase modulates angiogenesis in response to tissue ischemia. *The Journal of clinical investigation*. 1998;101:2567-2578
232. Tongers J, Knapp JM, Korf M, Kempf T, Limbourg A, Limbourg FP, Li Z, Fraccarollo D, Bauersachs J, Han X, Drexler H, Fiedler B, Wollert KC. Haem oxygenase promotes progenitor cell mobilization, neovascularization, and functional recovery after critical hindlimb ischaemia in mice. *Cardiovascular research*. 2008;78:294-300
233. Lee PJ, Jiang BH, Chin BY, Iyer NV, Alam J, Semenza GL, Choi AM. Hypoxia-inducible factor-1 mediates transcriptional activation of the heme oxygenase-1 gene in response to hypoxia. *The Journal of biological chemistry*. 1997;272:5375-5381
234. Peng YJ, Nanduri J, Raghuraman G, Souvannakitti D, Gadalla MM, Kumar GK, Snyder SH, Prabhakar NR. H_2S mediates O_2 sensing in the carotid body. *Proceedings of the National Academy of Sciences of the United States of America*. 2010;107:10719-10724